

INFORMATION TO USERS

This material was produced from a microfilm copy of the original document. While the most advanced technological means to photograph and reproduce this document have been used, the quality is heavily dependent upon the quality of the original submitted.

The following explanation of techniques is provided to help you understand markings or patterns which may appear on this reproduction.

1. The sign or "target" for pages apparently lacking from the document photographed is "Missing Page(s)". If it was possible to obtain the missing page(s) or section, they are spliced into the film along with adjacent pages. This may have necessitated cutting thru an image and duplicating adjacent pages to insure you complete continuity.
2. When an image on the film is obliterated with a large round black mark, it is an indication that the photographer suspected that the copy may have moved during exposure and thus cause a blurred image. You will find a good image of the page in the adjacent frame.
3. When a map, drawing or chart, etc., was part of the material being photographed the photographer followed a definite method in "sectioning" the material. It is customary to begin photoing at the upper left hand corner of a large sheet and to continue photoing from left to right in equal sections with a small overlap. If necessary, sectioning is continued again - beginning below the first row and continuing on until complete.
4. The majority of users indicate that the textual content is of greatest value, however, a somewhat higher quality reproduction could be made from "photographs" if essential to the understanding of the dissertation. Silver prints of "photographs" may be ordered at additional charge by writing the Order Department, giving the catalog number, title, author and specific pages you wish reproduced.
5. PLEASE NOTE: Some pages may have indistinct print. Filmed as received.

Xerox University Microfilms

300 North Zeeb Road
Ann Arbor, Michigan 48106

74-20,088

WUN, Wyman Woon-Man, 1941-
APPROXIMATE MACROMOLECULAR ORBITAL THEORY.

The City University of New York, Ph.D., 1974
Chemistry, physical

University Microfilms, A XEROX Company, Ann Arbor, Michigan

APPROXIMATE MACROMOLECULAR ORBITAL THEORY

by

Wyman W.M. Wun

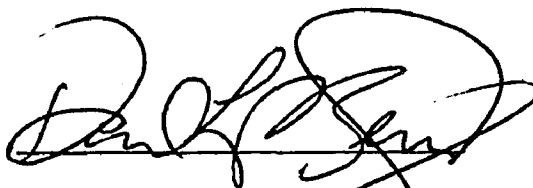
A dissertation submitted to the Graduate Faculty in Chemistry
in partial fulfillment of the requirements for the degree of
Doctor of Philosophy, The City University of New York.

1974

This manuscript has been read and accepted for the Graduate Faculty
in Chemistry in satisfaction of the dissertation requirement for
the degree of Doctor of Philosophy.

5/6/74

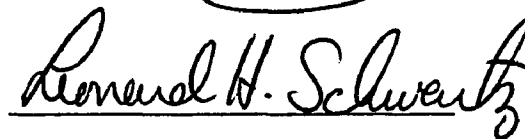
date



Professor David L. Beveridge
Chairman of Examining Committee

5/7/74

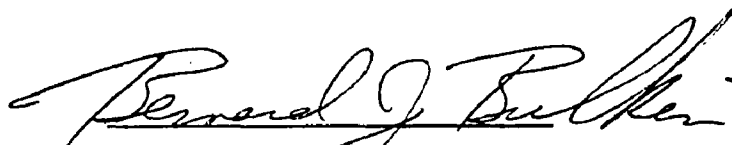
date



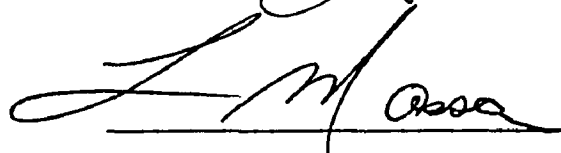
Professor Leonard H. Schwartz
Executive Officer

John Arents

Professor John S. Arents



Professor Bernard J. Bulkin



Professor Louis Massa

Supervisory Committee

The City University of New York

Abstract

APPROXIMATE MACROMOLECULAR ORBITAL THEORY

By

Wyman Woon-Man Wun

Adviser: Professor David L. Beveridge

The general formalism of INDO and MINDO/2 approximate macromolecular orbital calculations have been developed. The calculation of macromolecular properties, and the systematic analysis of one-dimensional macromolecular orbitals based on group theory has been presented. A test calculation of polyethylene is described in detail. Application of these methods to the calculation of the electronic structure, energy bands, and electrical properties of polyhydrogen, polyacetylene, polyethylene, F and NH₂-substituted polyacetylene, polypeptide, graphite and poly(hydrogenfluoride) have been carried out. The conformational potential energy surface of polyglycine calculated by INDO-MO and INDO-CMO methods in the free space approximation has been presented. A geometry at which the existence of metallic hydrogen might occur has been predicted by these methods. The semiempirical molecular orbital calculations with the parameters used in MINDO/2 yield a band structure of polyethylene in good agreement with experiment. The conformations of polypeptide predicted to be preferred in the free space approximation are discussed with the simple molecular orbital calculation. This result indicates that approximate macromolecular orbital calculations may be used in the same way as molecular orbital calculations for conformational analysis.

Acknowledgement

The author wishes to express his sincere gratitude to Professor David L. Beveridge of this Institution for his guidance and encouragement during this research work and his editing of the final form of this thesis. Appreciation is also due to Professor C.E. Hecht, for discussions.

A special note of thanks is due to my wife Esther and son Herrick for their patience and understanding. The encouragement of my parents and sister has a great contribution to the completion of my degree.

Table of Contents

- I. Introduction
- II. Background
- III. Theory and Methodology
- IV. Approximate Macromolecular Orbital Theory
- V. Applications
- VI. Concluding Remarks
- VII. Bibliography
- VIII. Appendix

I. Introduction

The purpose of this project is to develop a general approximate macromolecular orbital theory for infinite one-dimensional polymers. The project consists of four parts:

- 1) Derivation of the general formalism for self consistent field (SCF) macromolecular orbital (MMO) calculations at the ab initio level, and development of general approximate methods for treating all valence electrons;
- 2) Calculation of MMO's for prototype systems and analysis of the orbitals based on factor group, site group, and point group theory;
- 3) Application of the methods to the calculation of the electronic energy band structure, certain electrical and optical properties, and conformational stability of a set of representative polymers;
- 4) Assessment of capabilities and limitations of the method and prospects for future applications.

It has been recognized for some years that a useful perspective on the electronic structure of organic and biological macromolecules may be derived from the energy band theory of solid state physics. The quasiperiodic core potential of the macromolecular backbone gives rise to a manifold of energy levels resembling that expected for a one-dimensional crystal. The terminology of band theory can be used to describe the electronic structure of the polymer. In a valence electron treatment, the occupied manifold is referred to as the valence energy band. The unoccupied manifold is referred to as the

conduction band. The bands of levels are separated by forbidden zones or band gaps.

The electrical properties of the system are related to the band gap ΔE between the highest filled and lowest unfilled bands and the density of states (band shapes). The band gap is zero for a perfect conductor. There are free electrons in the conduction band due to thermal excitation. In an insulator, the magnitude of band gap is about 7 to 12 eV. Thermal population of the conduction band is completely negligible. Materials with band gaps between zero to 7 eV are called semiconductors. With band gaps in this range, thermal population of the conduction band is possible and increases with increasing temperature.

The optical properties of macromolecules can be related to the energy band structure in much the same manner as the absorption spectra of a simple molecule is related to the orbital levels. The wealth of experimental results now available in simple systems have already shown that the position and nature of the energy bands in a large number of materials could provide much information about the absorption of light in the visible and ultraviolet spectral. The band structure can be used directly to interpret and predict the photoelectron spectra of macromolecules in a simple way.

This thesis is concerned with the development, testing and evaluation of an approximate macromolecular orbital theory from the point of view described above. The following chapter develops the theoretical background of the project with regard

to both physical model and methodology. In chapter 3 the general formalism for crystal orbital calculation at the ab initio level is given and factor group analysis of macromolecular orbitals is described. The following chapter gives the details of approximate macromolecular orbital theory for valence electrons and parametrization of the methods. Chapter 5 is concerned with applications of the method to the calculation of the electronic structure, energy bands and the related conformational and electronic properties of representative polymers. An assessment of capabilities and limitations of the method and prospects for future applications are collected in chapter 6. The thesis is concluded with an appendix of the listing of the digital computer program used for approximate macromolecular orbital calculations.

II. Background:

Theoretical studies on macromolecules have been carried out using statistical mechanics and quantum mechanics. Statistical mechanics is used for large systems with highly approximate or empirical calculation of the conformational energy. Values of all thermodynamic quantities can be predicted by this method. Quantum mechanics is tractable only for relatively small systems or idealized representations of large systems, but provides a more accurate consideration of conformational energy. Quantum mechanics can provide expectation values of other molecular properties and information on electronic structure as well.

Models of macromolecules: Theoretical studies of macromolecules have been implemented using various models and methodology. The models are defined as follows:

1) Polymer Model: In the polymer model, the polymer is represented with explicit consideration of each of the monomeric units. Polymers with only a few monomeric units can be treated by quantum mechanics. Large polymers are computationally intractable using quantum mechanics. The problems encountered are purely computational in nature, and arise from the necessity of evaluation of the multicenter integrals. These systems can be treated in the polymer model using statistical mechanics. Many papers have been published¹ which have applied statistical mechanics to the calculation of the average dimensions, the probability of distribution of monomer, conformational stability, and phase transitions in macromolecular systems.

2) **Dimonomer Model:** The dimonomer model considers the structural features and molecular properties of two bonded monomers as representative of the macromolecule. This assumes that the macromolecular backbone and short-range interaction of side chains with the backbone in the macromolecule is the determinant factor in the establishing of the conformation of the macromolecule. The interactions with neighboring side chains are totally neglected. This model is of limited validity for large macromolecules where nonbonded interactions across chain segments and large entropy effects could be quite influential on the conformation. Macromolecular systems treated by the dimonomer model are tractable using molecular quantum mechanics. Extensive studies based on this model have been carried out on polypeptides using approximate molecular orbital theory.²

3) **One-dimensional crystal model:** In a perfect crystal, the interaction potential between each constituent atom is extended periodically throughout the crystal. For a highly idealized simple system, quantum mechanics is tractable for this method when Born-Van Karman cyclic boundary conditions³ are imposed on the problem. This is the method used in this thesis.

Methods of treating Macromolecules. In statistical mechanical studies the calculation of conformational energy is carried out by classical semiempirical methods. Bond lengths and bond angles are fixed and the energy of internal rotation about single bonds, non-bonded interactions, electrostatic interactions and hydrogen bonding are represented by various semiempirical pairwise potential functions.

It is customary to include entropy effects in these calculations, and estimate the statistical weights of the various conformations. These problems have been treated theoretically by Poland and Sheraga,¹ S.F. Edwards,⁴ M.E. Fisher,⁵ P.J. Flory and S. Fisk⁶ and by semiempirical methods using digital computer simulation. There are two approaches in computer simulation. One is the exact enumeration calculations by M.F. Sykes,⁷ M. Kumbar, S. Windwer,⁸ and K.K. Knaell and R.A. Scott.⁹ The other approach is the Monte Carlo method. Both of these methods involve the generation of non-self-intersection random walks. The difference between these two methods is the different way of calculating the properties of the system. In the Monte Carlo method, properties of the system are calculated for each random walk of length N. After a subset of the complete set of random walks of length N is generated, the average values of these properties are calculated in the limit of a long subset which is assumed to be approaching the values for the complete set. In the exact enumeration method, the properties of the system are calculated only when the complete set is generated.

Quantum mechanical studies of macromolecules have been carried out using the dimonomer and one-dimensional crystal model using a wide range of methods. Since the calculations presented herein are based on quantum mechanics, we review the quantum mechanical methods for polymers in some detail, including pi-

electron, valence electron, ab initio, molecular orbital and crystal orbital calculations.

The theoretical description of polymers as with other large organic molecules was first approached in the framework of the π - electron approximation, using free electron theory to simplify the computations to a tractable level. The Hückel theory of organic quantum chemistry has been applied extensively to polymeric systems by a number of workers, notably by Lennard-Jones,¹⁰ Ooshika,¹¹ Longuet-Higgins and Salem,¹² Tsuji, Huzinagn and Hasion,¹³ and Kutzelnigg.¹⁴ In Hückel LCAO approximation, each mobile or π - electron is considered to occupy a molecular orbital (MO) extending over the whole framework. This orbital is approximated by a linear combination of all p - π atomic orbitals. The desirable physical properties of the system are obtained by solving the Schrodinger equation with the corresponding effective hamiltonian operators. The Hückel method¹⁵ is a rather primitive and the results are generally considered too crude for the charge distribution, total energy and the geometry of the molecule. The π - electron approximation carries severe limitations, and is of very limited value in polymers with any degree of saturation or with any geometry other than planar. Improved methods for treating the electronic structure of polymers must provide for a consideration of all chemically effective electrons.

The extended Hückel theory (EHT) proposed by Hoffman¹⁶ is a logical extension of the ordinary Hückel method. In this

method, both σ and π electrons are treated explicitly. The basis set in EHT is a minimal Slater orbital set of electron atomic orbitals. The diagonal elements of the EHT matrix are given by the negative of the valence-state ionization potentials (VIP). The off diagonal elements of EHT matrix are related to the overlap integrals of the orbitals. The procedure to obtain the physical properties by this method is exactly analogous to simple Huckel theory. In comparison of theory and experiment, extended Huckel Theory gives often unsatisfactory bond lengths, charge distribution and exaggerated dipole moments. EHT can give a reasonable molecular conformations because of the mutual cancellation of errors in the final total energy calculation.¹⁷

In order to improve EHT, an iterative procedure was introduced to the EHT by Rein,¹⁸ Pullman,¹⁹ and Duke.²⁰ It is called Iterative Extended Huckel Theory (IEHT). This method has been shown to be a considerable improvement over EHT in terms of charge distribution in the orbitals. In IEHT, a parameter is assigned to each atomic orbital and it is minimized to get the best energy of the system. Integrals must be recalculated at each cycle of iteration. It has been shown that IEHT is a considerable improvements in iteration. The diagonal elements in IEHT are closer to the diagonal elements in SCF calculation because of the iteration in IEHT. But it is still not a very refine method, since either EHT or IEHT does not explicitly consider the electron repulsion terms.

The most elementary theory retaining the main feature of electron repulsion is the complete neglect of differential overlap method (CNDO) introduced by Pople, Santry, and Segal.²¹ Only valence electrons are treated explicitly; the inner shells are treated as part of a rigid core so that they modify the nuclear potential in the one electron part of the hamiltonian operator. The differential overlap approximation eliminates all three and four-center and most of the one and two-center integrals, leaving only the so-called coulomb integrals. The multicenter integrals are smallest in magnitude but the approximation is still severe. The CNDO method, particularly the CNDO/2²² procedure, has many advantages and some disadvantages.²³ Although most of the electron repulsion integrals are ignored, the important one, coulomb integrals are included. The method is simple enough to be generally useful for large molecules and avoids the multiplicity of parametrizations inherent in extended Huckel and other-empirical methods. Comparing theory and experiment CNDO has been shown to give good bond angles and a reasonable electron distribution as evidenced by electric dipole moments. Bond lengths are generally not predicted as well as bond angles, and binding energy and ionization potentials are predicted too high.

Several investigators have attempted to re-parameterize CNDO method.^{24,25} Unfortunately, as with the other semiempirical methods, a given parameterization which is suitable for the calculation of only one physical property, is generally found

to be poor for the others. So far, there is no unit approximate theory which is suitable for the calculation of all physical properties. Pople, Beveridge, and Dobosh have worked out a modified CNDO method known as INDO²⁶ (intermediate neglect of differential overlap) method. The two methods are closely related, for the basic approximations are the same except for monatomic terms. The mono-atomic differential overlap is retained in INDO, but only in one-center integrals. The detailed parameterization of INDO method will be given in the later section. The INDO method predicts molecular geometries as well as CNDO/2 or better, and is also capable of reasonable prediction of ESR hyperfine coupling constants.

The INDO method has been modified by Dewar and co-workers²⁷ for computing heats of formation of organic compounds. This modified INDO method is called MINDO, and differs from the INDO method by the electron repulsion integrals and the total energy of the molecules. Detailed MINDO/2 parameters will be also given in the later section. Excellent agreement with experiment for heats of formation and ionization energy of many hydrocarbons have been obtained by MINDO/2 method. Because of their advantages among available semi-empirical methods, MINDO/2 and INDO were chosen for the calculations on macromolecules using the crystal orbital model as described herein.

The series of papers by Ladik and co-workers²⁸ have detailed the application of independent electron crystal orbital theory

in the π -electron approximation, with extensive applications to the calculations to the calculation of π -bands in periodic models of nucleic acids. A parallel series of papers by Andre, Gouverneur and Leroy²⁹ have treated the electronic structure of polyene, polyacene, and graphite from a similar viewpoint.

Studies on polyethylene and poly(tetrafluoroethylene) using crystal orbital theory in the CNDO/2 approximation have been reported by Morokuma.³⁰ Calculations of electronic structures of polyethylene and polyglycine using extended Huckel and CNDO methods have been reported by Fujita and Imamura.³¹ Studies on polyene, polyhydrogen fluoride, and lithium hydride crystals using CNDO method have been reported by Bacon, O'Shea and Santry.³² Calculations using ab initio methods have been reported by Clementi, Andre and Leroy³³ on polyene and polyethylene.

During the progress of this project, studies of polyacetylene, polyethylene, and polyglycine using the crystal orbital theory at the levels of INDO and MINDO/2 was reported by Beveridge and Jano, and Ladik.³⁴ A comparison of ab initio, EHT, and CNDO band structures for polyene and polyethylene was reported by J.M. Andre, G.S. Kapsomenos and G. Leroy.³⁵ A series of papers concerning the electronic structure of periodic protein models have been reported by S. Suhai and J. Ladik.³⁶ These calculations will be described in more detail along with our own results in section II.

The interplay between the theoretical studies on the electronic structure of polymers and the experimental work on properties such as electrical conductivity has to date been very constructive and significant. For example the band gap for a two-dimensional polypeptide network was calculated by Suard-Sender³⁷ to be about 5 ev against an experimental value of about 2.4 ev. This appeared to rule out intrinsic semiconductivity. In reconsideration of the relationship between calculated and observed values it was recognized that the experimental studies of Burnel, Eley and Subramanyan³⁸ was to advance our knowledge of the conduction mechanism in DNA in light of recent theoretical work on the electronic energy structure by Ladik et al. The success of the conformational analyses of polyethylene and polypeptide by quantum mechanical calculations seems to be able to open a new way for the research of conformation of the structure of macromolecules. The comparison of the photoelectron spectrum and crystal orbital calculations of polyethylene by Wood, Barber, and Hillier³⁹ indicates that interpretation of spectra in terms of electronic structure macromolecular systems can be performed macromolecular orbital theory. Further considerations on these points will be presented in subsequent sections of this thesis.

II. Theory and Methodology

The theory and methodology for treating macromolecular systems in the quantum mechanical crystal detailed orbital model were developed especially by Ladik.⁴⁰ In this section we offer a review sufficient for specification of the theory and designation of notation and terms relevant to the discussion in succeeding sections. Consider a system of identical elementary cells in a cyclic array of order N . The electronic structure of the assemblage of polyatomic elementary cells can be described by a product wave function of one-electron crystal spin-orbitals. The spatial part of the spin-orbitals is considered as a linear combination of the atomic orbitals (LCAO) of all atoms contributing to the system,

$$\Psi_{1,p} = N^{-1/2} \sum_{j=0}^{N-1} \sum_{\mu=1}^n c_{1,p,j,\mu} \phi_{\mu}(r - ja) \quad (1)$$

where $\phi_{\mu}(r_A - ja)$ denotes the μ th atomic orbital centered on the A -th atom of the j -th elementary cell, n is the number of orbitals per elementary cell, N is the number of elementary cells and a is the elementary translation in the chain. The crystal orbital indices 1 and p take the values 1 to n and 0 to $N-1$, respectively. For an infinite polymer chain or one-dimensional crystal, $N \rightarrow \infty$ and the determination of linear expansion co-efficients by incorporating Eq. (1) into the Roothaan equations⁴¹ widely used for molecular self-consistent field calculations would be intractable since the matrix eigenvalue problem would be of order infinity.

The problem may be reduced to tractable form by recognizing for large N the infinite or quasi-infinite chain may be replaced with no essential loss of generality by a cyclic chain where the first and N -th elementary cells adjoin. The crystal orbitals are then subject to the Born-von Karman periodic boundary conditions:³

$$\psi_{1p}(r) = \psi_{1p}(r + Na) \quad (2)$$

according to which an orbital must have the same value for arguments differing by exactly N elementary translations. Equation (2) leads directly to the Bloch condition³ on the linear expansion coefficients:

$$C_{j\mu 1p} = \exp(2\pi i j p / N) C_{\mu 1p}. \quad (3)$$

As N becomes arbitrarily large, it is possible to define the wavenumber k accordingly as:

$$k = 2\pi p / N = 2\pi p a / L, \quad (4)$$

which to a first approximation changes continuously from 0 to 2π with L representing the total chain length. Substituting Eqs. (3) and (4) into Eq. (2), the LCAO expansion appropriate for the system reduces to

$$\psi_{1k} = N^{-1/2} \sum_j \sum_{\mu} \exp(ijk) C_{\mu 1k} \phi_{\mu A}(r - ja). \quad (5)$$

As a consequence of the Born-von Karman boundary conditions and the translational symmetry of the chain of elementary cells, the matrices entering a Roothaan-type treatment based on Eq.5 are cyclic hypermatrices, and thus can be unitarily transformed to the blocks are each Hermitian matrices of order n only, with the elements depending parametrically on the wavenumber k . The problem thus reduces to the solution of a complex matrix eigenvalue problem:

$$F'(k) C'(k) = S'(k) C'(k) \epsilon(k). \quad (6)$$

Here $C'(k)$ is a matrix of linear expansion coefficients and $\epsilon(k)$ is a diagonal matrix of orbital energies. The matrix $F'(k)$ of the Hartree-Fock Hamiltonian operator and the overlap matrix reduce further to:

$$F'(k) = \sum_q \exp(ikq) F(q), \quad (7)$$

$$S'(k) = \sum_q \exp(ikq) S(q), \quad (8)$$

where q is a running index over all unit cells. Thus the matrices $F'(k)$ and $S'(k)$ involve interactions within an elementary cell ($q=0$) as well as intercell interactions ($q \neq 0$).

Since intercell interactions are expected to fall off rapidly with distance, it is customary to use abridged forms of Eqs (7) and (8) including only nearest neighbor interactions

explicitly, i.e. restricting the summation over q to intra-cell ($q = 0$) and first neighbor ($q = \pm 1$) interactions.

Then

$$F'(k) = F(0) + \exp(ik) F(1) + \exp(-ik) F(-1), \quad (9)$$

and similarly for $S'(k)$. The elements $F_{\mu_0 \nu_q}$ of $F(q)$ in the nearest neighbor approximation are

$$F_{\mu_0 \nu_q} = H_{\mu_0 \nu_q} + \sum_{s,t=-1, (s-t) \neq 2} \sum_{\lambda_s \sigma_t} P_{\lambda_s \sigma_t}^{(s-t)} \times (u_0 \nu_q | \lambda_s \sigma_t) - 1/2 (u_0 \sigma_t | \nu_q \lambda_s), \quad (10)$$

where $(s-t)$ is a superscript label (not an exponent),

$$H_{\mu_0 \nu_q} = \int \phi_{\mu_0}^*(1) \left\{ -1/2 \nabla^2 - \sum_{s=-1}^1 \sum_A \left(\frac{Z_A}{|R_{1A} - R_A^s|} \right) \right\} \phi_{\nu_q}(1) d\tau_1 \quad (11)$$

and

$$(u_0 \nu_q | \lambda_s \sigma_t) = \iint \phi_{\mu_0}^*(1) \phi_{\nu_q}(1) r_{12}^{-1} \phi_{\lambda_s}^*(2) \phi_{\sigma_t}(2) d\tau_1 d\tau_2. \quad (12)$$

The elements $P_{\lambda_s \sigma_t}^{(s-t)}$ of the charge density - bond order matrices are obtained by numerical integration over the wave-number k ,

$$P_{\lambda_s \sigma_t}^{(s-t)} = (2\pi)^{-1} \int_0^2 P_{\lambda_s \sigma_t}^{(s-t)}(k) \exp[i(s-t)k] dk, \\ = \pi^{-1} \text{Re} \left\{ \int_0^\pi P_{\lambda_s \sigma_t}^{(s-t)}(k) \exp[i(s-t)k] dk \right\}, \quad (13)$$

where

$$P_{\lambda_s \sigma_t}^{(s-t)}(k) = 2 \sum_{l=1}^{\text{nocc}} C_{\lambda_s}^{l-1}(k) C_{\sigma_t}^{l-1}(k). \quad (14)$$

(14)

The computational procedure involved is quite analogous to matrix Hartree-Fock methods, with an initial guess at the n^2 elements of P used to generate a first F' matrix, diagonalization of the F' matrix for eigenvector matrices which are in turn used to construct a refined guess at P and a new F' . The process is repeated until the change in P on successive iterations is within a certain prescribed tolerance level. For each such iteration through the Hartree-Fock circuitry, the F' matrix is constructed and diagonalized for several values of the wavenumber k , generating $C(k)$. The evaluation of P by Eq. (13) at the end of each cycle is accomplished by numerical integration over k . The energy band structure of the system is specified by the extremums of $\epsilon_1(k)$ for each band l .

The $F'(k)$ matrices are Hermitian complex,

$$F' = F^r + iF^i, \quad (15)$$

where using Euler's relation $\exp(ik) = \cos k + i \sin k$

$$F^r = F(0) + [F(1) + F(-1)] \cos k, \quad (16)$$

and

$$F^i = F(1) - F(-1) \sin k. \quad (17)$$

With the real and imaginary parts of the crystal orbital Hartree-

Fock matrix expressed in this form, solution of the matrix eigenvalue problem in complex space is accomplished by numerical methods elaborated in Ref. 42.

The electronic energy per cell in the nearest neighbor approximation is given by the expression

$$E_{\text{electronic}} = E(0) + E_{\text{core}}(1) + E(-1), \quad (18)$$

where

$$E(q) = 1/2 \sum_{\mu_0 \nu_q}^P (\mu_0 \nu_q | H | \mu_0 \nu_q + F | \mu_0 \nu_q | \mu_0 \nu_q). \quad (19)$$

The total energy of the system per elementary cell is the sum of electronic energy and nuclear repulsion energy E_{core} , given by

$$E_{\text{core}} = E_{\text{core}}(0) + E_{\text{core}}(1), \quad (20)$$

where

$$E_{\text{core}}(q) = \sum_A^0 \sum_{B(\neq A_0)}^q Z_A Z_B Z_{AB}^{-1}, \quad (21)$$

where Z_A and Z_B are the core charges of atoms A and B respectively and R_{AB} is the internuclear separation. The summation \sum_B^q refers to all atoms B in cell q.

The end result of a crystal orbital calculation is thus the orbital energies $\mathcal{E}(k)$ as a function of the wavenumber k , the LCAO-CO coefficients $C(k)$ defining the electronic wavefunction, and the crystal orbital density matrix P . The $\mathcal{E}(k)$ determine the energy band structure of the system, from which the band widths and density of states function may be derived. Excitation energies in this formalism are calculated directly from the difference between the top of the highest filled band and the bottom of the lowest empty band, since the macromolecular coulomb and exchange integrals vanish as $N \rightarrow \infty$ ^{23d}. The P matrix may be subjected to an electron population analysis completely analogous to that suggested for molecules by Mulliken.⁴³

With the theory and methodology of the calculation of crystal wave functions thus specified, we now turn to general considerations on the calculation of macromolecular properties from the wave function. Of specific interest herein will be the electronic energy band structure, related electrical properties of the system, photoelectron spectral characteristics, and conformational stability.

When a system can be described in terms of the motion of electrons in a one-dimensional periodic potential, the wave functions of the electrons are characterized by the wave number k , equivalent to the electron momentum. The energy of the electron is a continuous function of the wave number k . The range of $\mathcal{E}(k)$ with respect to k defines an energy band for an electron.

In a many electron system, a manifold of energy bands develops due to quantization. The energy bands may be occupied or unoccupied (virtual). The band gap between bands occupied and unoccupied at 0° K and the respective band shapes define theoretical values for the intrinsic electrical conductivity of the macromolecular system.

An intrinsic semiconductor is characterized by a relatively small band gap. At normal temperatures, some electrons are thermally excited to levels in the conduction band, creating conduction electrons and so-called "holes" in the valence band. In the presence of an applied electric field, the electrons at the top of a conduction band move in the opposite direction of the field, while the holes move in the direction of the field, since they have negative and positive effective mass respectively. The total conductivity of a semiconductor can be calculated in terms of the motion of electrons and holes. The equation derived for intrinsic conductivity is⁴⁴

$$\sigma_0 = \frac{16}{3} \frac{KTe^2L}{h^3} \left(m_e^{*1/4} m_h^{*3/4} + m_e^{*3/4} m_h^{*1/4} \right) \quad (22)$$

where m_e^* and m_h^* are the effective mass of the electrons and holes respectively, e is the electronic charge, h is Plank's constant, and L is the mean free path of a charge carrier, taken to be the spacing between elementary cell.

The effective mass of a carrier in a semiconductor is evaluated from the curvature of the conduction band (for electrons)

or valence band (for holes) at the band edge. For an electron in free space,⁴⁵ $\mathcal{E}(k)$ is proportional to k^2 according to the equation

$$\mathcal{E}(k) = \frac{(\hbar k)^2}{2m^*} \quad (23)$$

For electrons in the conduction band, $\mathcal{E}(k)$ can be expressed as

$$\mathcal{E}(k) = \mathcal{E}_v + \frac{(\hbar k)^2}{2m^*} \quad (24)$$

where \mathcal{E}_v is the energy of carriers at the conduction band edge. The quantity \mathcal{E}_v is customarily set to zero, i.e. referred to a condition of zero average kinetic energy. Then the motion of the carrier in a periodic lattice just is analogous to that of a free electron, except the mass m is replaced by the effective mass m^* . From equation (3), the equation for effective mass of carriers is

$$m^* = \hbar^2 \left(\frac{\partial^2 \mathcal{E}(k)}{\partial k_x^2} \right)^{-1}_{k=0} \quad (25)$$

A similar expression can be obtained for the effective mass of holes. Equation (4) can be evaluated by numerical methods. In most semiconductors m^* for electrons is considerably smaller than the free electron mass. The conductivity (σ) of a semiconductor can be calculated by the equation⁴⁴

$$\sigma = \sigma_0 e^{-E/2KT} \quad (26)$$

where σ_0 is the intrinsic conductivity, E is the energy band gap, K is Boltzmann's constant and T is the absolute temperature.

The orbital energies of a molecule or energy band structure of a crystal can be directly studied in principle by photoelectron spectroscopy.⁴⁶ In this technique, electron ionization is induced by vacuum ultra violet radiation. It is thus concerned with the ejection of electrons from valence orbitals of the system. This information is obtained by measuring the experimental ionization potentials, which are most closely related to the energy of the molecular orbitals. According to the Einstein's photoelectric equation,⁴⁷ the kinetic energy E_i of a photoelectron released from the i th highest occupied orbital is given in terms of the impacting photon frequency, ν , by

$$E_i = h\nu - I_i \quad (27)$$

where h is Planck's constant, I_i is the relevant ionization potential, In photoelectron spectroscopy ν and h are known. E_i is found from the spectrum, and thus the ionization potentials I_i 's are obtained. The most energetic photoelectron corresponds to the lower ionization potential, and is therefore responsible for the highest observed band in the photoelectron spectrum. Photoelectrons with lower kinetic energies correspond to the ionizations from deeper molecular orbitals (higher ionization potentials). A photoelectron spectrum is effectively a distribution curve of the energies of electrons emitted from a molecule by the action of monochromatic radiation. Koopman's⁴⁸ theorem equates the ionization potential with the negative of

the Hartree-Fock orbital energy, and thus the photoelectron spectrum of a molecule is related to the orbital energy level diagram.

Molecular orbital theory has already been of great help in the interpretation of photoelectron spectra, and the use of macromolecular orbital theory to interpret photoelectron spectra of polymers is an important potential application of the theory. This problem is taken up in more detail for polyethylene in chapter V.

The conformation stability of the system can be determined from the variation in the total energy with geometry. The total energy can be considered as a function of the $3n-6$ normal coordinates Q_i of the system.

$$E = E (Q_1, Q_2, \dots, Q_{3n-6}) \quad (28)$$

The geometries corresponding to the global and local minima in this function specify the theoretically stable conformations of the macromolecule. In practice, calculations are usually carried out with respect to one or two critical internal coordinates of the system. The calculated total energy of the system per unit cell can be partitioned into electronic energy E_{ele} and nuclear repulsion energy E_{core} both contributed from the original and neighboring cells. The expression for E_{ele} and E_{core} can be found through equation 18 to 21 in section II.

III. Factor group analysis of macromolecular orbital

The symmetry of a linear polymer can be described in terms of line groups. A line group is a one-dimensional space group.⁴⁹ There are two types of special symmetry operations in an infinite chain-like molecules: the reflection symmetry with respect to the plane passing through the center of the chain, and the translational operation throughout the chain. When the infinite or quasi-infinite chain is replaced by a cyclic chain where the first and the N-th elementary cells adjoin, the translational operation in an infinite linear chain becomes an infinitesimal rotational operation with respect to the center of the N-side polygon. Each unit is rotated by an infinitesimal angle of $2\pi/N$, where N is a very large number. The reflection operation with respect to the plane passing through the center of the chain becomes a reflection operation in a plane perpendicular to the plane of the infinite polygon passing through the center of the polygon and one of its atoms. Besides the translational and reflection operations characterizing the chain, there are also a point symmetry operation characterizing each individual unit cell. If there are H symmetry elements in each individual unit cell, then the order of symmetry in this line group is $2NH$, while the $2N$ translational operation form a self-conjugate subgroup of the line group. The translational group has H nonequivalent cosets which form the factor group of the line group. The factor group elements $ET, R_2T, \dots, R_H T$ are sufficient to characterize a

line group, where E, R_2, \dots, R_H are the elements of the point group. This is because of the factor group is independent of the order of the translational group. Therefore, no matter whether the line group is finite or infinite, it has the same factor group. The factor group of a line group is always isomorphous with a point group and therefore has the same character table.

The next thing to formulate is a systematic procedure for the symmetry classification of a linear macromolecules based on the factor group analysis. This procedure is analogous to the procedure given by Cotten⁵⁰ for point groups. Since there are almost no incidence of $T, T_h, T_d, O, O_h, I, I_h$ in linear infinite chain liked polymers, therefore, we can forget about those special groups and follow the following sequence of steps to find a correct classification.

1. Determine whether or not the molecule has any point symmetry operations plus screw rotation and glide reflection. If any are found, we proceed to step 5. If only the point symmetry operations are found, and the atoms in a unit cell is linear, it can belong to group $D_{\infty h}$ and $C_{\infty v}$, depending on whether it has a center of symmetry or not.
2. We next look to see if there is an n-fold rotational axis C_n . If so, we proceed to step 3, if not, it can belong to $C_i, C_s,$ or C_1 . Then we look for a center of symmetry. If any is found, it can belong to group C_i . If we find a plane of symmetry instead of a center of inversion, it can belong to the group C_s . If none of any symmetry elements can be found, it must be belong to the group C_1 .
3. When a rotational axis C_n is present, we must look for whether there is a two-fold axis C_2 perpendicular to it. If so, we proceed to step 4. Otherwise, the symmetry described by the groups generated by C_n .

If there are not any symmetry elements except the identity and n fold rotational axis, the system belongs to the group C_n . If in addition to these two elements, there is also a horizontal plane and an inversion center, the molecule can belong to the factor group C_{nh} . If there is no center of inversion, but instead there is a set of vertical planes perpendicular to the C_n rotational axis and also to the horizontal plane, the molecule can belong to the symmetry group C_{nv} .

4. In addition the C_n rotational axis, there are a set of C_2 rotational axis perpendicular to the C_n axis, but there is no other symmetry elements, the molecule can belong to symmetry group $D = V$. If we still can find a center of inversion and a set of planes of symmetry, the molecule can belong to the $D_{2h} = V_h$ group.

5. In addition to the point symmetry operations, the molecule also possesses a screw rotations and glide reflection operations, the classification should follow the following steps: first we look for screw rotational operations. If found, we proceed to step 6, if not, the molecule can belong to the group C_s if it possesses a plane of glide reflection.

6. If a molecule possesses a screw rotation C_n , then we look for whether there is two-fold rotational axis perpendicular to it. If so, we proceed to step 7. If not, the molecule can belong to the group C_n , if there are no other additional elements. Next, we look for a horizontal plane of symmetry. If found, the molecule can belong to the group C_{nh} or C_{nv} depending on whether the molecule has a center of inversion or a glide reflection plane.

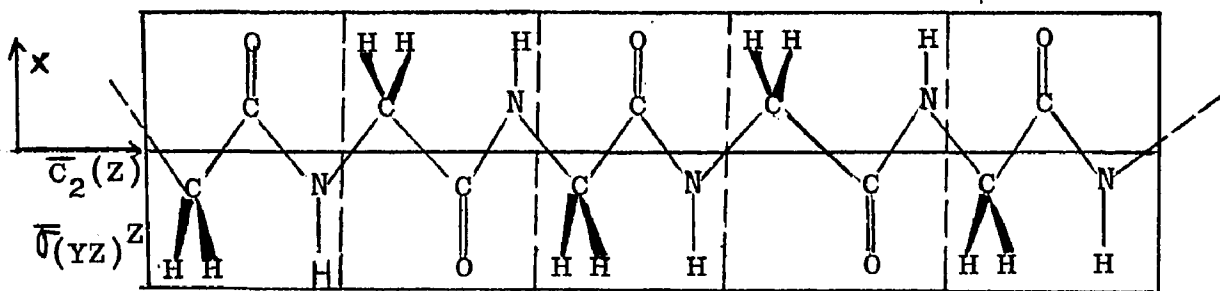
7. At last, if a molecule has a screw rotational axis and also a two-fold rotational axis perpendicular to it, the molecule can belong to

the group $D=V$ or D_{2h} , depending on whether the molecule has a horizontal plane of symmetry and a set of glide reflection planes.

The steps of sequences of systematic classification of groups can be summarized in the table 1. The symbols in this table are defined as follows (the Chain axis coincides with the z-axis of a coordinate system).

- E identity operation
- σ_h reflection at the xy plane
- σ_v^1 reflection at a plane parallel to the z-axis
- σ_v^2 reflection at the yz-plane
- σ_v^3 reflection at the xz-plane
- C_n rotational around the z-axis by the angle $k360/n$, where $k=1, 2, \dots, p^{-1}$
- C_2^1 rotation around the z-axis by 180°
- C_2^2 rotation around y-axis by 180°
- i inversion at a center
- σ_v^1 glide reflection at the yz-plane along the z-axis
- σ_v^2 glide reflection at the xz-plane along the z-axis
- C_n screw rotation around the z-axis by the angle $k360/n$, where $k=1, 2 \dots p^{-1}$

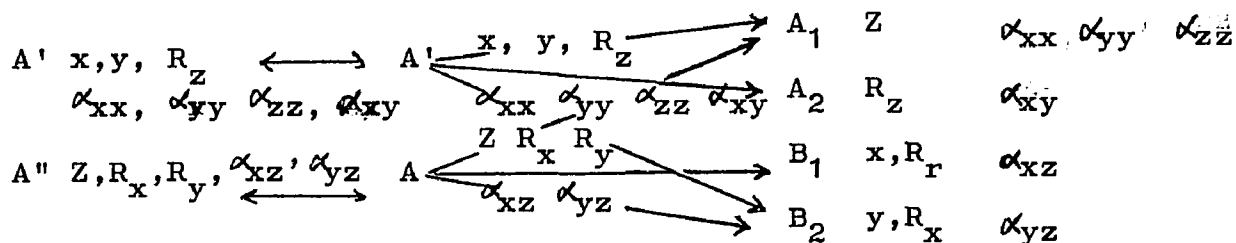
Planar polyglycine - $(C_2H_3O N)_n$ -



Isolated molecule (Factor group)	Site group	planar polyglycine
-------------------------------------	------------	-----------------------

C_s	C_s	C_{2v}
Symmetry elements	Symmetry elements	Symmetry elements
E, $\sigma(x,z)$	E, $\sigma(x,z)$	E, $\sigma(xz)$, $\sigma(y,z)^{*1}$, $C_2(z)^{*2}$

Characters



Correlation Diagram of planar polyglycine

- *1. two fold screw rotation along the chain
- *2. glide reflection at YZ plan along the Zaxis

IV. Approximate Macromolecular Orbital Theory:

Quantum theoretical calculations on the electronic structure of molecules based on matrix self-consistent field (SCF) methods increase in size as $\sim n^4$, where n is the number of atomic orbitals included in the LCAO expansion. Thus detailed studies of large molecules, not to mention polymers, often require vast amounts of computer time. In view of this, considerable research effort in recent years has been directed towards the development of computationally rapid approximate LCAO-SCF schemes suitable for large molecules. The general approach has been to systematically neglect some polycenter electron repulsion integrals and introduce estimates based on experimental data for others. The more recent procedures, such as the CNDO²⁰ method, the PND⁵¹ method, and the INDO²⁶ and MINDO²⁷ methods treat all valence electrons explicitly and have been somewhat successful in accounting for a variety of molecular properties. Any of them can be adapted for macromolecular orbital calculations, and as we have been mentioned in chapter II, concurrently with the research described herein, the CNDO method has been applied to macromolecular orbital calculations by a number of authors.^{31,32} The CNDO method has been shown to give generally good molecular geometries and electric dipole moments. The INDO method is a modified CNDO procedure which accomodates nuclear spin coupling constants and hyperfine copling constants.²³ Ionization potentials and heats of formation are computed by the CNDO and INDO methods are

uniformly too high.²³ Ionization energies in a molecular orbital theory are related to orbital energies by Koopman's theorem,⁴⁸ and in macromolecular orbital calculations to the energy band structure. Thus the INDO macromolecular orbital calculation might be satisfactory for geometry but unsatisfactory for electronic energy bands. A modification of INDO which gives improved agreement with experimental results of ionization and electron affinity has been developed by Dewar and is called MINDO.²⁷ Thus the INDO and MINDO/2 are chosen for the macromolecular orbital calculations in this project.

Formalism and Parameters for INDO and MINDO/2. In going from the exact formulation to the approximate form characteristic of INDO level approximate self-consistent field theory, the basis functions ϕ_μ are restricted to valence orbitals centered on the atoms in the elementary cell, and the macromolecular orbitals are calculated for the motion of valence electrons in the field of non-polarizable cores constituted of atomic nuclei and inner shell electrons. The details of the reduction are completely analogous to the reduction of the Roothaan equations to the INDO level described by Pople, Beveridge and Dobosh,²⁶ wherein atomic integrals are approximated with expressions involving semiempirical parameters. The principal approximation is the neglect of differential overlap in polycentric electron repulsion integrals. With the neglect of overlap, Eq. 6 in Chapter II reduces to

$$F'(k) C'(k) = C'(k) \mathcal{E}(k) \quad (29)$$

and the elements of $F_{\mu_0\mu_0}$ are given by

$$F_{\mu_0\mu_0} = U_{\mu_0\mu_0} + \sum_{\sigma}^A P_{\sigma\sigma} (\mu_0\mu_0 | \sigma_0\sigma_0) - 1/2 (\mu_0\sigma_0 | u_0\sigma_0) \quad (30)$$

$$+ \sum_{t=-1}^1 \sum_{B \neq A_0} (P_{B_t B_t} - Z_{B_t}) Y_{A_0 B_t},$$

where $U_{\mu_0\mu_0}$ is a one center atomic core integral, $Y_{A_0 B_q}$ is a two center atomic coulomb integral over valences orbitals centered on atoms A and B. Furthermore,

$$F_{\mu_0\nu_0} = P_{\mu_0\nu_0} \left[3/2 (\mu_0\nu_0 | \mu_0\nu_0) - 1/2 (\mu_0\mu_0 | \nu_0\nu_0) \right], \quad (31)$$

and

$$F_{u_0\nu_q} = H_{\mu_0\nu_q} - 1/2 P_{\mu_0\nu_q} Y_{A_0 B_q}, \quad \mu_0 \in A, \nu_q \in B. \quad (32)$$

The diagonal two center core matrix elements are

$$H_{\mu_0\mu_0} = U_{\mu_0\mu_0} - \sum_{q=1}^1 \sum_{B(\neq A_0)} Z_B Y_{A_0 B_q} \quad (33)$$

and the off diagonal two center core matrix elements are calculated by

$$H_{\mu_0\mu_q} = 1/2 (\beta_A^0 + \beta_B^0) S_{\mu_0\mu_q}, \quad (34)$$

where the β_A^0 and β_B^0 are empirical parameters, and their values are given in table I. $S_{\mu_0\mu_q}$ is the overlap integral

matrix elements computed over Slater orbitals with Slater exponents, and the remaining atomic integrals are assigned on the basis of values derived from atomic spectra. The detail calculations of the integrals are given by Pople and Beveridge.⁵¹ Using the notation of Slater,⁵² and assuming 2s and 2p orbitals to have the same radial parts, we may write the nonvanishing integrals.

$$(ss | ss) = (ss | xx) = F^0 = \gamma_{AA} \quad (35)$$

$$(sx | sx) = 1/3 G^1 \quad (36)$$

$$(xy | xy) = 3/25 F^2 \quad (37)$$

$$(xx | xx) = F^0 + 4/25 F^2 \quad (38)$$

$$(xx | yy) = F^0 - 2/25 F^2 \quad (39)$$

and similar expression for $(ss | zz)$, etc. The Slater-Condon parameters F^0 , G^1 , and F^2 are two-electron integrals involving the radial parts of the atomic orbitals. The values of those parameters are given in table II A and II B.

The core integrals U_{ufl} are

Hydrogen

$$-1/2 (I + A)_s = U_{ss} + 1/2 \gamma_{HH} \quad (40)$$

Lithium

$$-1/2 (I + A)_s = U_{ss} + 1/2 F^0 \quad (41)$$

$$-1/2 (I + A)_p = U_{pp} + 1/2 F^0 - 1/12 G^1 \quad (42)$$

Beryllium

$$-1/2 (I + A)_s = U_{ss} + 3/2 F^0 - 1/12 G^1 \quad (43)$$

$$-1/2 (I + A)_p = U_{pp} + 3/2 F^0 - 1/4 G^1 \quad (44)$$

Boron to Flourine

$$-1/2 (I + A)_s = U_{ss} + (Z_A - 1/2)F^0 - 1/6(Z_A - 3/2)G^1 \quad (45)$$

$$-1/2 (I + A)_p = U_{pp} + (Z_A - 1/2)F^0 - 1/3G^1 - 2/25(Z_A - 5/2)F^2 \quad (46)$$

The MINDO/2 method involved modification of the $\beta_{u_o \nu_q}$ formulation to

$$\beta_{u_o \nu_q} = B (I_u + I_\nu) S_{u_o \nu_q} \quad (47)$$

where I_μ is a valence state ionization potential of ϕ_μ , and modification of the core repulsion expression to

$$E_{core}^e(q) = \sum_A^o \sum_{B(\neq A_o)}^q Y_{A_o B_q} + (Z_A Z_B R_{AB}^{-1} - Y_{A_o B_q}) \exp(-\alpha R_{AB}) \quad (48)$$

and evaluation of electron repulsion integrals by the formula

$$Y_{A_o B_q} = R_{A_o B_q}^2 + (\rho_A + \rho_B)^2 - 1/2 \quad (49)$$

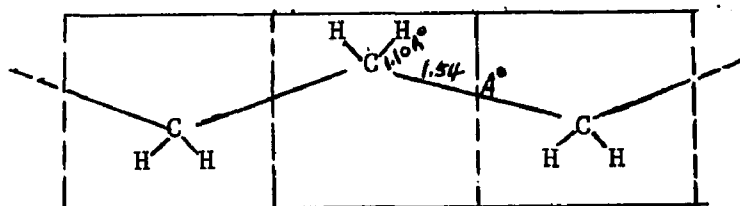
where

$$\rho_A = .26459 / Y_{AA} \quad ; \quad \rho_B = 0.26459 / Y_{BB} \quad (50)$$

The disposable parameters α and β were chosen by least squares refinement techniques. Numerical values for the parameters are given in Table III.

The INDO and MINDO versions of macromolecular orbital theory were programmed for the CDC 6600 digital computer and the program listing and test calculation are given as Appendix I. The full details of the test calculation are given below.

SCF-MMO (INDO) Test Calculation for Polyethylene: To carry out a calculation of the energy band structure of polyethylene, one must first specify the position of the atoms in the elementary cell. The geometry chosen for the test calculation is as follows:



Coordinates of atoms

No. of atom	Symbol	X	Y	Z
1	C	0.00000000	0.00000000	0.00000000
2	H	0.00000000	0.00000000	1.10000000
3	H	1.03708994	0.00000000	-.36666667
4	C	-.72596298	-1.25740472	-.51333334
5	H	-1.68797558	-.96810387	-.96148150
6	H	-.19985346	-1.64986001	-1.39604939

The atomic orbital basis set is the valence orbitals of the constituent atoms in a unit cell. They are $2s$, $2p_x$, $2p_y$, and $2p_z$ Slater functions on each carbon, and $1s$ on each hydrogen atom. The following functions are used for testing the calculation.

Carbon:

$$\phi_1 = \phi (C; 2s) = \left(\frac{5}{3\pi} \right)^{1/2} r \exp \left(- \int_2 r \right)$$

$$\phi_2 = \phi (C; 2p_x) = \left(\frac{5}{\pi} \right)^{1/2} x \exp \left(- \int_2 r \right)$$

$$\phi_3 = \phi(C; 2p_y) = \left(\frac{\zeta_2^5}{\pi} \right)^{\frac{1}{2}} y \exp(-\zeta_2 r) \quad (50)$$

$$\phi_4 = \phi(C; 2p_z) = \left(\frac{\zeta_2^5}{\pi} \right)^{\frac{1}{2}} z \exp(-\zeta_2 r)$$

Hydrogens:

$$\phi_5 = \phi(H_1; 1s) = \left(\frac{\zeta_3^3}{\pi} \right)^{\frac{1}{2}} \exp(-\zeta_3 r) \quad (51)$$

$$\phi_6 = \phi(H_2; 1s) = \left(\frac{\zeta_3^3}{\pi} \right)^{\frac{1}{2}} \exp(-\zeta_3 r)$$

The values of the exponents are chosen according to Slater's rules so that

$$\begin{aligned} \zeta_1 &= 8.7 \\ \zeta_2 &= 2.6 \\ \zeta_3 &= 1.0 \end{aligned} \quad (52)$$

Using these functions, we may calculate the zero cell overlap and coulomb integrals using formulae given in Ref. 42. The results are:

$$S_{\mu\nu}^0 = \begin{bmatrix} 1.0000 & 0.0000 & 0.0000 & 0.0000 & 0.5133 & 0.5133 \\ 0.0000 & 1.0000 & 0.0000 & 0.0000 & 0.0000 & 0.4577 \\ 0.0000 & 0.0000 & 1.0000 & 0.0000 & 0.0000 & 0.0000 \\ 0.0000 & 0.0000 & 0.0000 & 1.0000 & 0.4855 & -0.1618 \\ 0.5133 & 0.0000 & 0.0000 & 0.4855 & 1.0000 & 0.1805 \\ 0.5133 & 0.4577 & 0.0000 & -0.1618 & 0.1805 & 1.0000 \end{bmatrix} \quad (53)$$

$$Y_{AB}^0 = \begin{bmatrix} 0.5903 & 0.4317 & 0.4317 \\ 0.4317 & 0.7500 & 0.2920 \\ 0.4317 & 0.2920 & 0.7500 \end{bmatrix} \quad (54)$$

The intercell and coulomb overlap integral matrices are:

$$S_{\mu\nu}^+ = \begin{pmatrix} 0.3404 & 0.1721 & -0.2981 & 0.1217 & 0.1161 & 0.1161 \\ -0.1712 & 0.0762 & 0.2005 & -0.0819 & -0.1149 & -0.0473 \\ 0.2981 & 0.2005 & -0.1554 & 0.1418 & 0.0820 & 0.0820 \\ -0.1217 & -0.0819 & 0.1418 & 0.1340 & -0.0096 & -0.1052 \\ 0.1161 & 0.0473 & -0.0820 & 0.1052 & 0.0601 & 0.0226 \\ 0.1161 & 0.1149 & -0.0820 & 0.0096 & 0.0226 & 0.0601 \end{pmatrix} \quad (55)$$

$$Y_{AB}^+ = \begin{pmatrix} 0.3313 & 0.2430 & 0.2430 \\ 0.2430 & 0.2116 & 0.1719 \\ 0.2430 & 0.1719 & 0.2116 \end{pmatrix} \quad (56)$$

Using equations 33, 34, 40, 45, 46 and the Slater-Condon parameters listing in table II, the 6 x 6 core hamiltonian matrices H_{μ}^0 of the zero-cell can be calculated as follows:

$$H_{\mu\nu}^0 = \begin{pmatrix} -6.9568 & 0.0000 & 0.0000 & 0.0000 & -0.2830 & -0.2830 \\ 0.0000 & -6.6466 & 0.0000 & 0.0000 & 0.0000 & -0.2523 \\ 0.0000 & 0.0000 & -6.6466 & 0.0000 & 0.0000 & 0.0000 \\ 0.0000 & 0.0000 & 0.0000 & -6.6466 & -0.2676 & 0.0892 \\ -0.2830 & 0.0000 & 0.0000 & -0.2676 & -5.3691 & -0.0597 \\ -0.2830 & -0.2523 & 0.0000 & 0.0892 & -0.0591 & -5.3691 \end{pmatrix} \quad (57)$$

The intercell 6 x 6 two center core hamiltonian matrices are calculated by Equation 34.

$$H_{\mu\nu}^+ = \begin{pmatrix} -0.2627 & -0.1328 & 0.2300 & -0.0939 & -0.0640 & -0.0640 \\ 0.01328 & -0.0588 & -0.1548 & 0.0632 & 0.0633 & 0.0261 \\ -0.2300 & -0.1548 & 0.1199 & -0.1094 & -0.0452 & -0.0452 \\ 0.0939 & 0.0632 & -0.1094 & -0.1035 & 0.0580 & 0.0580 \\ -0.0640 & -0.0261 & 0.0452 & -0.0580 & -0.0199 & -0.0075 \\ -0.0640 & -0.0633 & 0.0452 & -0.0053 & -0.0075 & -0.0199 \end{pmatrix} \quad (58)$$

Let us consider the sequence of events on typical iteration of the Hartree-Fock circuitry. Suppose a wave function is available from the previous cycle in the form:

$$\begin{pmatrix} \psi_1 \\ \psi_2 \\ \psi_3 \\ \psi_4 \\ \psi_5 \\ \psi_6 \end{pmatrix} = \begin{bmatrix} \text{Matrices of real} \\ \text{part coefficient } C^r \end{bmatrix} + \begin{bmatrix} \text{Matrices of imaginary} \\ \text{part coefficient } C^i \end{bmatrix} \begin{pmatrix} 1 \\ 2 \\ 3 \\ 4 \\ 5 \\ 6 \end{pmatrix} \quad (59)$$

The calculation of the density matrix by eight point Gaussian numerical integration goes as follows, based on the procedure described by Nielsen⁵³. For an Gaussian integration of a function $f(x)$ over an upper and lower bound a and b ;

$$I = \int_a^b f(x) dx \quad (60)$$

with an interval transformation:

$$x = \frac{1}{2} (b-a) v + \frac{1}{2} (a+b) \quad (61)$$

in our case we have $b = \pi$, $a = 0$. Therefore we have a linear transformation

$$\begin{aligned} x &= \frac{1}{2} (\pi - 0) v + \frac{1}{2} (\pi + 0) \\ dx &= \frac{\pi}{2} dv \\ I &= \int_a^b f(x) dx = \frac{b-a}{2} \int_{-1}^{+1} \varphi(v) dv = \frac{\pi}{2} \sum \epsilon_i \varphi_i(v_i) \end{aligned} \quad (62)$$

In comparison with equation 13

$$\begin{aligned}
 V_i &= K_i \\
 \varphi_i(V_i) &= P_{\lambda_s}^{(s-t)} \sigma_t(k_i) \\
 &= 2 \sum_{l=1}^s C_{\lambda_s l}(k_i) C_{\sigma_t l}(k_i)
 \end{aligned} \tag{63}$$

In an 8 point Gaussian numerical integration, for $k = 0$, 0.06237655 and $g_1 = 0.1012$, the real part coefficient of the wave function are:

$$\text{CR} = \begin{bmatrix} -0.8374 & -0.0000 & -0.0743 & -0.4247 & 0.0000 & 0.0318 \\ -0.0824 & 0.4491 & 0.1863 & -0.1113 & 0.1714 & 0.0806 \\ -0.0264 & 0.0000 & 0.1471 & -0.4220 & 0.0000 & -0.1173 \\ -0.0582 & -0.6351 & 0.1317 & -0.0787 & -0.2424 & 0.0570 \\ -0.3524 & -0.4234 & 0.0555 & 0.5378 & 0.2727 & -0.0299 \\ -0.3524 & 0.4234 & 0.0555 & 0.5378 & -0.2727 & -0.0299 \end{bmatrix} \tag{64}$$

The imaginary part of the coefficient of the wave function are:

$$\text{CI} = \begin{bmatrix} -0.1677 & 0.0000 & 0.2587 & -0.0882 & 0.0000 & -0.0948 \\ -0.0256 & 0.0874 & -0.6096 & -0.0302 & -0.3077 & -0.4828 \\ 0.0045 & 0.0000 & -0.4750 & -0.0840 & 0.0000 & 0.7437 \\ -0.0181 & -0.1230 & -0.4310 & -0.0214 & 0.4351 & -0.3414 \\ -0.0721 & -0.0824 & -0.1798 & 0.1189 & -0.4895 & 0.1760 \\ -0.0721 & 0.0824 & -0.1798 & 0.1189 & 0.4895 & 0.1760 \end{bmatrix} \tag{65}$$

The corresponding coefficient of the wave function for different wave vector k 's are listed in the appendix. The calculated value of the first diagonal element of the density matrix can be summarized as the following:

$$\begin{array}{llll}
 k_1 = 0.062477 & P_{11}(k_1) = 0.3509 & \varepsilon_1 = 0.1012 & P_{11}(k_1)\varepsilon_1 = 0.0355 \\
 k_2 = 0.3194 & P_{11}(k_2) = 0.3557 & \varepsilon_2 = 0.2224 & P_{11}(k_2)\varepsilon_2 = 0.0791 \\
 k_3 = 0.7453 & P_{11}(k_3) = 0.3787 & \varepsilon_3 = 0.3139 & P_{11}(k_3)\varepsilon_3 = 0.1188 \\
 k_4 = 1.2827 & P_{11}(k_4) = 0.4400 & \varepsilon_4 = 0.3627 & P_{11}(k_4)\varepsilon_4 = 0.1596 \\
 k_5 = 1.8589 & P_{11}(k_5) = 0.5796 & \varepsilon_5 = 0.3627 & P_{11}(k_5)\varepsilon_5 = 0.2102 \\
 k_6 = 2.3963 & P_{11}(k_6) = 0.6587 & \varepsilon_6 = 0.3137 & P_{11}(k_6)\varepsilon_6 = 0.2066 \\
 k_7 = 2.8222 & P_{11}(k_7) = 0.6459 & \varepsilon_7 = 0.12224 & P_{11}(k_7)\varepsilon_7 = 0.1437 \\
 k_8 = 3.0792 & P_{11}(k_8) = 0.6979 & \varepsilon_8 = 0.1012 & P_{11}(k_8)\varepsilon_8 = 0.0706
 \end{array}
 \tag{66}$$

The first diagonal element of the charge density matrix is calculated by the following equation

$$P_{11}^0 = \sum_i P_{\downarrow\downarrow}(k_i)g_i = 1.0991 \tag{67}$$

The other elements of the same matrix are calculated in the same way.

The final density matrix for zero cell are obtained as below:

$$P_{\mu\nu}^0 = \begin{bmatrix} 1.0991 & -.0771 & -.0026 & -.0545 & .04630 & .4630 \\ -.0771 & .9876 & .0576 & .0383 & -.0452 & .7433 \\ -.0026 & .0576 & .8852 & .0407 & .2011 & .2011 \\ -.0545 & .0383 & .0407 & .9605 & .8044 & -.3107 \\ .4630 & -.0452 & .2011 & .8044 & 1.0338 & -.0328 \\ -.4630 & .7433 & .2011 & -.3107 & -.0328 & 1.0338 \end{bmatrix} \tag{68}$$

The charge density matrix of the neighboring cell is calculated in the same way as the P⁰, but has to be multiplied by a factor exp(i(s-t)k). This matrices are

$$P_{\mu\nu}^+ = \begin{bmatrix} .3139 & -.2205 & .1403 & -.1559 & .0131 & .0131 \\ .0157 & .1554 & .2632 & -.0143 & .0222 & .0341 \\ -.4667 & .4743 & -.2643 & .3354 & .0080 & .0080 \\ .0111 & -.0143 & .1861 & .1655 & .0283 & .0115 \\ -.0168 & -.0369 & .0225 & -.0133 & -.1852 & -.0096 \\ -.0168 & -.0250 & .0225 & -.0303 & -.0096 & -.1852 \end{bmatrix} \tag{69}$$

The diagonal elements of the Hartree-Fock zero cell matrices are calculated by equation 30, where $P_{B_t B_t}$ is the electronic density of atom B at the location in the t cell. For this particular example of polyethylene, the diagonal elements of Hartree-Fock matrices for hydrogen and carbons are

$$\begin{aligned}
 & \qquad \qquad \qquad t=0 \quad B \text{ atom} \quad C \text{ atom} \\
 F_{ss}^0 &= U_{ss}^0 + P_{ss}(ss|ss) - \frac{1}{2}P_{ss}(ss|ss) + (P_{B_0 B_0} - Z_{B_0}) Y_{A_0 B_0} + (P_{C_0 C_0} - Z_{C_0}) Y_{A_0 C_0} \\
 & \quad P_{ss}(ss|xx) - \frac{1}{2}P_{ss}(sx|sx) \\
 & \quad P_{ss}(ss|yy) - \frac{1}{2}P_{ss}(sy|sy) \\
 & \quad P_{zz}(ss|zz) - \frac{1}{2}P_{zz}(sz|sz) \\
 & \qquad \qquad \qquad t = 1 \quad B^+ \text{ atom} \quad C^+ \text{ atom} \quad A^+ \text{ atom} \\
 & + (P_{B_+ B_+} - Z_{B_+}) Y_{A_+ B_+} + (P_{C_+ C_+} - Z_{C_+}) Y_{A_+ C_+} + (P_{A_+ A_+} - Z_{A_+}) Y_{A_+ A_+} \\
 & \qquad \qquad \qquad t = -1 \quad B^- \text{ atom} \quad C^- \text{ atom} \quad A^- \text{ atom} \\
 & + (P_{B_- B_-} - Z_{B_-}) Y_{A_- B_-} + (P_{C_- C_-} - Z_{C_-}) Y_{A_- C_-} + (P_{A_- A_-} - Z_{A_-}) Y_{A_- A_-}
 \end{aligned} \tag{70}$$

The off diagonal matrix elements are calculated by equation 31.

Thus the 6 x 6 Hartree-Fock matrices are

$$F_{\mu\nu}^0 = \begin{bmatrix} -0.0832 & 0.0124 & 0.0004 & 0.0088 & -0.3829 & -0.3829 \\ 0.0124 & -0.1939 & -0.0148 & -0.0098 & 0.0098 & -0.4128 \\ 0.0004 & -0.0148 & -0.1676 & -0.0105 & -0.0434 & -0.0434 \\ 0.0088 & -0.0098 & -0.0105 & -0.1869 & -0.4413 & 0.1563 \\ -0.3829 & 0.0098 & -0.0434 & -0.4423 & -0.2773 & -0.2773 \\ -0.3829 & -0.4128 & -0.0434 & 0.1563 & -0.0549 & -0.2773 \end{bmatrix} \quad (71)$$

The 6 x 6 intercell Hartree-Fock matrices are calculated by equation 32

$$F_{\mu\nu}^+ = \begin{bmatrix} -0.3147 & -0.0963 & 0.2068 & -0.0681 & -0.0656 & -0.0656 \\ 0.1302 & -0.0845 & -0.1983 & 0.0655 & 0.0607 & 0.0219 \\ -0.1527 & -0.2333 & 0.1637 & -0.1637 & -0.0461 & -0.0461 \\ 0.0921 & 0.0655 & -0.1403 & -0.1309 & 0.0018 & 0.0566 \\ -0.0620 & -0.0216 & 0.0425 & -0.0563 & -0.0003 & -0.0066 \\ -0.0620 & -0.0603 & 0.0425 & -0.0016 & -0.0066 & -0.0003 \end{bmatrix} \quad (72)$$

The Hartree-Fock matrices of zero cell $F_{\mu\nu}^0$ and intercell $F_{\mu\nu}^+$ are diagonalized by Jacobi's method⁵³ to obtain the eigenvalues and eigenvectors and this matrices also can serve for next iteration to calculate a new charge density matrices. The cycle goes on and on as stated in equation until the difference of charge density between two successful iteration converges. The orbital electronic energies of the final iteration calculated as a function of wave vector k_i , define the energy band structure of the system. The effective mass of charge carriers are calculated by curve fitting technique based on Lagranges interpolating method⁵³. For eight points the Lagrange interpolating polynomial is

$$P_8(k) = \sum_{i=1}^8 A_i \prod_{\substack{j=1 \\ i \neq j}}^8 (k - k_j) \quad (73)$$

where A_i is given by

$$A_i = \frac{E(k_i)}{(k_i - k_1)(k_i - k_2)(k_i - k_3) \dots (k_i - k_{i-1})(k_i - k_{i+1}) \dots (k_i - k_j)} \quad (74)$$

where i, j , and $E(k_i)$ is the energy point corresponding to the wave vector K_i . The values of the eight wave vectors are given in equation 66. By substituting the corresponding values of k_i into the equation 74 and 73, and differentiating equation 73 twice, the curvature of the energy band structure can be obtained in terms of the calculated energy points;

$$\left[\frac{\partial^2 P(k)}{\partial k^2} \right]_{k=0} = 50.4537E_0 - 110.1330E_1 + 100.4546E_2 - 76.8840E_3 \quad (75)$$

$$+ 92.1648E_4 - 43.3753E_5 + 24.0567E_6 - 6.9653E_7$$

then, the effective mass of carriers, intrinsic and extrinsic conductivity can be obtained by equation 25, 22 and 26 respectively.

V. Applications

In this section we describe selected applications of macromolecular orbital theory to some representative physical problems. The systems considered are polyhydrogen, polyethylene, polyacetylene, polyglycine, polyaniline, graphite, and one-dimensional polymers of hydrogen fluoride.

A. Polyhydrogen

There are two alternate theoretical descriptions of solid hydrogen: as an atomic crystal consisting of equivalent interacting hydrogen atoms or as a molecular crystal based on equivalent interacting hydrogen molecules.⁵⁴ The electronic structural characteristics of two representations are depicted in Figure 1. In an atomic crystal, the 1s orbitals of neighboring hydrogen atoms interact to form a 1s energy band. With one electron contributed per atoms, the 1s band is half filled, and the energy band gap is zero. According to this picture solid hydrogen should be an electrical conductor.

On the other hand, one knows that two hydrogen atoms covalently bind to form a stable hydrogen molecule, and alternatively solid hydrogen may be considered as a crystal of H_2 molecules held together by van der Waals forces. Just as the energy band structure of an atomic crystal is derived from the atomic energy levels of constituent atoms, the energy bands for a molecular crystal can be developed in terms of the molecular orbital energy levels of the constituent molecules. For a crystal of hydrogen molecules, the N bonding $\sigma(1s)$ molecular orbitals of constituent molecules interact to form an N -level $\sigma(1s)$ band in the crystal. The antibonding $\sigma^*(1s)$ molecular orbitals likewise form a $\sigma^*(1s)$ band. The energy bands in the molecular crystal should be rather narrow as a consequence of the relatively weak crystal force between H_2 molecules. The ground

state molecular electronic configuration is $\sigma(1s)^2$, and with two electrons per molecule the $\sigma^*(1s)$ band of the molecular crystal will be totally filled and the $\sigma^*(1s)$ band would be completely empty. The band gap would be unequal to zero, and depending on its magnitude, solid hydrogen considered as a molecular crystal should be an electrical semiconductor or insulator. Weak intermolecular forces would favor the latter. The known experimental characteristics of solid hydrogen favor the molecular crystalline form under normal pressures. The existence of metallic hydrogen in the core of Jupiter has been postulated by astrophysicists to explain the powerful magnetic field, the density and the heat source of this planet.⁵⁵ Recently, Soviet scientists have reported converting gaseous hydrogen very briefly into a metal. The conversion occurred under explosive compression at 2.8 Mbar. At that pressure, the density of the hydrogen jumped from 1.08 to 1.30 grams per cubic centimeter. The possibility of metallic hydrogen has been considered by Bernal in the early 1925, who suggested that if any substance subjected to high enough pressure it would become metallic. Particularly, for a diatomic molecule, such as hydrogen, the intermolecular distance decreases with high pressure until an individual atom does not know whether it belongs to its own molecule or to the next one. The material becomes metallic with all atoms approximately equidistant, and all electrons are uniformly distributed. In 1935, Wigner and Huntington,⁵⁶ based on their lattice energy calculation, had predicted that hydrogen would form a metal with roughly the density reported by the Russian scientists. It was subsequently estimated that about 2 Mbar. Pressure would be required for the conversion of hydrogen into metal, which was considered to be outside the scope of the technique at that time. According to the

Bardeen-Cooper-Schrieffer (BCS) theory of superconductivity,⁴⁵ some theorists have proposed that the metallic hydrogen may be superconductor at room temperature. If so, and if hydrogen were metastable in the metallic phase, it could have many practical application; it could be a really great scientific invension. For a variety of reasons, many researchers in the United States are joining the band that is searching for metallic hydrogen, such as Hawke and his associates at Livermore, Arthur Ruoff in Cornell, and Ian Spain in Maryland.

Almost without exception, experiments on polyhydrogen are difficult to execute and interpret. The basic properties of possible metallic hydrogen are either uncertain or completely unknown. By contrast, theoretical calculation are much easier done, and can predict the conditions under which it may be formed. The quantitative theoretical study of the electronic structure property of solid hydrogen requires a detailed quantum mechanical calculation. We have carried out calculations on polyhydrogen at the INDO and MINDO/2 level of approximation using macromolecular orbital theory.

The present calculation of the polyhydrogen has a three fold purpose: To estimate the transition point between normal and metallic hydrogen, and determine the metallic equilibrium geometry of the system, to study the influence of changes in molecular geometry on the band structure of the system, and to compare the results of INDO and MINDO/2 macromolecular calculations for a simple system, enumerating the similarities and differences in the methods.

The parameters for the molecular geometry of the elementary cell of polyhydrogen chosen for the INDO and MINDO/2 calculations are shown in the

Figure 2. The intracell bond length is denoted as r , and the intercell parameter is R . The INDO and MINDO/2 electronic energy band structure are given in Figure 3 and 4, respectively. The molecular energy level diagrams of these methods are also shown in the same figure for the convenience of comparison between the crystal molecular orbital theory and the molecular orbital theory. By varying the values of intra (r) and inter (R) molecular distance of the polyhydrogen crystal, the values of energy band gap, band width, and total energy per unit cell of the polyhydrogen crystal can be obtained as a function of geometry. The energy band structure of the INDO and MINDO/2 calculations of polyhydrogen crystal are plotted in Figure 5 and 6 respectively as a function of intermolecular distances, when the intra molecular distance is kept constant at 0.74 \AA throughout all the calculations. The INDO and MINDO/2 energy band gap of polyhydrogen is presented as a function of r and R simultaneously in the contour plots of Figures 7 and 8. The INDO and MINDO/2 energy curves of the polyhydrogen crystal are plotted in Figure 9 and 10 as a function of the intermolecular distance, when the intramolecular distance is kept constant (0.74 \AA).

Figures 3 and 4 show how the energy manifold of polyhydrogen at $r=R=0.74 \text{ \AA}$ is resolved into a valence and conduction band. The widths of the conduction and valence band are theoretically supposed to be of the same order of magnitude. In INDO and MINDO/2 results, the conducting band appears much narrower in width than the valence band, with the band width in MINDO less than that of the INDO method. This effect is a result of the zero differential overlap approximation, and was recognized for molecules even in Huckel theory. The calculated values of the energy band are 14.37 eV and 7.73 eV respectively for the INDO and MINDO/2 methods.

This indicates that polyhydrogen crystal would be a non-conductor at this geometry.

Figure 5 and 6 show that the energy band width increases as the intermolecular distance of the polyhydrogen crystal decreases. The increase is more or less linear when the two molecules are considerably separated. When the intermolecular distance reaches about 0.54 \AA , the energy band gap widths increase sharply and the band gap decreases drastically, becoming zero at the intermolecular distance about 0.44 \AA . In order to have a clear picture of the energy band gap as a function of geometry, the INDO and MINDO/2 energy band gap contour surfaces of polyhydrogen are in Figure 7 and 8. From Figure 7, the INDO method predicts the zero band gap appears first at the geometry with inter and intramolecular distances both equal to 0.44 \AA . This is consistent with Bernal's suggestion; the material becomes metallic with all atoms approximately equidistant and all electrons uniformly distributed. From Figure 8, the geometry of metallic hydrogen predicted by MINDO/2 method is $(0.85 \text{ \AA}, 0.65 \text{ \AA})$. This result is not consistent with Bernal's suggestion. Based on molecular calculations, the MINDO/2 method does not necessarily give good result on molecular geometry, and the INDO result is probably more reliable.

Based on the law of conservation of energy, the increased internal energy of each hydrogen molecule must be equal to the external mechanical work done by the high pressure on each individual molecule. Therefore, the pressure required to compress the solid polyhydrogen crystal to the geometry $(0.44 \text{ \AA}, 0.44 \text{ \AA})$ is the minimum external pressure to make the metallic hydrogen. From Figure 9, we find that the energy curve of the polyhydrogen for unit cell decreases as the intermolecular distances

increases. It approaches the limit of the energy of a single monomer at the point corresponding to the intermolecular distance about 3.24\AA . This is exactly the experimental value for intermolecular distance in solid hydrogen. The energies per unit cell of polyhydrogen crystal for the geometries E (0.44\AA , 0.44\AA) and E (0.44\AA , 3.24\AA) are obtained to be $-.4937$ and -1.4746 a.u respectively by INDO quantum mechanical calculations. The corresponding pressure required to compress the polyhydrogen crystal from the geometry (0.74\AA , 0.324\AA) to the geometry (0.44\AA , 0.44\AA) is calculated to be 4.579 Mbar. This calculated pressure is in the same order of magnitude with the experimental result which is recently reported by the Russian scientists.

The energy curve of the polyhydrogen per unit cell calculated by MINDO/2 method (Figure 10) is very similar to the result of INDO method. MINDO/2 also predicts the dissociation limit when the two hydrogen molecules are separated by the distance of 3.24\AA .

In conclusion, the energy band calculations of one-dimensional hydrogen crystal have been carried out, and a geometry at which the existence of metallic hydrogen might occur has been predicted by both INDO and MINDO/2 methods. The external pressure required to turn hydrogen crystal into a metal has been calculated to be the same order of magnitude as found by experiment, using the INDO method. The MINDO/2 method can give qualitatively the same results in energy band structure as the INDO method, but with a smaller energy band gap. The INDO results predicts the equilibrium geometry of metallic hydrogen to have equal interatomic spacings.

B. Polyacetylene and polyethylene: Polyacetylene

The elementary cell and molecular geometry chosen for the calculation on polyacetylene is shown in Figure 11. Only the planar trans extended form of the polymer was considered, with all bond angles taken as 120° . The electronic energy band structure of the polymer calculated with INDO method is given in Figure 12, juxtaposed with the calculated orbital energy levels of the isolated elementary cell. Considerable band overlap is evident, so that the highest occupied and lowest unoccupied bands are of mixed σ and π character. The calculated gap between the highest occupied band and lowest unoccupied band is 10.14 eV. The $\epsilon(k)$ curves for each band are given at the right hand side of the diagram. The calculated charge distribution is recorded in Figure 11, and reflects the low polarity expected for the C-H bond. The calculated effective mass of charge carriers are .1752 for electrons and .7520 for holes, in units of electron rest mass.

A comparison between the INDO calculated structure and the corresponding CNDO calculation is available by comparison of our Figure 11 with Figure 3 given by O'Shea and Santry.³² The results as expected are very similar, considering the slight difference in geometrical parameters. Note that for overlapping bands in our methodology, the σ/π nature of a given band may change as k changes, and resolution in to pure bands is necessary for direct comparison with their calculations. This is readily accomplished by inspection of the $G(k)$ matrices.

The calculated intrinsic conductivity is $.7586 \Omega^{-1}/\text{cm}$. For the MINDO/2 calculations, the C-H bond length was increased to 1.19 \AA as recommended by Dewar et. al.²⁷ for molecular calculations. The calculated band structure is given in Figure 13. The MINDO/2 results are qualitatively similar to the INDO results, but differ in quantitative detail. In particular, the calculated band gap was 6.97 eV , substantially lower than the INDO value. The MINDO/2 calculated net atomic charges are recorded in parentheses in Fig. 11, and shows C-H with slightly less charge separation than the INDO values. The calculated effective mass of carriers are $.614$ and $.7947$ respectively for electrons and holes, and the calculated intrinsic conductivity is $.8139 \Omega^{-1}/\text{cm}$.

The elementary cell and molecular geometry chosen for the INDO calculations on polyethylene are shown in Figure 14. Only the planar trans extended geometry was considered, and all bond angles were taken as $109^{\circ}28'$. The electronic energy band structure of the polymer is given in Fig. 15. Here as well considerable overlap in the highest occupied and lowest unoccupied bands is evident, and the calculated band gap is 13.64 eV . The INDO calculated charge distribution is also given in Figure 14, and shows $\text{C}^{\delta+} - \text{H}^{\delta-}$ with only a small charge separation. The calculated effective mass of carriers are $.6285$ and $.4703$ for electrons and holes in the units of electron rest mass, and the calculated intrinsic conductivity is $.5403 \Omega^{-1}/\text{cm}$.

In the MINDO/2 calculations on polyethylene, the C-H bond length was again increased to 1.19\AA , but other geometrical parameters were kept the same as above. Again the calculated MINDO/2 band structure and electronic charge distribution was qualitatively similar to the INDO results, with the bandgap substantially lower at 9.56eV . The MINDO/2 calculated effective mass of carriers are .2397 and .9630 for electrons and holes in the units of electron rest mass, and the calculated intrinsic conductivity is $5.3114\ \Omega^{-1}/\text{cm}$. Smaller band gap and better intrinsic conductivity are predicted by MINDO/2 than by INDO method. For reasons described earlier, the MINDO/2 values are probably more reliable than the results. Both INDO and MINDO/2 values would characterize polyethylene as an electrical insulator in agreement with experimental measurements.⁵⁷

Previous calculations of polyethylene using extended Huckel and CNDO methods in analogous formulations given gaps of $12.35\ \text{eV}$ and $19\ \text{eV}$ ^{31,32} respectively. Various values of the effective mass (.48 , .38, and .17)⁵⁸ were obtained by the extended Huckel method and the results depends very much on the parameters used in the calculations. The discrepancy in the CNDO value and INDO value reported herein is due in part to difference in choice of elementary cell and our use of the nearest neighbor approximation.

The applicability of the one-dimensional crystal model as a useful representation of real systems is yet to be adequately documented. The measurement of electrical properties of polymeric materials is subject to well-known experimental uncertainties, and macromolecular conformational

stability is known to depend in part on correlation effects beyond an orbital approximation. More promising in this regard are recently developed techniques in photoelectron spectroscopy, which provide an experimental probe of the manifold of ionization energies. Comparison of the observed photoelectron spectrum of a polymer with the calculated crystal orbital energy band structure tests the theory within the limits of Koopman's theorem.⁴⁸

The system for which the most representative theoretical and experimental data are presently available is polyethylene. Calculations including at least valence electrons for polyethylene have been reported by Imamura⁵⁹ using the extended Huckel theory, by Morakuma³⁰ using the CNDO approximations, by Beveridge et al with the INDO and MINDO/2 methods,³⁴ and at the ab initio level by Andre and Leroy.²⁹ The experimentally observed photoelectron spectrum of $C_{36}H_{74}$ has been reported by Wood, Barber and Hiller,³⁹ and interpreted with crystal orbital theory and a modification CNDO parameters due to Whitehead and Sichi.⁶⁰ We have compiled a comparison of the calculated and observed results for polyethylene, and the results are presented in Figure 17.⁶¹

The observed spectrum shows three distinct bands below 25 eV. The calculated valence energy band structures all appear to be higher in energy than the observed results with the effect in calculations at the MINDO/2 level less pronounced.

MINDO/2 is also the only method giving three distinct hyperbands, and the calculated bandwidths are in reasonable agreement with experiment. The interpretation of the spectrum based on the **MINDO/2** results parallels that offered by Wood et al. The low energy peak (I) is assigned to be due to ionization from the four topmost bands (A, B, C, D in Figure 17) having predominantly carbon 2p and hydrogen 1s atomic components. The experimental width of this band (~ 8 eV) is slightly smaller than the result predicted by **MINDO/2** (~ 12 eV) as shown in Figure 17. A slight band gap (1-2 eV) is predicted to occur at higher energy, in agreement with the observed spectrum, before the appearance of Peaks II and III. This observed band correlates to the ionization from the second lowest calculated band (E in Figure 17). The experimental width of the second band (~ 4 eV) is in excellent agreement with the calculated **MINDO/2** result. The last observed band correlates to the ionization from the lowest band (F in Figure 17) which cover an energy range of ~ 20 eV. These values are in good agreement with the calculated **MINDO/2** results. These two lower bands are calculated to be mainly carbon 2s character. Thus, Peak II and III are expected to be more intense than Peak I in view of the larger photoionization cross section, and this is the experimental result in the photoelectron spectrum.

The **MINDO/2** energy band structure calculated here is in good agreement with the experimental results. The relatively poor agreement produced by the **CNDO/2** and **INDO** methods is as expected since these methods are well known to give poor ionization

energies. Most surprising is the relatively poor agreement between experiment and theory at the initio level. Thus, with the parameters used in MINDO/2 , relatively simple semiempirical molecular orbital calculations yield a band structure of polyethylene in good agreement with experiment. This indicates that reliable calculation of the electron of the electronic structure of more complicated periodic systems may be performed by such approximate methods.

C. Substituted Polyacetylenes. The purpose of the present calculation of substituted polyacetylene is to study the influence of substituted group on the energy band structures, and their polarity for the band between the substituted group and the carbon atom on the chain. The functional groups considered are the F, and NH_2 substituted polyacetylenes.

The elementary cell and molecular geometry chosen for the INDO calculation on the F-substituted polyacetylene is shown in Figure 18. The geometry of the carbon chain is the same as the polyacetylene. The C - F bond length taken as a 1.35\AA . The electronic energy band structure of the polymer calculated with INDO method is given in Figure 19. Considerable change of valence band structures are evident, the top two substituted polyacetylene bands are similar in shape to the corresponding two top bands in nonsubstituted polyacetylene. The band widths are considerable narrower. The conducting bands greatly resemble the conducting bands of the nonsubstituted polyacetylene. The calculated gap between the highest occupied band and the lowest unoccupied band is 9.62 eV. The calculated charge distribution is recorded in Figure 18, and accurately reflects the large polarity expected for the C-F band. The effective mass of electron and hole are .1781 and .5583 in unit of electron rest mass respectively, and the intrinsic conductivity is $.7034 \Omega^{-1}/\text{cm}$. The elementary cell and molecular geometry chosen for the INDO calculation on the NH_2 -substituted polyacetylene is given in Figure 20. The geometry of the carbon

chain is the same as the polyacetylene, the hydrogen atom is substituted by the -NH_2 group, the N-C and N-H bond are taken as 1.37 and 1.00 A° respectively. The electronic energy band structure of NH_2 -substituted polyacetylene calculated with INDO method is given in Figure 21. In comparison with the nonsubstituted and the F-substituted polyacetylene, the energy bands of NH_2 -substituted polyacetylene have smaller degree of change in their shapes. The three top NH_2 -substituted energy bands greatly resemble the corresponding three top energy bands of nonsubstituted polyacetylene. The other two lowest bands in nonsubstituted polyacetylene are preserved their band shape in the NH_2 -substituted polyacetylene. Once again, the conducting band is not much affected by the substitution. The calculated gap between the highest occupied and the lowest unoccupied band is 9.25 eV. The calculated charge distribution are recorded in Figure 20. The effective mass for electron and hole are .2223 and .4814 in unit of electron rest mass respectively, and the intrinsic conductivity is $.7034 \text{ } \Omega^{-1}/\text{cm}$. They are also presented in table IV.

D. Polypeptide

The elementary cell and molecular geometry chosen for the INDO calculations on polyglycine are shown in Figure 2'. The conformation of the molecules is specified in terms of the dihedral angles ψ and ϕ . The bond lengths chosen are based on an approximate energy minimization of glycine using molecular orbital theory. Here two geometries were explicitly considered: planar ($\psi = 0, \phi = 0$) and α -helical ($\psi = 123^\circ, \phi = 132^\circ$). The INDO calculated crystal orbital electronic energy band structure is given in Figure 2.3 and 2.4. The calculated band gaps are 9.53 eV for the planar polyglycine and 8.51 for the α -helical form. The calculated charge distribution for planar and α -helical polyglycine are given in Figure 2.5 and 2.6 respectively. The results are uniformly consistent with chemical intuition, with the expected polarity of the carbonyl bond and peptide bond qualitatively reproduced. The polarity of both bonds appears to decrease in going from the planar to helical form.

In the MINDO/2 calculations, the C-H bond lengths given in Figure 2.2. was increased by 0.1 Å and the N-H bond length increased by 0.15 Å as recommended by Dewar. The MINDO/2 calculated electronic energy band structure is given in Figure 2.7 and 2.8 respectively. The band gap calculated by the method were 6.14 eV for planar polyglycine and 5.7 eV for the α -helical form. The MINDO/2 calculated net atomic charges are given in parentheses in Figures 2.5 and 2.7. The qualitative

considerations remain approximately the same as for but bond polarities are substantially more pronounced.

The MINDO/2 value of 5.7 eV is in good agreement with the band gaps estimated in the Suard-Sender work. The description of dielectric lowering and the comparison of theory and experiment by Rosenberg and Postow⁶² indicates that band gaps between 4.9 and 5.9 eV are consistent with experimental data on electrical conduction in protein systems. It should be mentioned, however, that in reality only high frequency a.c. conductivity measurements could give more reliable experimental information about the band gap, because the d.c. measurements refer rather to the intermacromolecular potentials than to the activation energy of conductivity within a single protein molecule.

The elementary cell and molecular geometry chosen for the INDO calculation on the α helical poly(glycine-aniline) are shown in Figure 29. The geometry of the polyglycine backbone remains the same. One of the hydrogens at the C^α position is replaced by a methyl group, with the CH_3-C and CH_2-H bond lengths taken as 1.54 and 1.09 Å respectively. The electronic energy band structure of the α helical polymer calculated with INDO method is given in Figure 30. The energy band structures of the polyglycine-aniline resembles greatly the electronic energy band structure of the polyglycine-L-glycine. The calculated charge distribution is recorded in Figure 30. The electron donating methyl group produces

a considerable change in electronic density at the nitrogen atom and the adjacent C^{α} , with the nitrogen becoming more negative while the C^{α} becomes less electropositive. This can be explained by the higher intrinsic electronegativity of the nitrogen atom carbon. There is not affect from the CH_3 group on the electron density at the carbonyl group, because the spatial separation between the CH_3 -group and the carbonyl group is relatively large.

The calculated band gap in poly(glycine-aniline) is 9.39 eV. This large band gap indicates poly(glycine-aniline) is likely to be intrinsically an insulator. Some electrical properties of polypeptide calculated both by INDO and MINDO/2 methods are presented in table 5. Unfortunately, this calculation is still in its earliest stage, there have no experimental or other theoretical results concerning the effective mass of the carriers in polypeptides for comparison. To clarify finally the problem of band gap and the effective mass of carriers in proteins further work is needed both on the theoretical and experimental side.

Studies of polypeptide conformations using the statistical mechanics was first introduced by Ramachandran.⁶³ Recently a number of new variations on methods have been added. This approach to this problem involves the use of a hard-sphere model and various potential functions for interatomic interactions. The bond lengths and bond angles are fixed, and the amine plane is fixed in the planar trans configuration. The conformational energy is studied with respect to rotation about the N-C^α and C^α-C' single bonds of the polypeptide backbone.⁶³ The various atoms or group of atoms are assumed to interact pairwise as specified by selected pairwise potential functions. These potential functions represent such effects of barriers of internal rotations, hydrogen-bonding, nonbonding and electrostatic interactions etc. All these potential functions are semi-empirical, and have been deduced from the many experimental studies in physical chemistry. They are far from being well established, and different investigators often use different formulae and parameters. Therefore, these methods and models possibly suffer from incompleteness and arbitrariness.

A satisfactorily account for the overall zone of conformational stability of residues in globular proteins using the PCILO method has been reported by Pullman.² Calculations on dipeptides also have been reported by the CNDO and the EHT methods. The dipeptide model of course can yield some

information on the polypeptide structure, but the conformation of the polypeptide chain is definitely different from the stable dipeptide conformations. This is because of the high specificity of the model. This limitation of the dipeptide model has been recently discussed in detail by Pullman and Margret². The alternative model for representing a macromolecule for the theoretical studies is the one-dimensional crystal model, the real polymer structure may be intermediate between the results of the dipeptide and the crystal orbital model. It is interesting to compare the results produced for energy conformational maps by these two models at the various levels of approximation.

The dipeptide model chosen for INDO conformational analysis is shown in Figure 32. Two amide planes are joined by the tetrahedral bonds of the α carbon, the rotation parameters are ϕ (C - N bond) and ψ (C - C'). Direction of rotations are shown in the picture. The zero position in both ϕ and ψ occurs with the two peptide planes themselves coplanar. The elementary cell geometry for polyglycine chosen for conformational analysis is given in Figure 33 with all the bond length taken as those shown in Figure 24. The steric conformational map of dipeptide glycine is represented in Figure 34. The capital letters F, B and C indicate the nonbonded interatomic distances are less, equal and greater than 0.5\AA but less than 1\AA respectively. The INDO-MO dipeptide and INDO-CMO polypeptide energy conformational maps are presented

in Figure 35 and 36 . The most stable conformational structure of dipeptide glycine molecule calculated by INDO-MO method is shown in Figure 37. The most stable conformation corresponding to the global minimum in Figure 35 is predicted for the region $\phi = 120^\circ$ and $\psi = 300^\circ$ and the symmetric position $\phi = 240^\circ$, $\psi = 60^\circ$ by the INDO-MO method. The most stable conformation predicted by the INDO-CMO method is $\phi = 120^\circ$, $\psi = 200^\circ$, and its symmetrical position $\phi = 240^\circ$, $\psi = 160^\circ$. This conformation, leading to a seven membered ring, is called C_7 by Pullman and is shown in Figure 37. This conformation is stabilized by a strong intramolecular hydrogen bond between oxygen atom O^1 and the hydrogen atom H^2 in the neighboring cell.

The second most stable conformation, corresponding to the secondary local minima, appears 2 kcal/mole above the preceding global minimum in the regions $\phi = 0^\circ - 60^\circ$, and $\phi = \psi = 90^\circ - 120^\circ$ (their symmetrical positions $\phi = \psi = 360^\circ - 300^\circ$ and $\phi = \psi = 270^\circ - 240^\circ$) by the INDO-MO method. The local minimum appears in the region $\phi = \psi = 0^\circ - 20^\circ$ and $\phi = 180^\circ$, $\psi = 90^\circ$ (and their symmetrical areas) using the CMO method. The first secondary minima corresponding to the extended form of the molecule is stabilized by a weak intramolecular hydrogen bond between the oxygen atom O^2 and hydrogen atom H^1 . This conformation, leading to a five member ring structure, is called C_5 by Pullman.

Comparing the INDO-MO , INDO-CMO and PCILO methods, the global and two local minimas are predicted by all these three

methods, but the locations are slightly different from each other. The energy minimum at $\phi = 180^\circ$, $\psi = 90^\circ$ in the PCILO result which is called region M by Pullman is reproduced by the INDO-CMO method in exactly the same region. INDO-MO method predicts this region in the sterically allowed area. There is argument on the significance of these region M involving several investigators, since it is located in the sterically forbidden area produced by empirical potential methods, and has not yet observed experimentally. It is however also predicted by A. Pullman using a more accurate ab initio method. In general the INDO-CMO energy conformational map is closer to the PCILO conformational energy map rather than the INDO-MO results. This difference may have to do with the INDO-CMO method accounting for intercell interaction.

E. Graphite

Graphite is an excellent example of a substance illustrating the effects of greatly differing bonding character in different crystallographic directions. The atoms are arranged in hexagons in each layer and it can be considered to be a single large layer aromatic molecule. The spacing between layers is considerably greater (3.35\AA) than that between atoms in a given layer (1.42\AA). As a consequence of the large interlayer spacing in graphite, there is covalent bonding between the atoms within the layer, whereas the bonding between planes is of nonbonding character. Therefore, it exhibits strong anisotropic behavior. Most of the optical properties of graphite can be well understood on the basis of a single-layer two dimensional model. This simple model was first introduced by Wallace,⁶⁴ and it has been found that it is quite adequate for treating graphite in this way. This model is chosen for this calculation.

The elementary cell and molecular geometry chosen for the INDO and MINDO/2 calculations on graphite is shown in the Figure 38. The inter-atomic distance between carbons is 1.40\AA . The angles between carbons are all 120° . The electronic energy band structure of graphite calculated by INDO and MINDO/2 methods are shown in Figures 39, and 40 respectively. Considerable band overlap is also evident, the highest valence band and the lowest conduction band are of mixed σ and π character. The INDO method gives 7.17 eV energy band gap, while MINDO/2 method gives only 5.46 eV . The calculated energy band structures in these two methods were qualitatively similar to each other. A comparison of energy band structures of graphite by different methods is summarized in table 6, and the wave functions are symmetry classified in the figures of the energy band structure. The allowed transitions which is induced by incident radiation of polarized light are also summarized in table 7.

In comparing the energy band structure of graphite as calculated by different methods, it is found that the INDO method in general predicts larger band width than the ab initio and MINDO/2 methods. On the other hand, the MINDO/2 method predicts smaller band width than the values predicted by the other two methods, except for the lowest band. The total valence band width predicted by the semiempirical methods are larger than the ab initio method;⁶³ this is consistent with some results of applications to other polymers. The energy band gap of graphite calculated by INDO and MINDO/2 methods are 7.07 and 5.44 eV respectively. These values are all higher than the 4.6 eV given by the ab initio method. The electron density of graphite calculated by these two methods are both zero, as determined by symmetry.

Greenaway et al.⁶⁵ observed a peak in reflectivity for polarization with the electrical field perpendicular to the surface of the layer at about 4.6 eV, which they ascribed to the $\pi - \pi$ transition. This transition has been claimed by Painter and Ellis⁶⁶ to be in very good agreement with their ab initio results. The INDO and MINDO/2 methods both predict a higher value for this transition. For $\sigma_3 - \sigma_3^*$ transition, the ab initio method predicts 16.3 eV, when the INDO and MINDO/2 predict 12.52 and 8.07 eV respectively. In comparison with the experimental value 14.5 eV, the ab initio value is higher, and the values of the two semiempirical methods are smaller than the actual experimental result. For polarization with the electrical field parallel to the surface of the graphite, all these methods predict reflectance structure above 10eV for the $\sigma_2 - \pi^*$ transition. This has been claimed by Painter and Ellis to be qualitative agreement with the observed increase in reflectivity above 10eV in Greenaway's experiment. Unfortunately, there have been no reflectivity measurements above 10eV for the electrical field parallel to the surface.

In summary, the INDO and MINDO/2 methods can account for the energy band structure of graphite to a certain extent. They also can predict the existence of the $\sigma - \pi^*$ transition above 10 eV range. These results support the suggestion by Painter and Ellis to extend the reflectivity measurements for the electrical field parallel to the surface of the graphite into the energy range above the range of 10 eV. Some discrepancies between the ab initio, INDO and MINDO/2 methods do occur in their results, when compared with the experimental results. This may be due to the use of one-dimensional crystal model to describe the two dimensional graphite crystal. Therefore, the two and three dimensional crystal model for graphite in these semiempirical levels should be an interesting subject for further investigation.

F. Hydrogen-bonded polymers: Polymer of hydrogen fluoride

Polymer formation through hydrogen bonding occurs rather widely in nature. Examples range from water to macromolecules having both electronegative atoms and labile hydrogen atoms. A number of theoretical studies of hydrogen bonding have been reported using quantum mechanical calculations. Most of these calculations have used a dimer model and LCAO-SCF theory. This dimer model can yield some information on some hydrogen bonding systems, but many of the important macromolecular systems involved not only two but a large number of individual molecules. The inter and intramolecular interaction in a crystal or a linear polymer is clearly different from that of a dimer model, and should influence any hydrogen bonds to certain extent. This shortcoming of the dimer model has been recognized by a number of investigators.⁶⁷

Polyhydrogen fluoride is the simplest and a good representative example of this type system. Studies of linear and cyclic HF polymers have been reported by Kollman and Allen.⁶⁷ Calculations on a one dimensional hydrogen bond chain have been reported by Sabin.⁶⁸ It has been found that the strength of individual hydrogen bonds depends on the polymer chain length. Studies of three dimensional HF crystal was reported by Bocon and Santry⁶⁹ using molecular orbital theory for infinite systems. This theory treats the entire crystal field as a perturbation on the isolated molecular orbitals. Since some of the hydrogen bonds are most chainlike even in the solid state, this can be treated as an infinite linear polymer rather than three dimensional crystal. Study of the hydrogen bonding using the CMO method should provide a comparison between the dimer model and the one-dimensional crystal model. The similarity and differences between the

perturbation theory used by Santry⁷⁰ and our crystal molecular orbital theory are also of interest. Thus we have carried out calculations on poly(hydrogenfluoride) using both molecular orbital and macromolecular orbital methods.

The model system chosen for this study is one dimensional linear chain with the geometry of polyhydrogen fluoride taken from the theoretically found equilibrium distance for dimer by Kollman and Allen. In each case, the F - F and F - H distances are kept at 2.45 \AA and 1.00 \AA respectively. The calculated results on poly(hydrogen-fluoride) linear system using the INDO molecular orbital (MO) theory are given in table 8. The similar calculated results using the INDO crystal molecular orbital (CMO) theory is presented in table 9. The intra and intermolecular density submatrices for polyhydrogen fluoride linear chain calculated by INDO crystal molecular orbital theory with the z-axis along the chain is shown in table 10. The electron population for each constituent atom of the same system calculated by both INDO molecular orbital and crystal molecular orbital theories are given in table 11 and 12 respectively. Finally the energy band structure of poly(hydrogen-fluoride) is shown in Figure 41, with the energy levels of FH monomer shown side by side for the purpose of comparison between these two methods.

Comparing the INDO results with the CNDO results reported by Kollman and Allen, the average energy gained per H-bond is higher for INDO method is both CMO and MO calculations. There is no such maximum energy gained per H-bond at the pentamer case as it was found in their CNDO calculation. Instead, the energy gained per H-bond increases monotonically to a limiting value about 17.5 kcal per mole for INDO-MO calculation about 18.0 kcal per mole for INDO-CMO calculation when the chain length increases

to infinite. This is what one would expect as the electrostatic interaction between neighboring fragments increases. This is consistent with the experimental results of Bellamy and Pace, who found that the existence of a hydrogen bond at a nucleophilic center increases the strength of another H-bond to that side. INDO crystal molecular orbital calculation of poly(hydrogenfluoride) predicts 12.0394 kcal per hydrogen bond for single FH fragment in a unit cell. This value is in good agreement to the 11.9 kcal per hydrogen bond calculated by Santry, and it is very close to the value of 12.368 kcal per H-bond formed reported by Sabin for hexamer. The limiting theoretical value of energy per H-bond should be close to the value of 18.0 kcal per mole for infinite poly(hydrogenfluoride) linear chain. As Sabin already mentioned in his paper, the actual value is expected to be lower than this, as both CNDO and INDO both methods generally overestimate the bond energies.

From table 11 and 12, it is found that there is a charge transfer from the hydrogen atom to the fluorine atom. The addition of each FH fragment to the chain increases the charge transfer from the donor hydrogen atom to the fluorine atom, and it is also monotonically increased to a limiting value. In comparing the MO to the CMO result, it is found that the charge transfer from hydrogen atom to the fluorine atom is greater in CMO than in MO calculation. There is only one maximum negative charge on the first fluorine atom and the amount of negative charge on the successful fluorine atoms are monotonically decreased with a corresponding increase of positive charge on the successful hydrogen atoms. In the MO calculation, instead of a monotonic increase of positive charge on the successful hydrogen atoms,

there is a maximum positively charged hydrogen atom near the middle of the chain of the hydrogen atoms.

Figure 41 shows that the energy levels in poly(hydrogenfluoride) calculated by CMO method is a band-like structure with an energy band gap about 22.78 eV, such a large energy band gap definitely indicates poly(hydrogenfluoride) is an absolute insulator. In fact, hydrogenfluoride has been found to take hexameric form in a gas phase using electron diffraction methods. The band-like structure at orbital energies for the hexamer were mentioned by both Kollman and Sabin in their papers. The difference of the calculated energy levels between the crystal molecular orbital and the simple molecular orbital is that they are a continuous function of wave vector in the first method and discrete in the later.

VII. Concluding remarks:

The general formalism of INDO and MINDO/2 approximate macromolecular orbital calculations, the calculation of macromolecular properties, and the systematic analysis of one-dimensional macromolecular orbitals based on group theory have been presented. A test calculation on polyethylene is described in detail. Application of these methods to the calculation of the electronic structure, energy bands, and electrical properties of polyacetylene, polyethylene, F- and NH_2 -substituted polyacetylene, polypeptides, graphite and poly(hydrogen-fluoride) have been carried out. The conformational potential energy surface of polyglycine calculated by INDO-MO and INDO-CMO methods in the free space approximation have been presented. On the basis of the study described herein, the following conclusion are drawn:

- 1) Approximate macromolecular orbital calculations are feasible for the calculation of wavefunctions and properties of systems of chemical interest.
- 2) Among the approximations, studied the INDO method gives a good result of molecular geometry, but the calculated energy band gap is too high. The MINDO/2 method is less reliable for geometry of the polyhydrogen, but it gives a good description of the valence bands. The shape of the energy band structure calculated by INDO and MINDO/2 methods are similar, with the conduction band is significantly narrower than the valence band due to the neglect of differential overlap. An improved description of

conduction bands could be obtained from an approximate SCF calculation including overlap approximation.

3) Comparison of theoretical and the experimental results for the molecular energy band structure using the MINDO/2 method is encouraged, on the basis of comparison with the photoelectron spectra of polyethylene.

4) Comparison of the theoretical and experimental results for electrical properties is complicated by experimental difficulties and limited by the number of systems where intrinsic conductivity and band conduction have been unequivocally established. Until further experimental and theoretical work have been carried out significant conclusions be drawn.

5) Approximate macromolecular orbital calculations may be used in the same way as molecular orbital calculations for conformational analysis. From the results of the poly(hydrogenfluoride) and conformational analysis of polyglycine, it seems that the one dimensional crystal model is a better model than the dimer model for the description of the macromolecule.

Figures

1. Electronic Structure of solid hydrogen as an atomic crystal and as a molecular-crystal.
2. Elementary cell geometry and calculated net atomic charges for polyhydrogen using the INDO and MINDO/2 methods.
3. Electronic energy band structure of polyhydrogen calculated using the INDO method.
4. Electronic energy band structure of polyhydrogen calculated using the MINDO/2 method.
5. Electronic energy band structure of polyhydrogen calculated as a function of intermolecular distances using the INDO method.
6. Electronic energy band structure of polyhydrogen calculated as a function of intermolecular distances using MINDO/2 method.
7. Energy band gap surface of polyhydrogen calculated using the INDO method.
8. Energy band gap surface of polyhydrogen calculated using the MINDO/2 method.
9. Energy per unit cell of polyhydrogen calculated as a function of intermolecular distances using INDO method.
10. Energy per unit cell of polyhydrogen calculated as a function of intermolecular distances using MINDO/2 method.
11. Elementary cell geometry and calculated net atomic charges for polyethylene .
12. Electronic energy band structure of polyacetylene calculated using the INDO method.

13. Electronic energy band structure of polyacetylene calculated using the MINDO/2 method.
14. Elementary cell geometry and calculated net charges for polyethylene using the INDO and MINDO/2 methods. MINDO/2 values are in parenthesis.
15. Electronic energy band structure of polyethylene calculated using the INDO method.
16. Electronic energy band structure of polyethylene calculated using the MINDO/2 method.
17. Experimentally observed photoelectron spectrum of $C_{36}H_{74}$ compared with theoretical 1-D crystal calculations on polyethylene by various methods a) EHT (30); b) CNDO/2 (32); c) INDO (34); d) CNDO (31); e) MINDO/2 (34); f) ab initio (33).
18. Elementary cell geometry for F-substituted polyacetylene.
19. Electronic energy band structure of F-substituted polyacetylene calculated using the INDO method.
20. Elementary cell geometry for NH_2 -substituted polyacetylene.
21. Electronic energy band structure of NH_2 -substituted polyacetylene.
22. Elementary cell geometry for polyglycine.
23. Electronic energy band structure of planar polyglycine calculated using the INDO method.
24. Electronic energy band structure of α -Helical geometry of polyglycine calculated using the INDO method.
25. Calculated INDO and MINDO/2 net atomic charges for planar polyglycine. MINDO/2 values in parentheses.

26. Calculated INDO and MINDO/2 net atomic charges for α -helical polyglycine. MINDO/2 values in parentheses.
27. Electronic energy band structure of planar polyglycine calculated using the MINDO/2 method.
28. Electronic energy band structure of α -helical geometry of polyglycine calculated using the MINDO/2 method.
29. Elementary cell geometry for poly(glycine-aniline).
30. Calculated INDO net atomic charges for α -helical poly(glycine-aniline).
31. Electronic energy band structure of polyethylene calculated using the INDO method.
32. Molecular structure of dipeptide for INDO conformational analysis.
33. Molecular structure of polyglycine for INDO conformational analysis.
34. Steric conformational map of dipeptide glycine, the capital letters F, B, and C indicate the nonbonded interatomic distances are less, equal and greater than 0.5\AA but less than 1.0\AA .
35. INDO calculated potential energy surface for dipeptide glycine as a function of ϕ (C^{α} -N bond), (C^{α} - C^{β} bond).
36. Calculated potential energy surface for polyglycine as a function of ϕ (C^{α} -N bond), (C^{α} - C^{β} bond) using INDO method.
37. Molecular structure of most stable conformation of dipeptide glycine using INDO method.
38. Elementary cell geometry of graphite.
39. Electronic energy band structure of graphite calculated using the INDO method.
40. Electronic energy band structure of graphite calculated using the

MINDO/2 method.

41. Electronic energy band structure of poly(hydrogenfluoride) calculated using the INDO method.

Tables

1. Flow chart for line group classification
2. Table II INDO parameters for first-row elements (electron volts).
3. Table III MINDO/2 parameters for first-row elements (electron volts).
4. Electrical properties of polyacetylene, polyethylene and F, NH₂-substituted polyacetylene calculated by INDO and MINDO/2 methods
5. Electrical properties of α -helix and planar polyglycine, and helix poly(glycine-aniline) calculated by INDO and MINDO/2 methods.
6. Comparison of energy band structure of graphite calculated by ab initio, INDO and MINDO/2 methods.
7. Comparison of allowed transition of graphite calculated by ab initio, INDO and MINDO/2 methods.
8. Energies of one-dimensional poly(hydrogenfluoride) crystal calculated by INDO-MO method.
9. Energies of one-dimensional poly(hydrogenfluoride) crystal calculated by INDO-CMO method.
10. Intra and intermolecular density submatrices for one-dimensional poly(hydrogenfluoride) crystal calculated by INDO-CMO method with the Z-axis along the chain.
11. Electron population for poly(hydrogenfluoride) one-dimensional crystal calculated by INDO-MO method.
12. Electron population for poly(hydrogenfluoride) one-dimensional crystal calculated by INDO-CMO method.

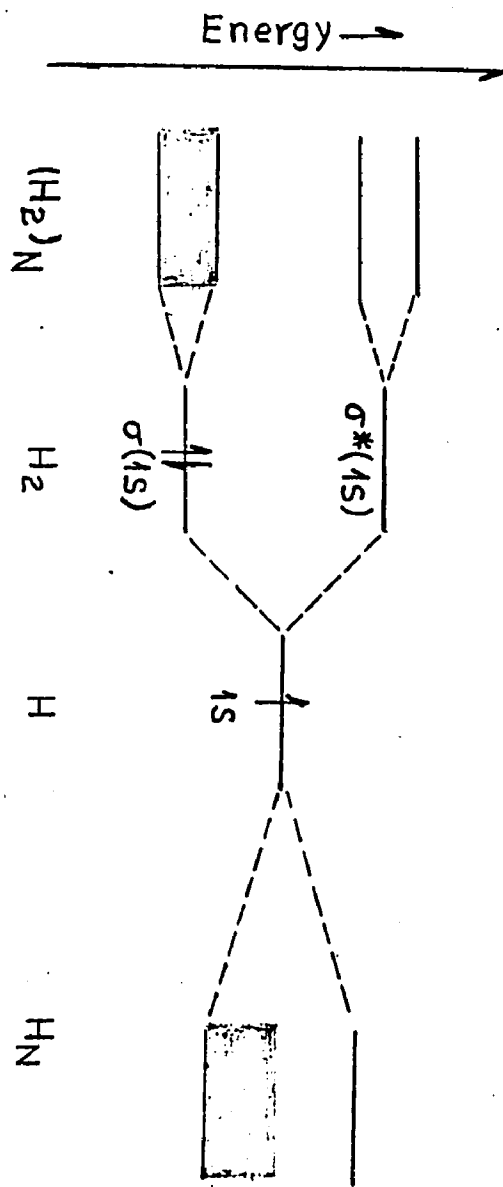


Figure 1

Figure 2

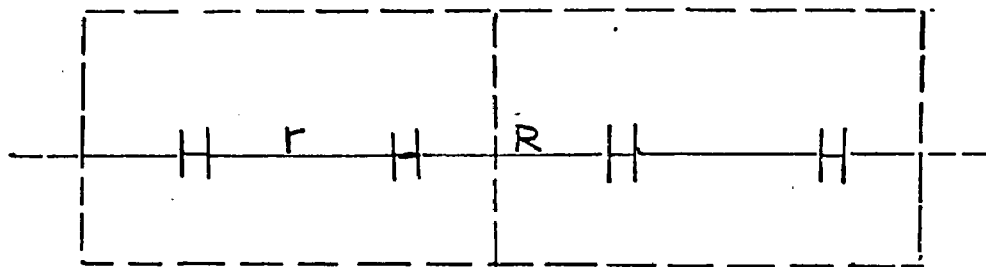


Figure 3

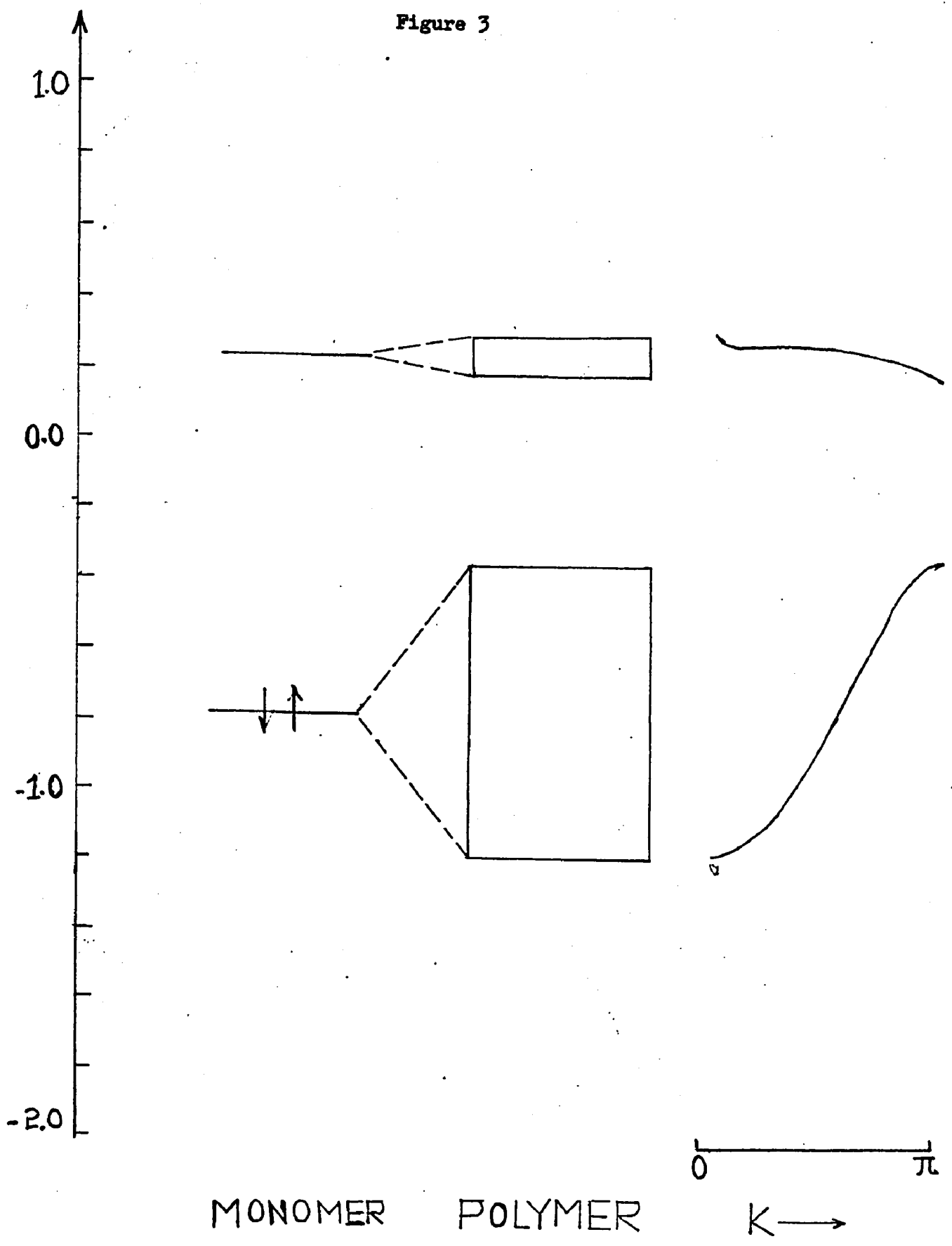


Figure 4

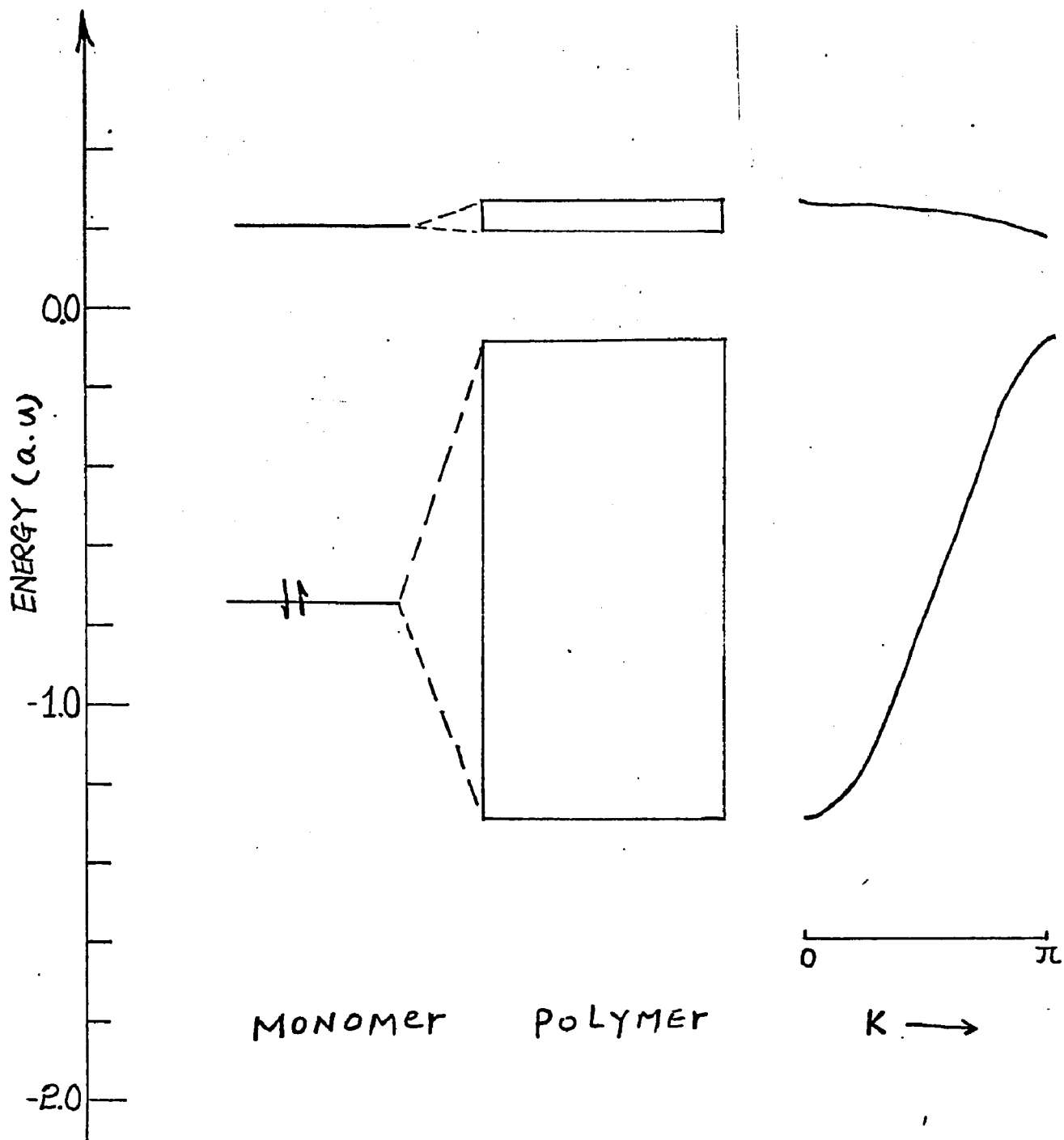


Figure 5

Fig. 5. Electronic energy band structure of polyhydrogen calculated as a function of intermolecular distances using the INDO method.

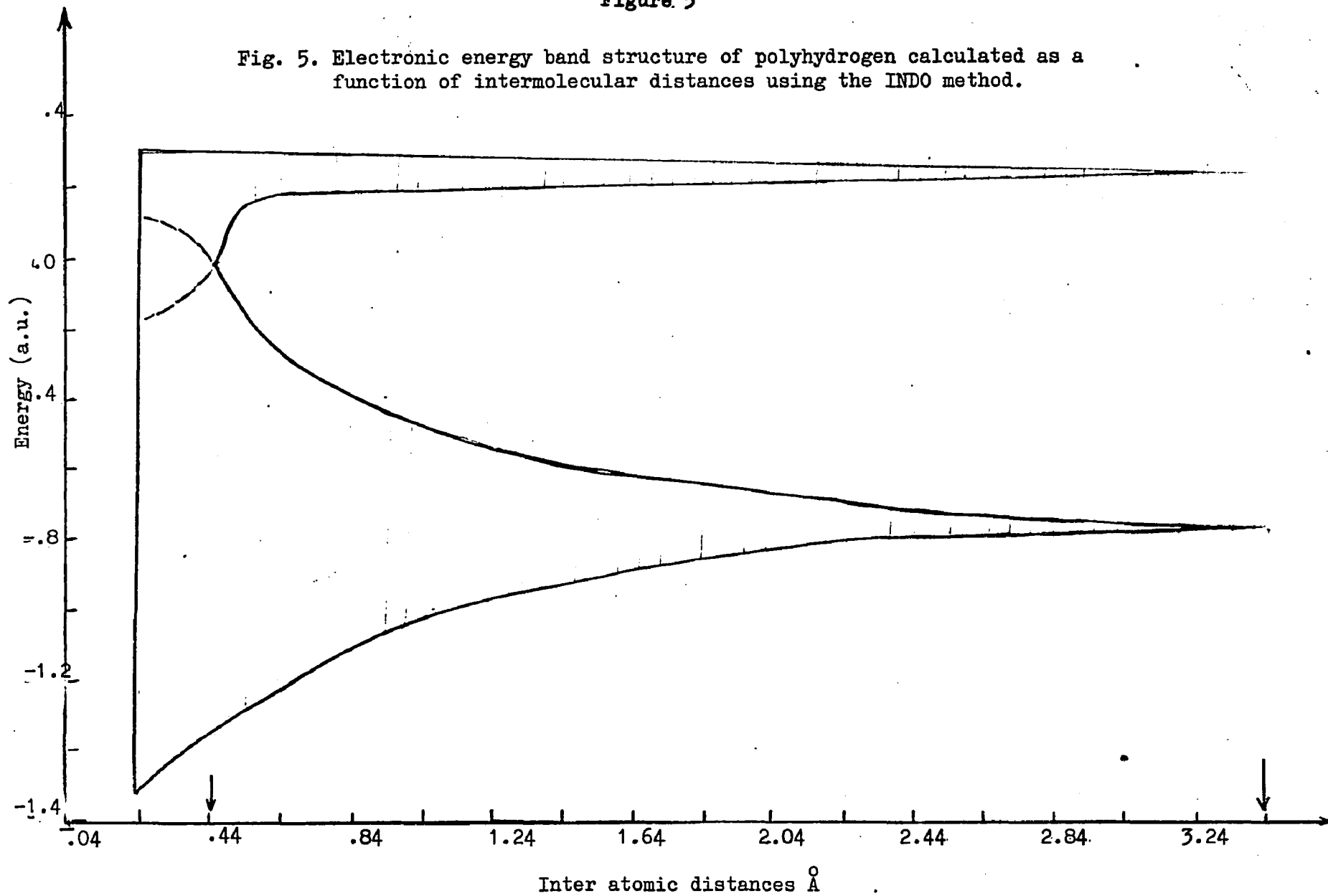
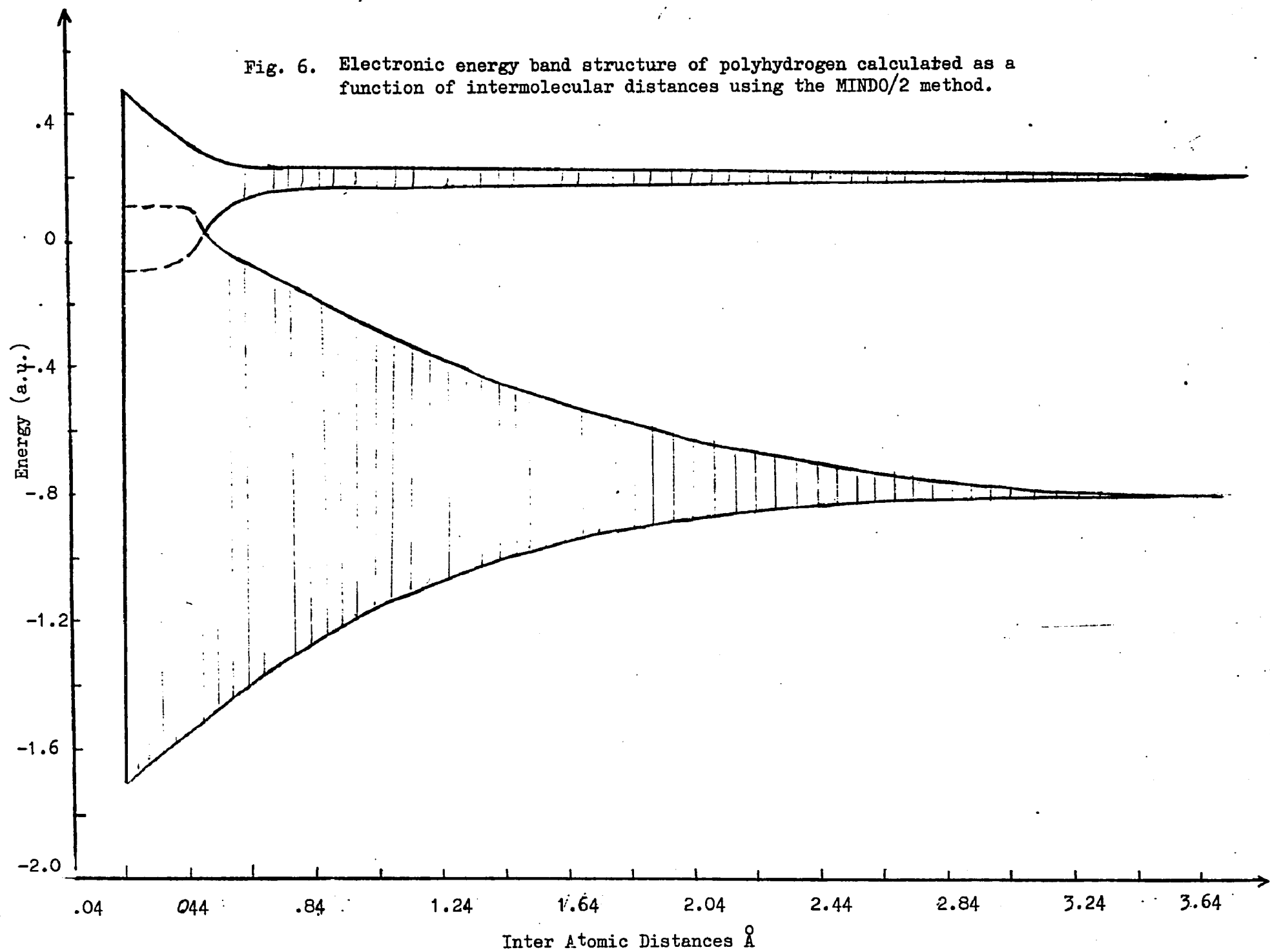


Fig. 6. Electronic energy band structure of polyhydrogen calculated as a function of intermolecular distances using the MINDO/2 method.



895

AFPH995 I.O. 508101 BEVERIDGE 11.17.58. 02/

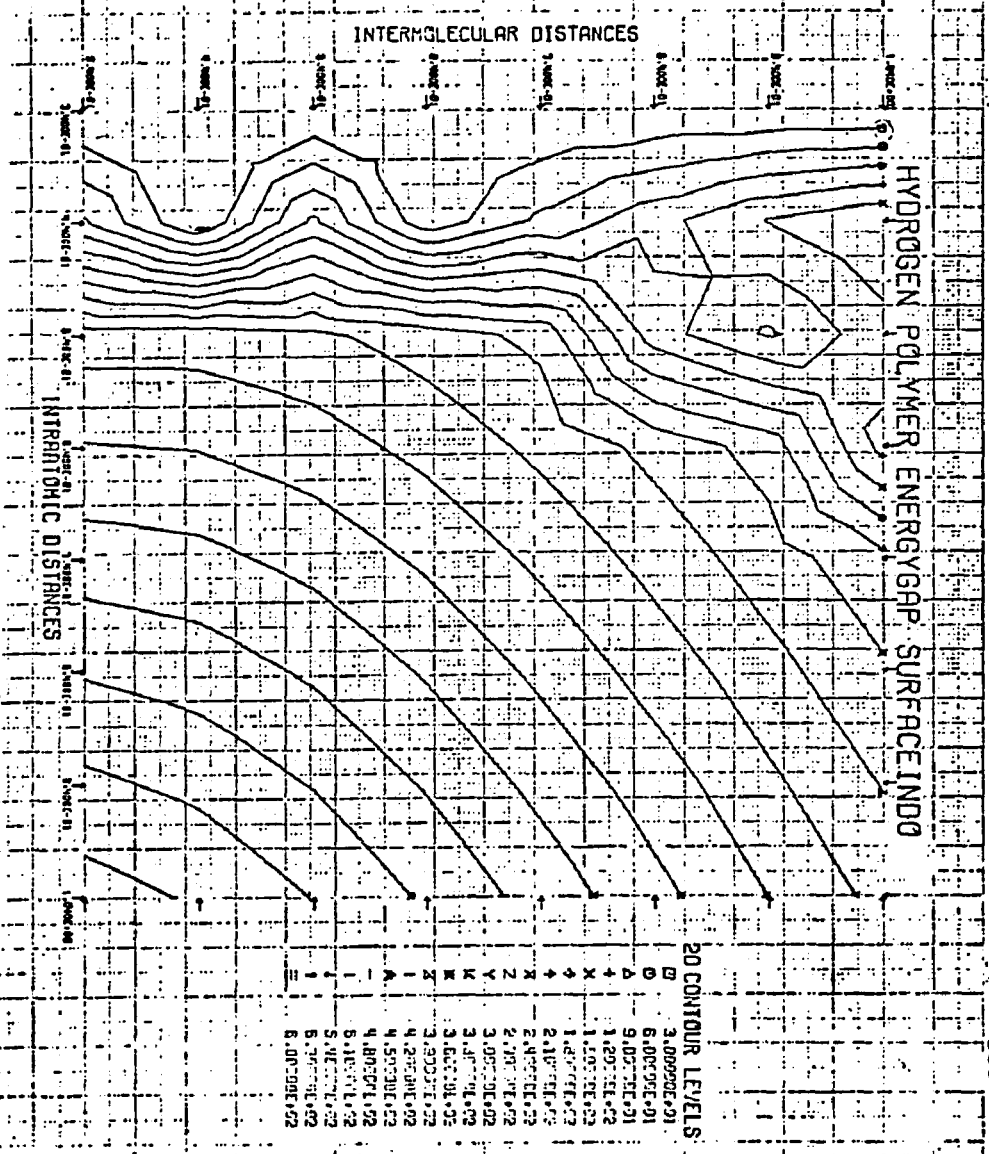


Figure 7

JUNSON SIGLOW INC.

896

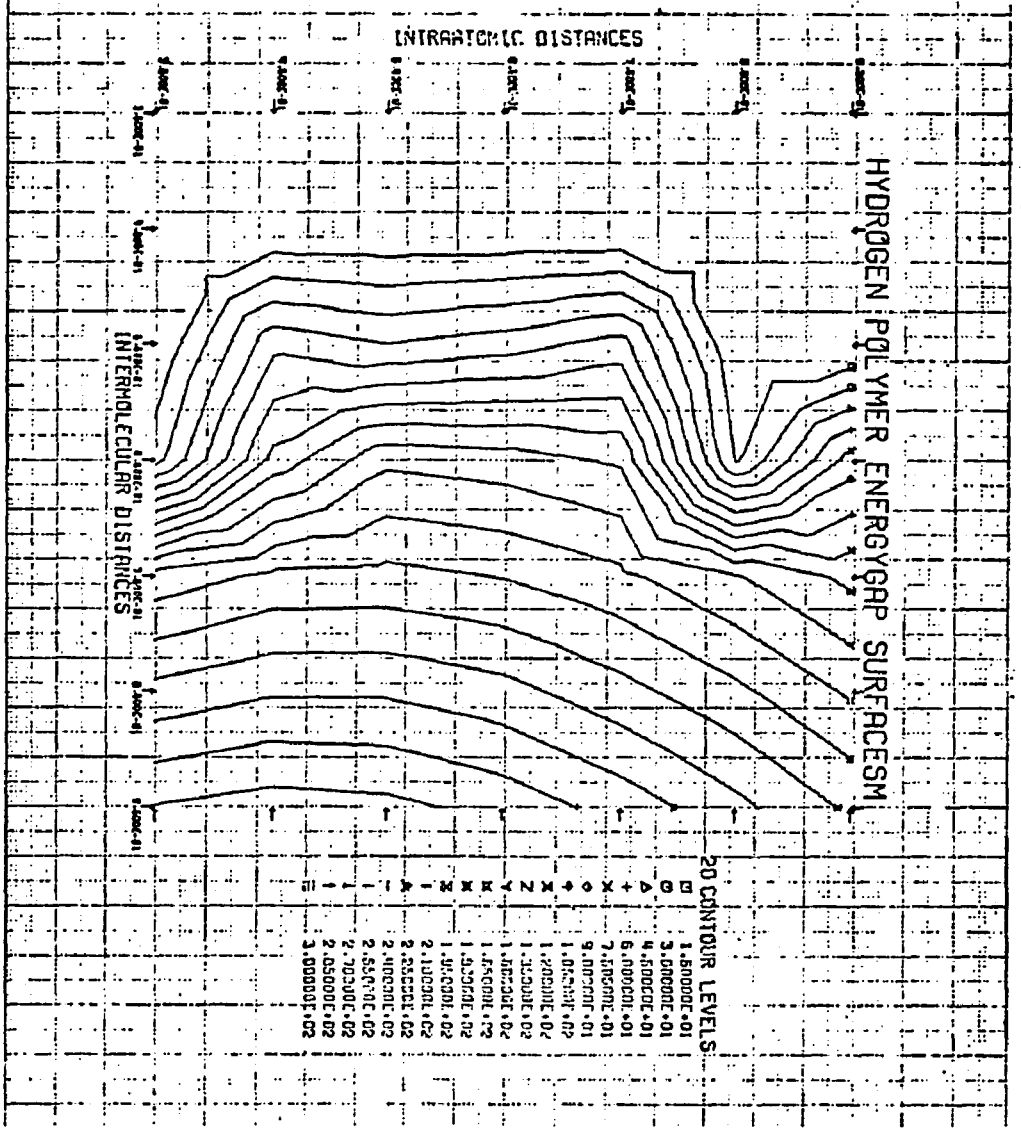


Figure 8

Fig. 9. Energy per unit cell of polyhydrogen calculated as a function of intermolecular distances using the INDO method.

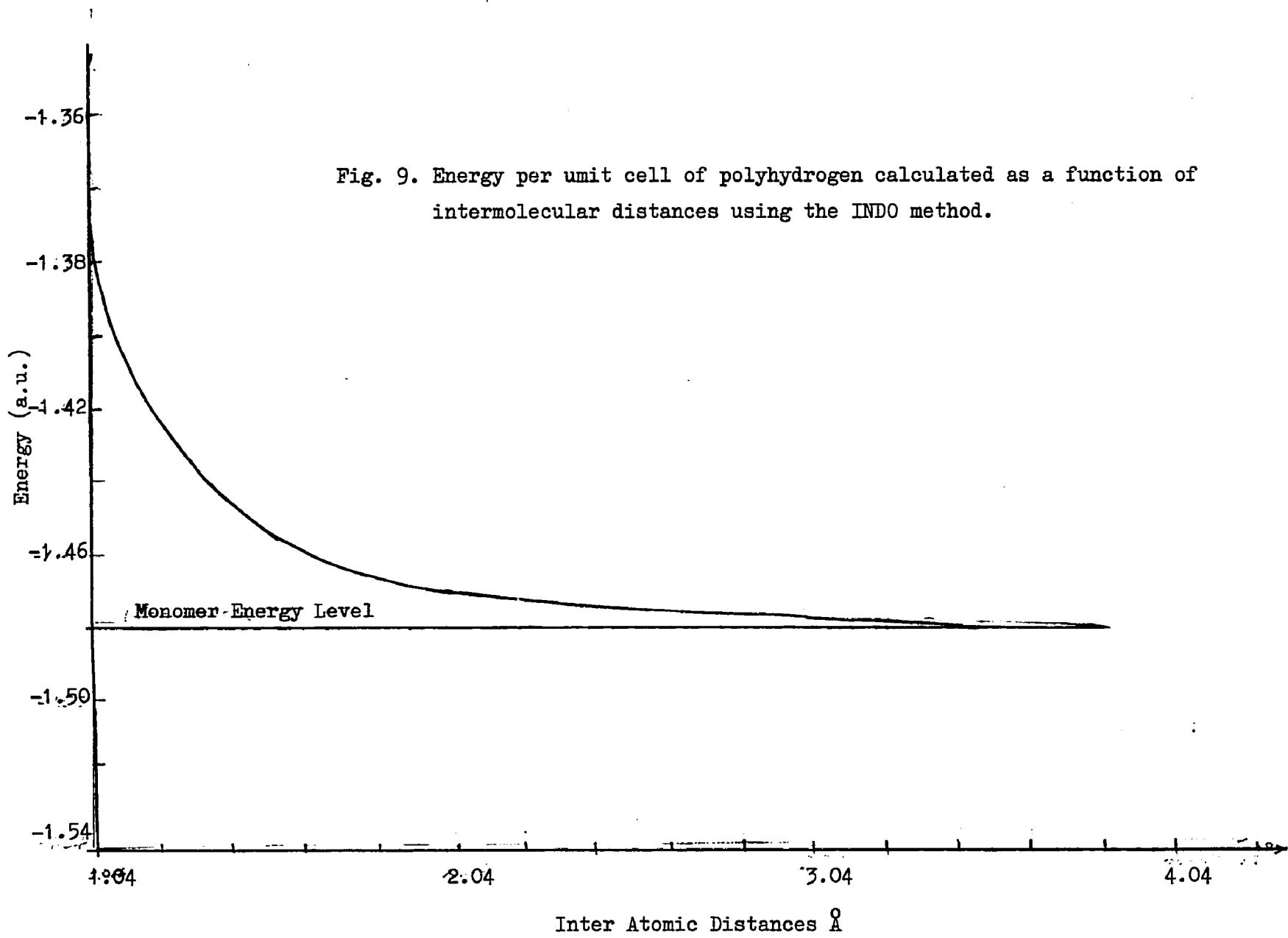


Fig. 10. Energy per unit cell of polyhydrogen calculated as a function of intermolecular distances using the MINDO/2 method.

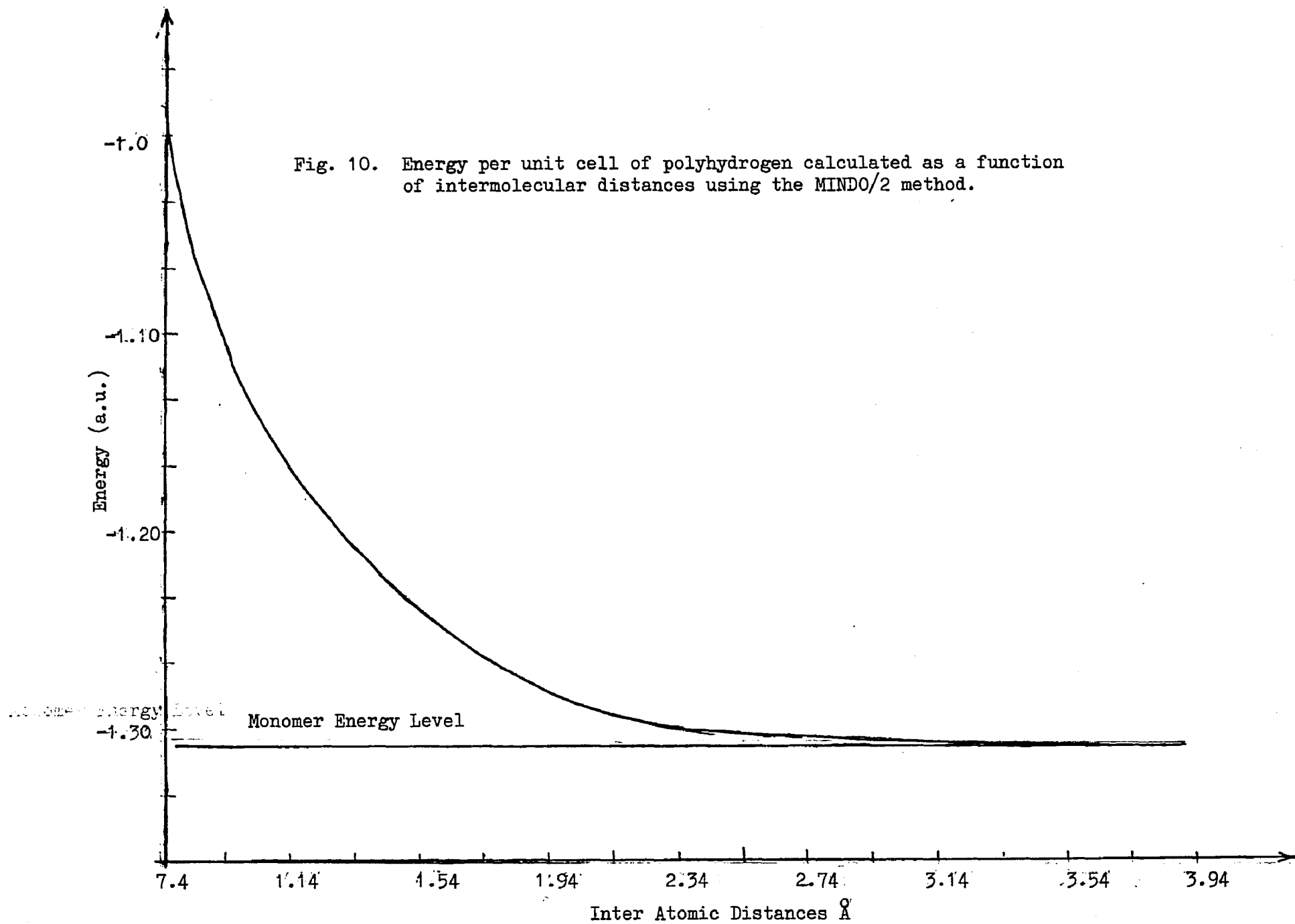


Figure 11

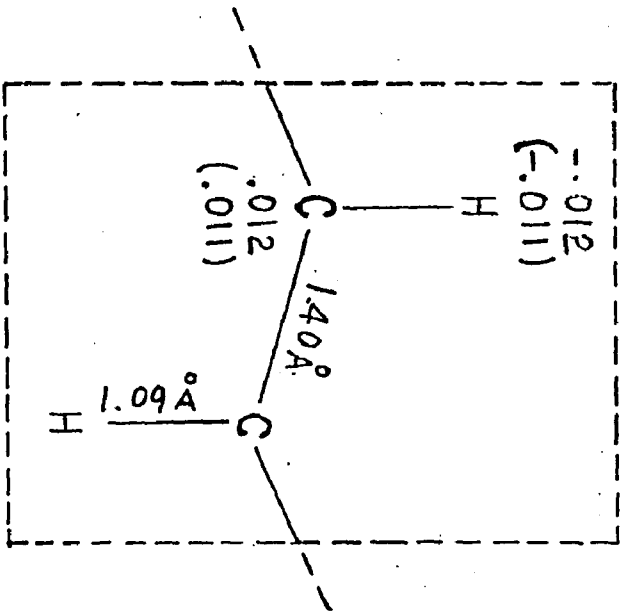


Figure 12

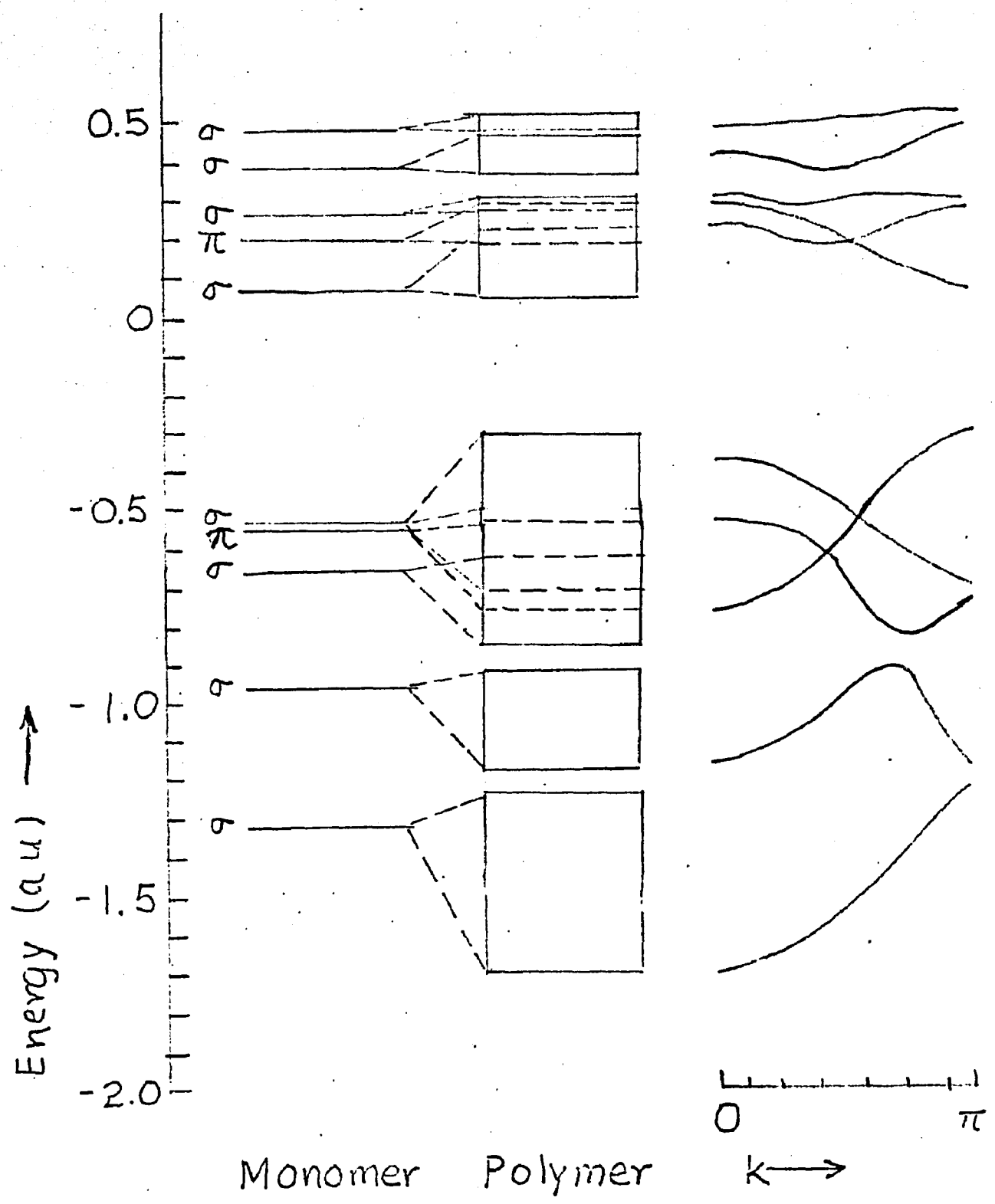
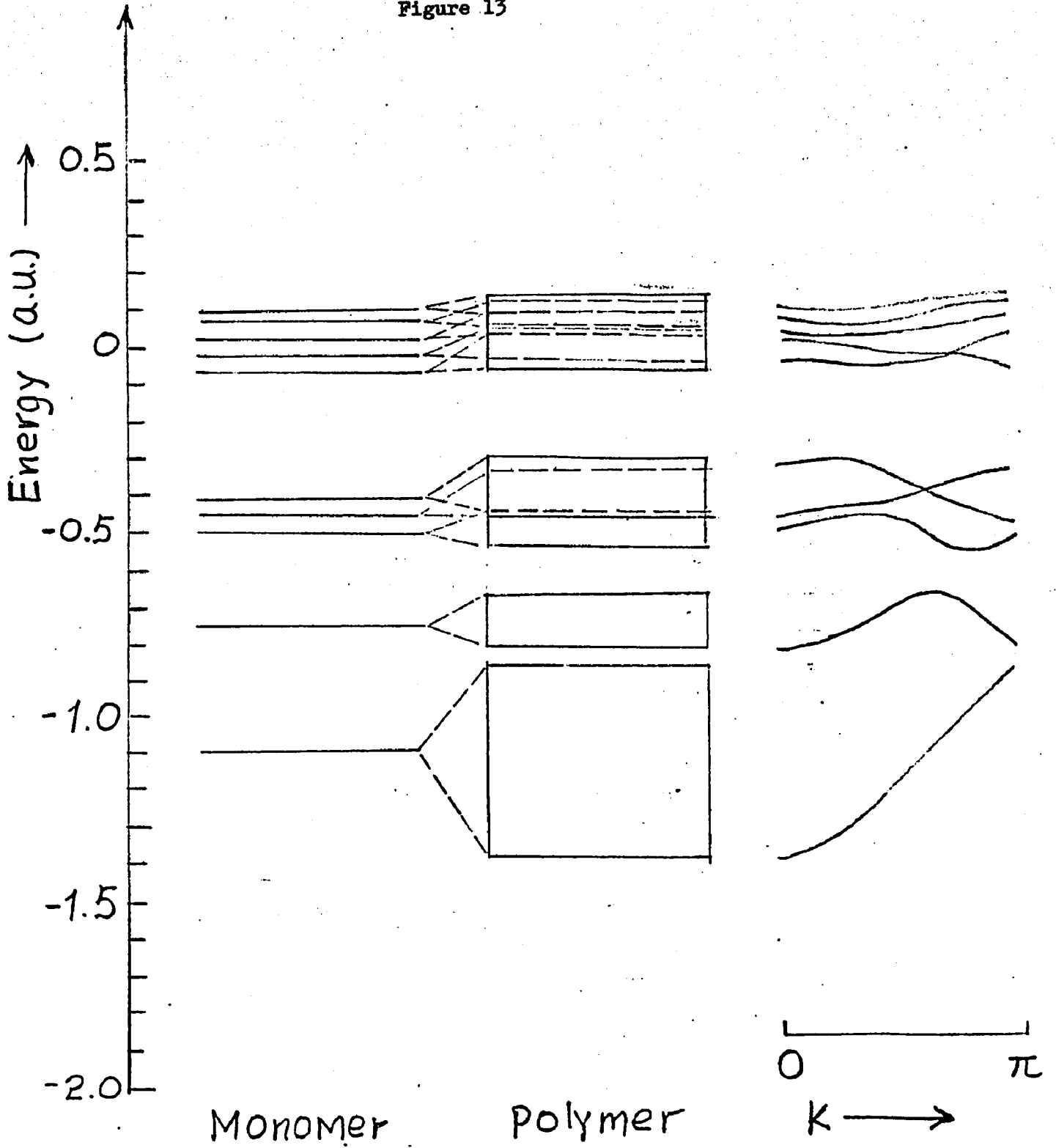


Figure 13



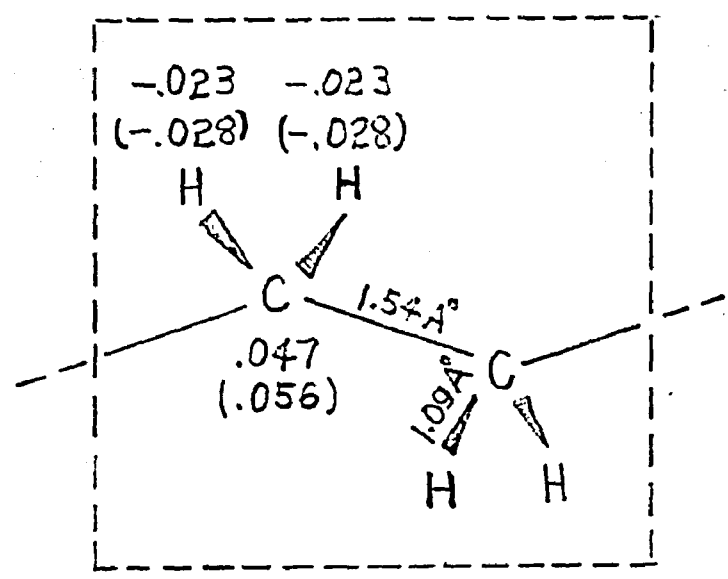


Fig. 14 Elementary cell geometry and calculated net atomic charges for polyethylene using the INDO and MINDO/2 methods. MINDO/2 values are in parentheses.

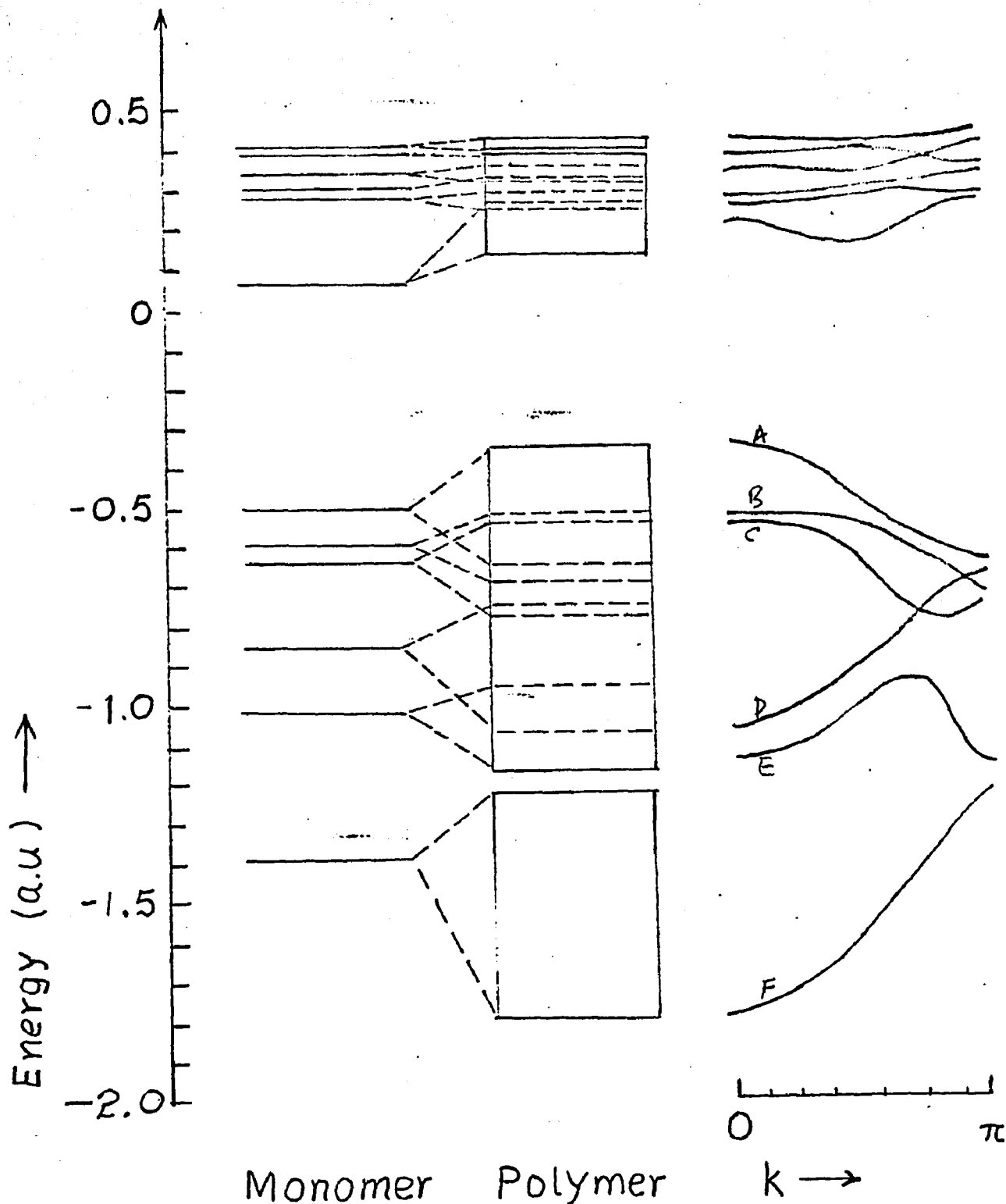


Fig. 15 Electronic energy band structure of polyethylene calculated using the INDO method.

Figure 16

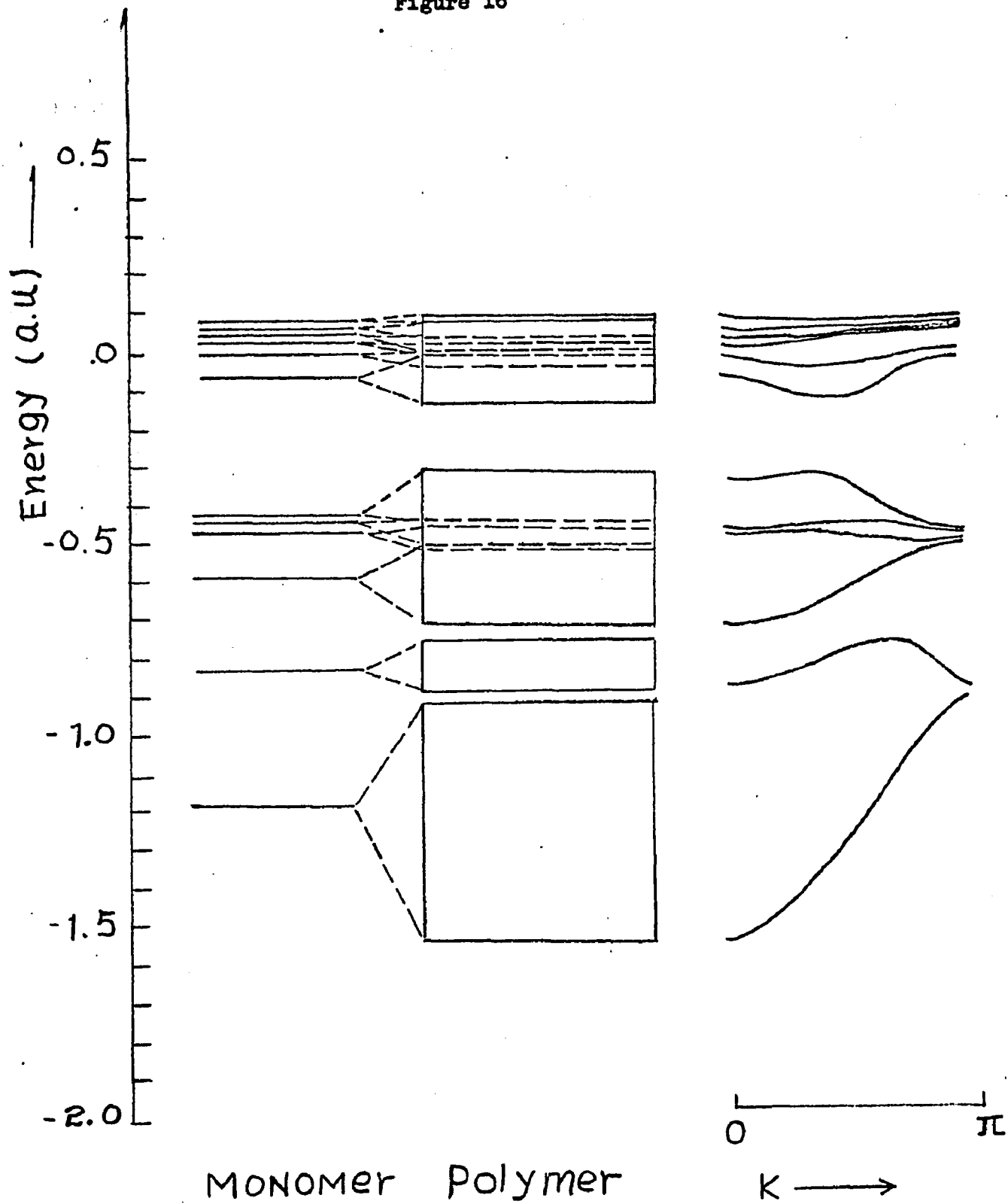


Figure 17

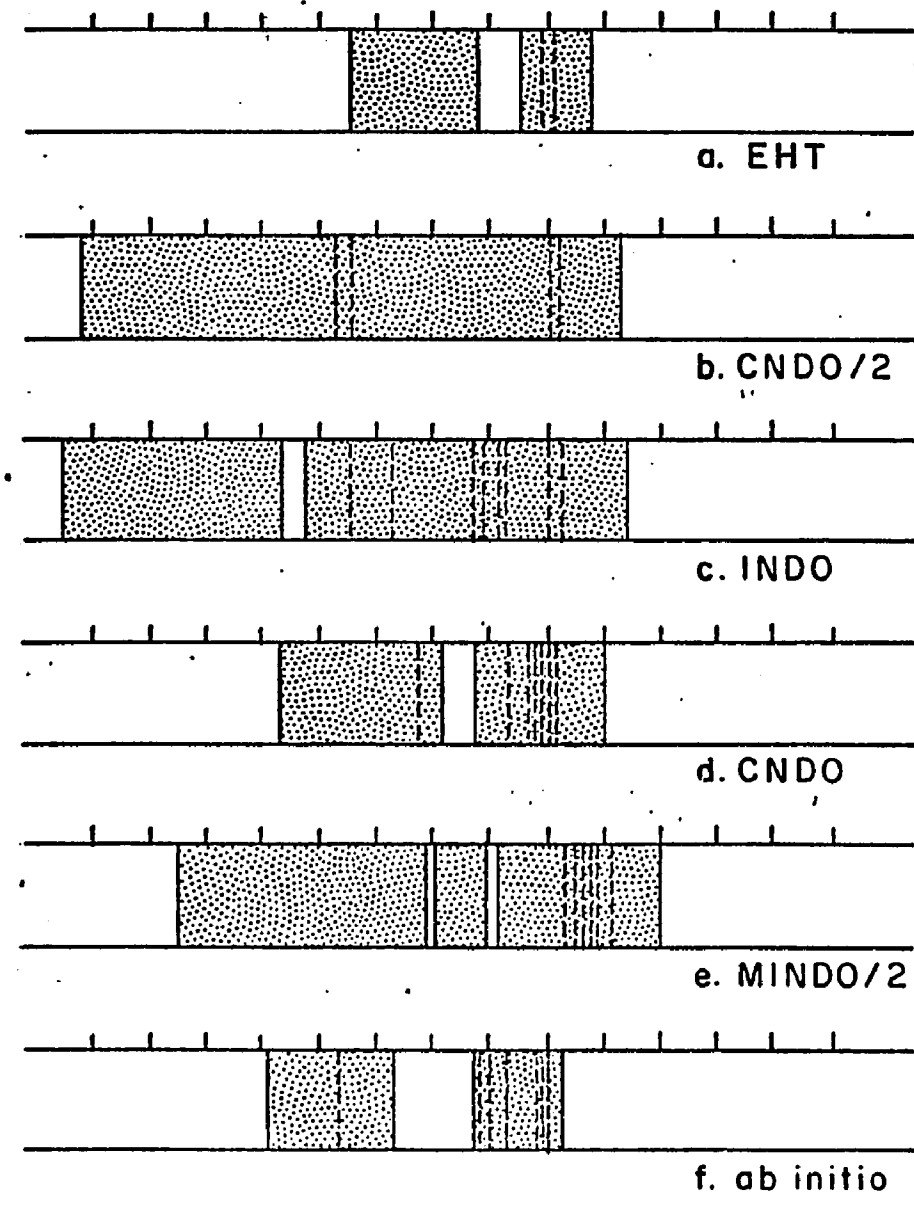
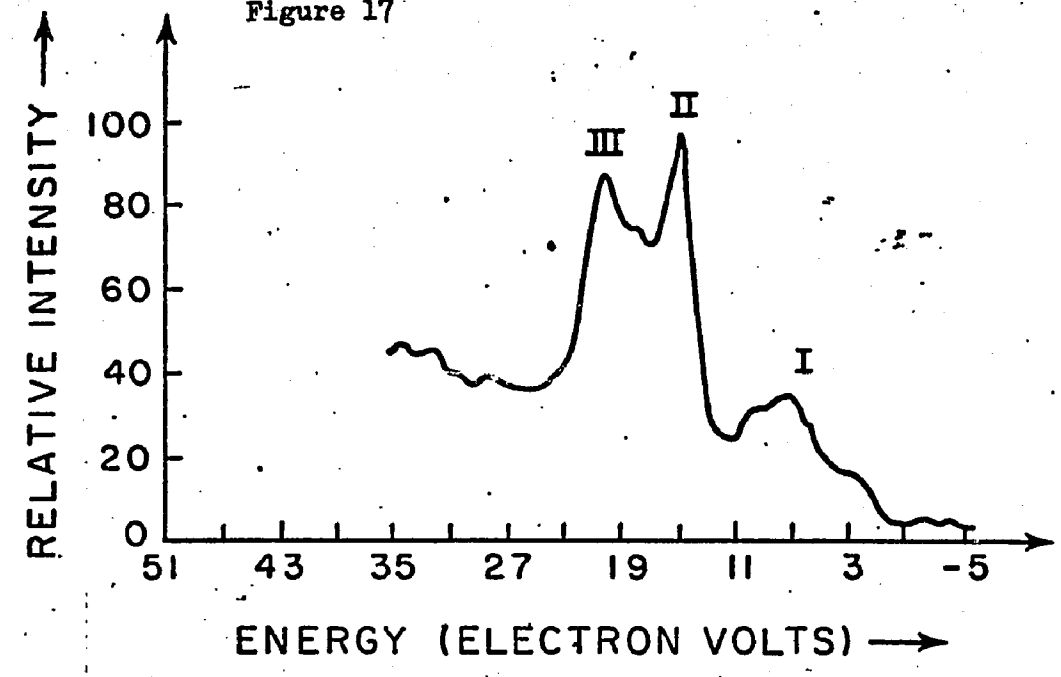


Figure 18

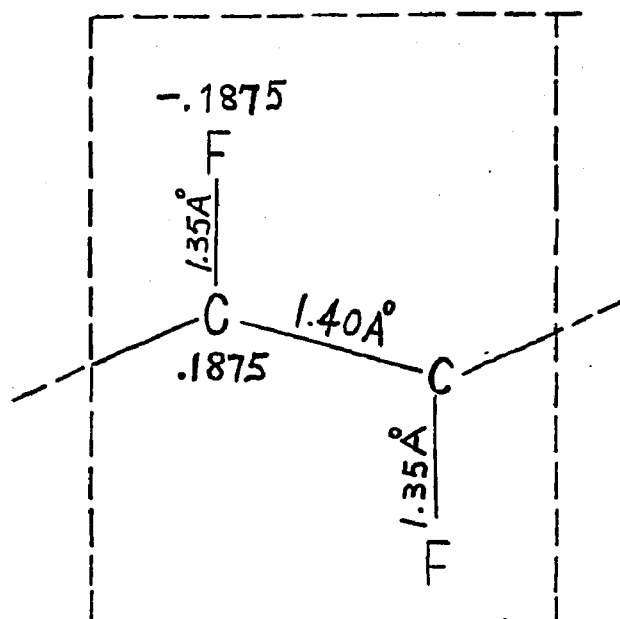


Figure 19

ENERGY BAND STRUCTURES F-SUBSTITUTED POLYACETYLENE

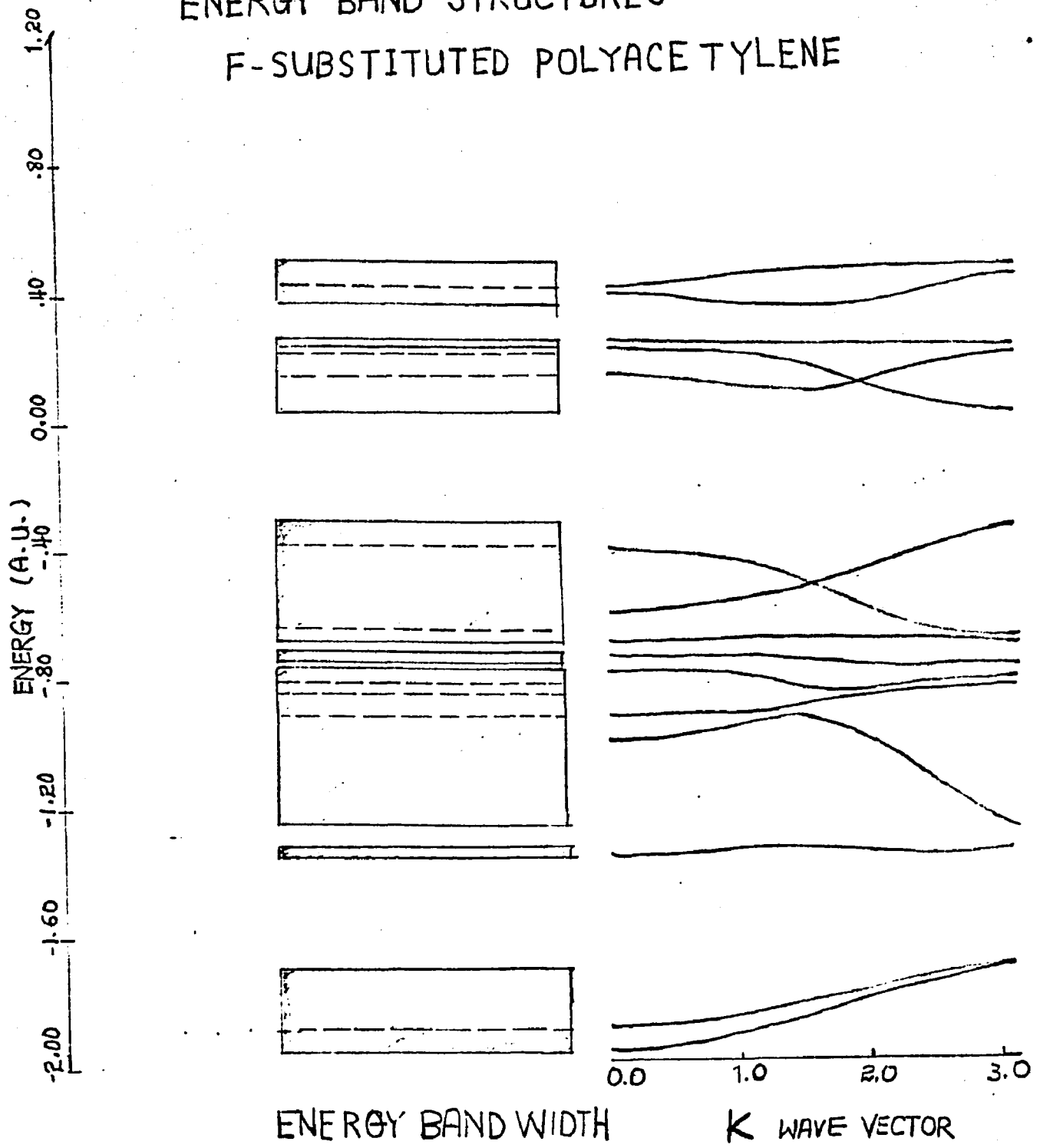


Figure 120

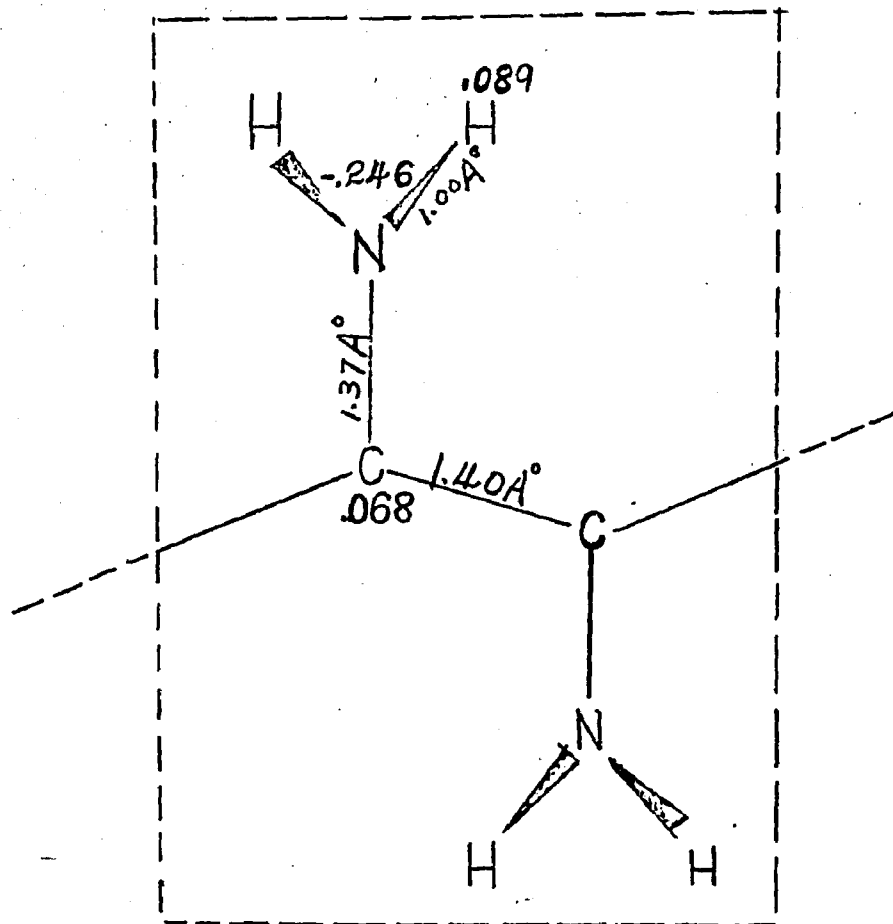


Figure 21

ENERGY BAND STRUCTURES NH₂-SUBSTITUTED POLYACETYLENE

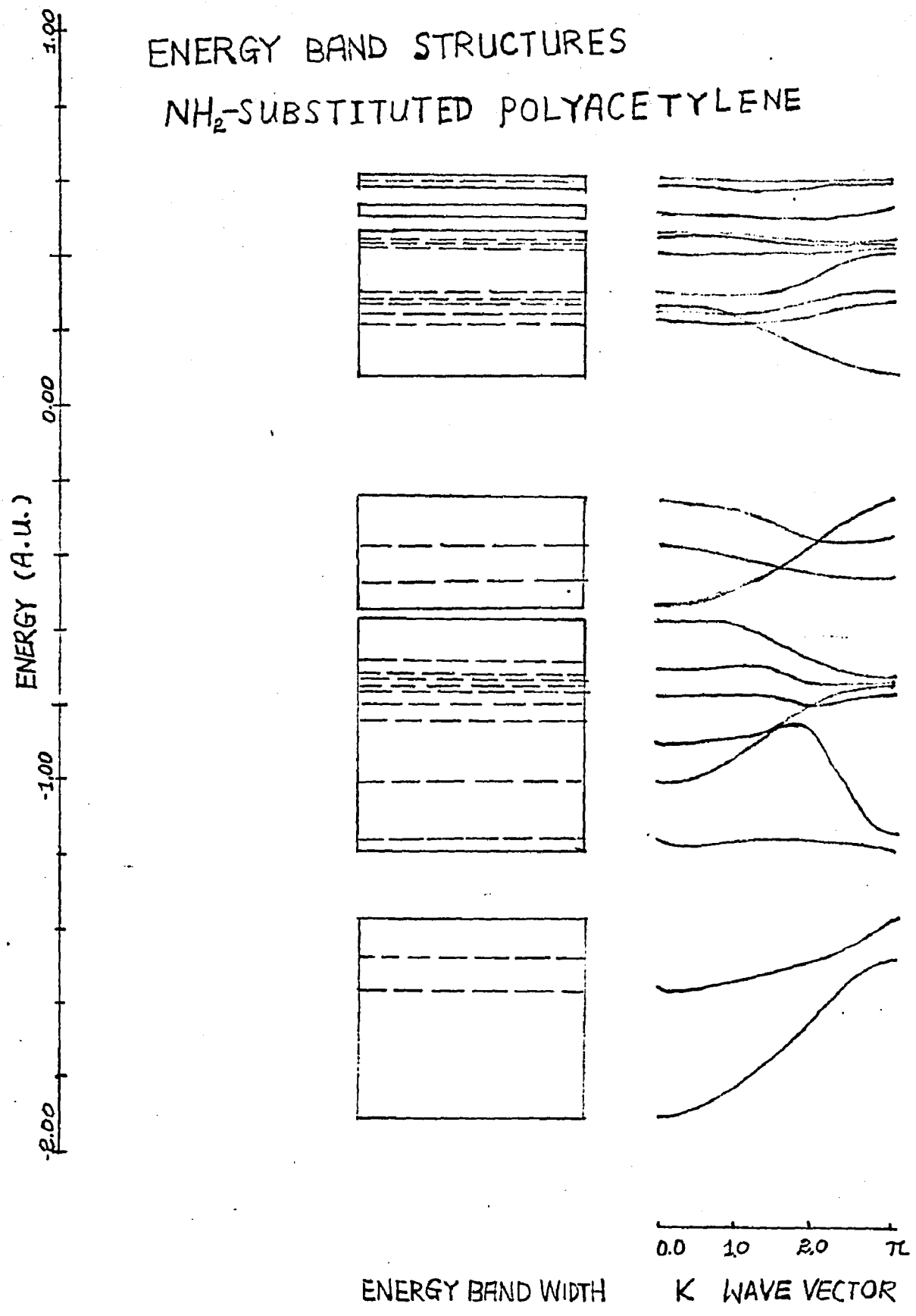


Figure 23

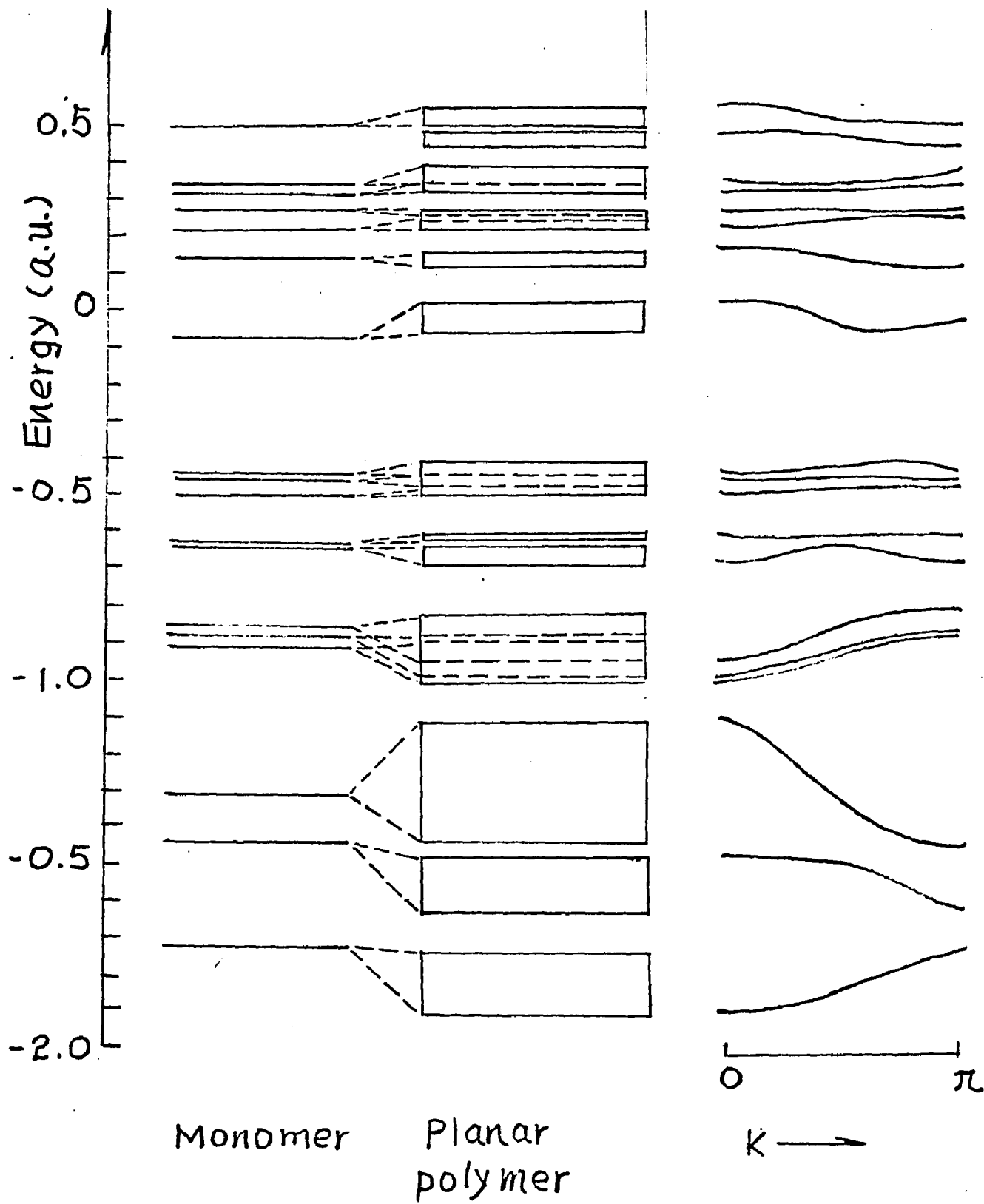


Figure 24

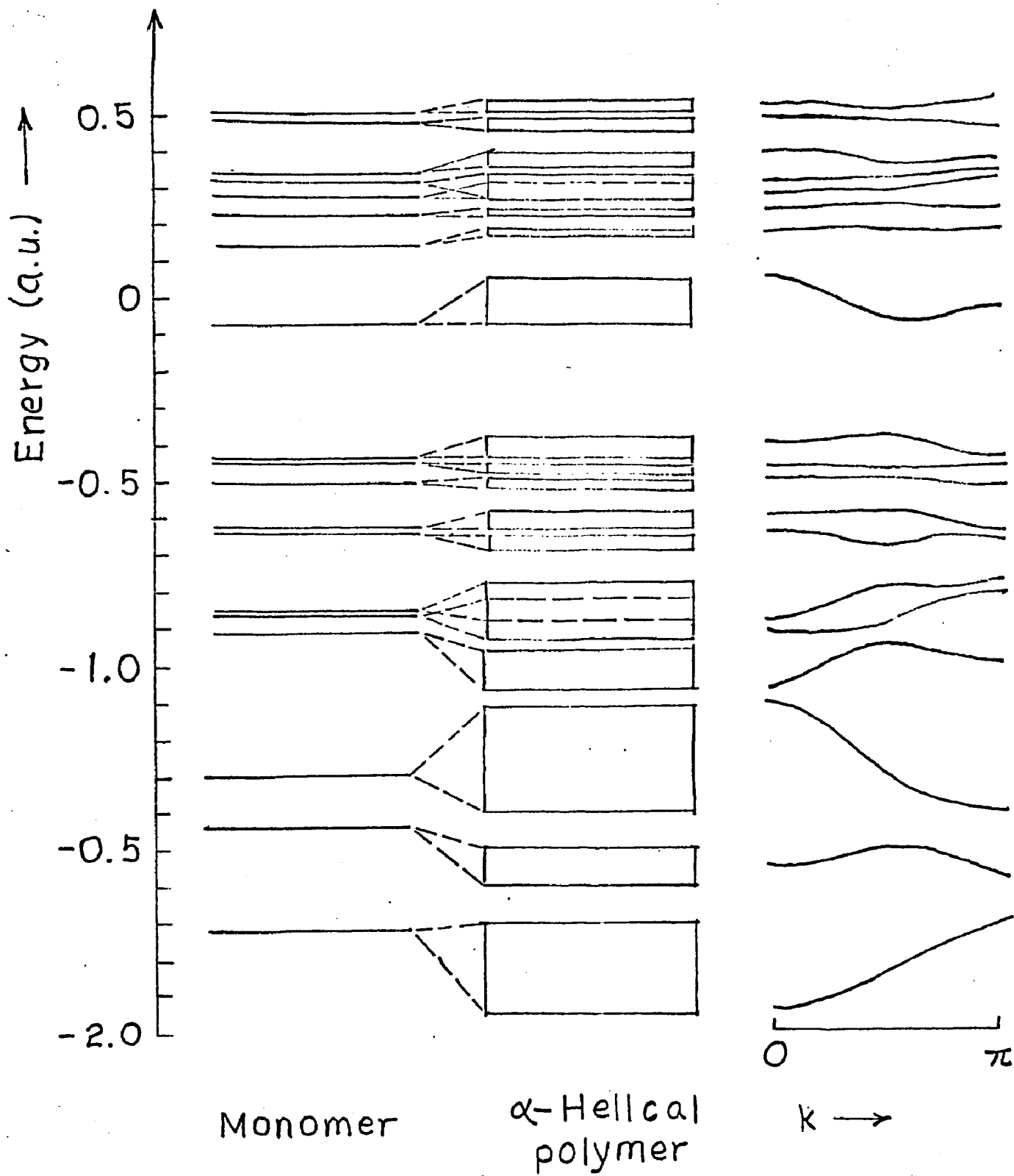


Figure 25

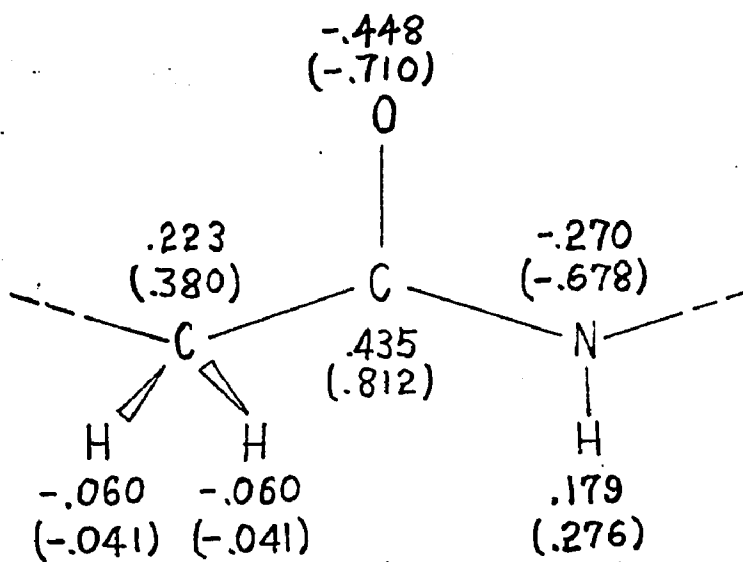


Figure 26

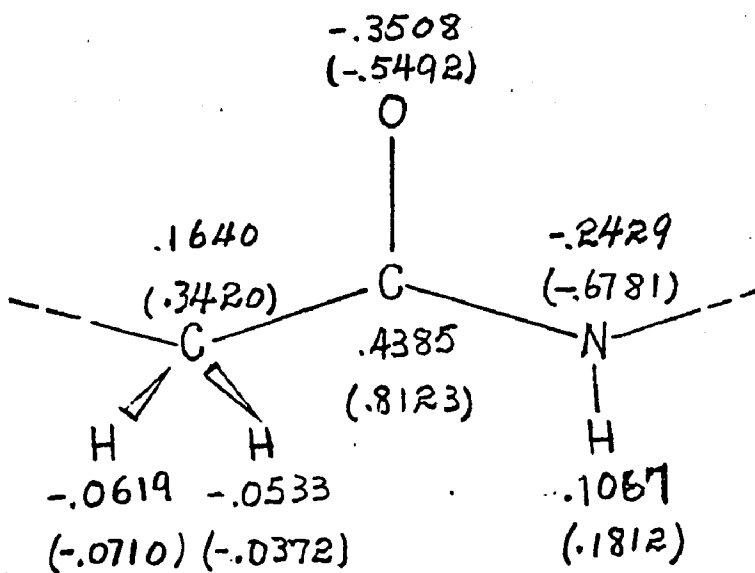


Figure 27

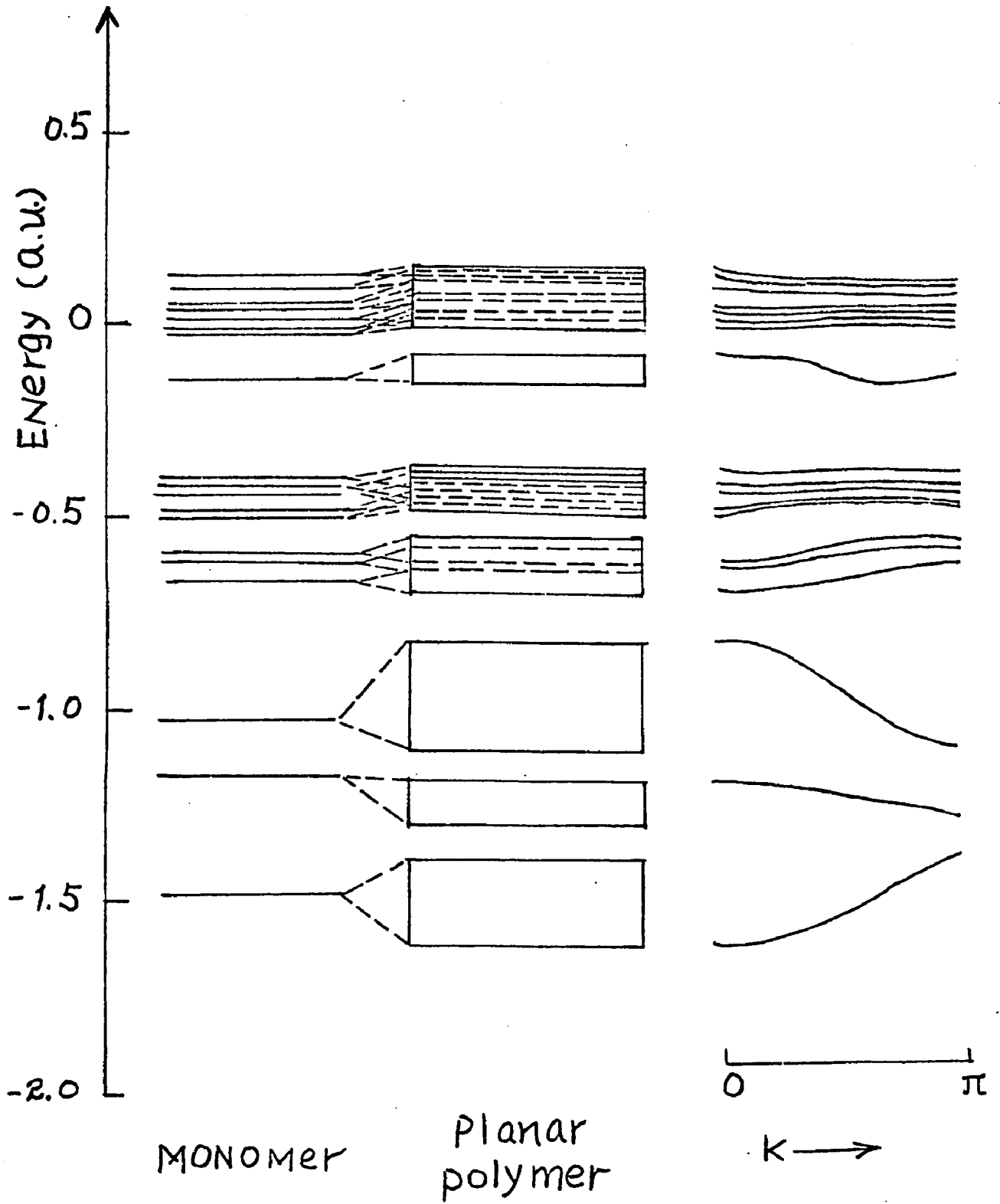


Figure 28

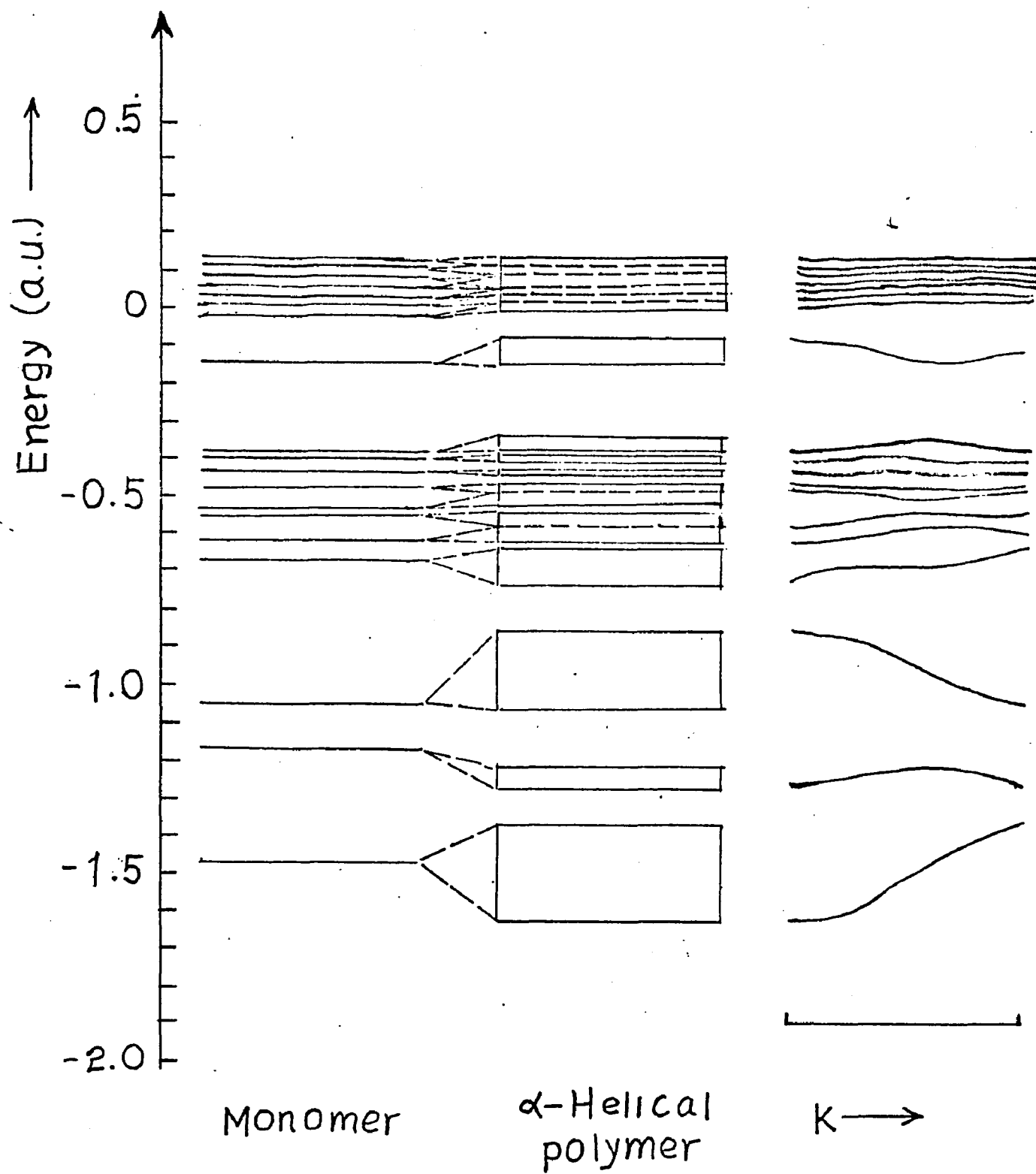


Figure 29

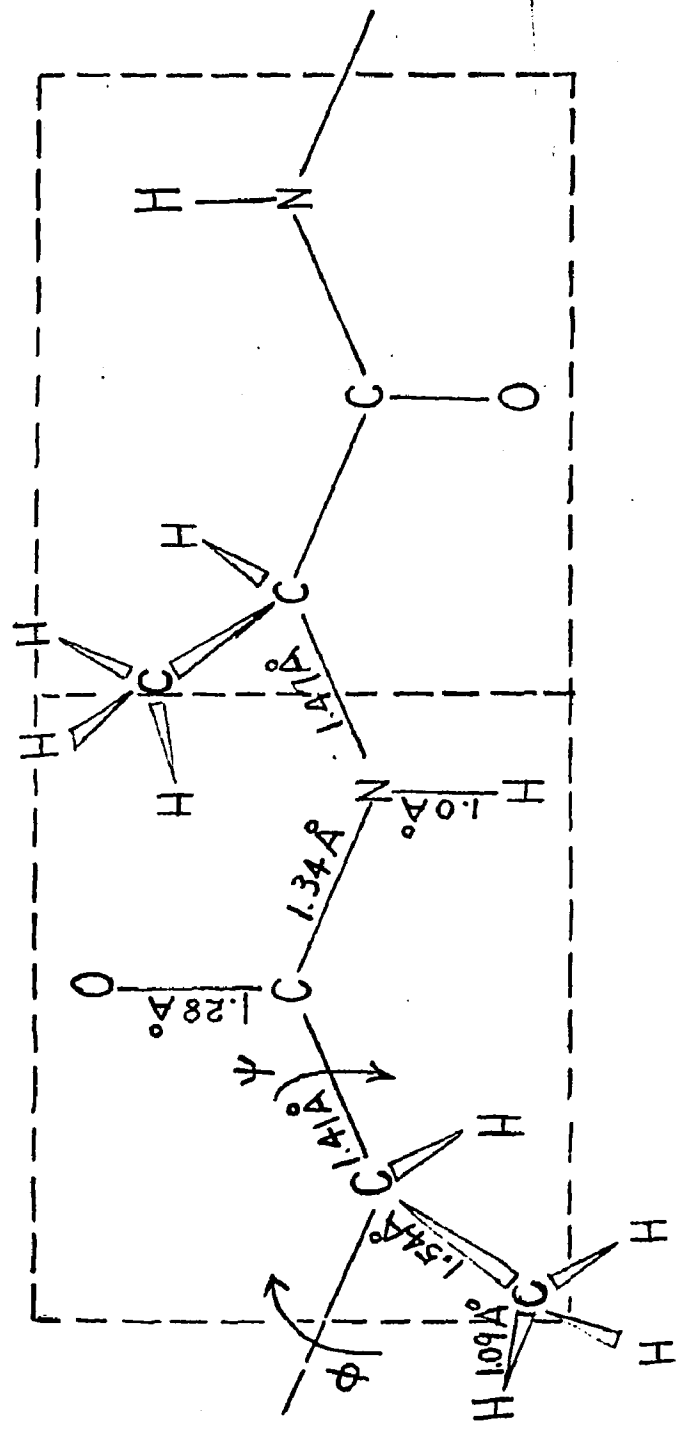


Figure 30

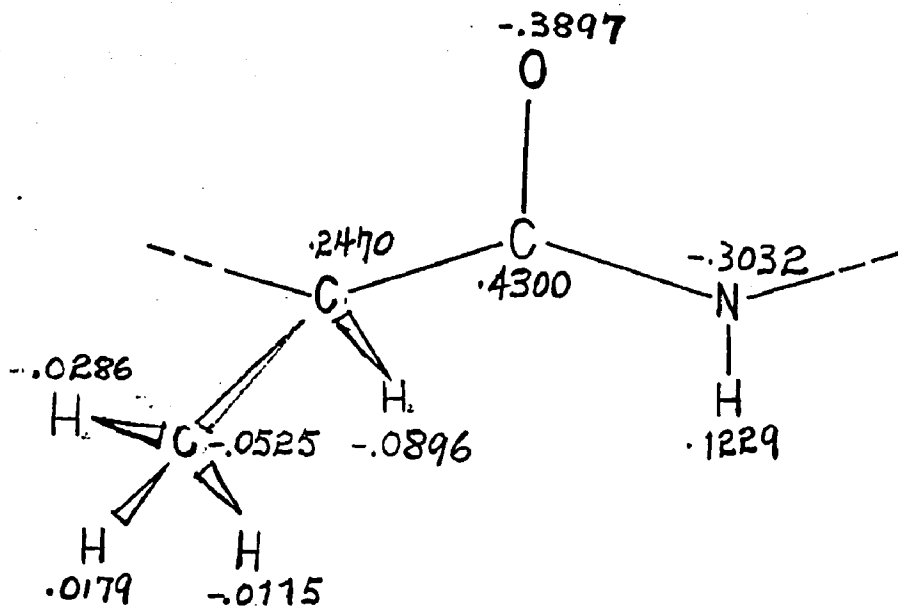


Figure 31

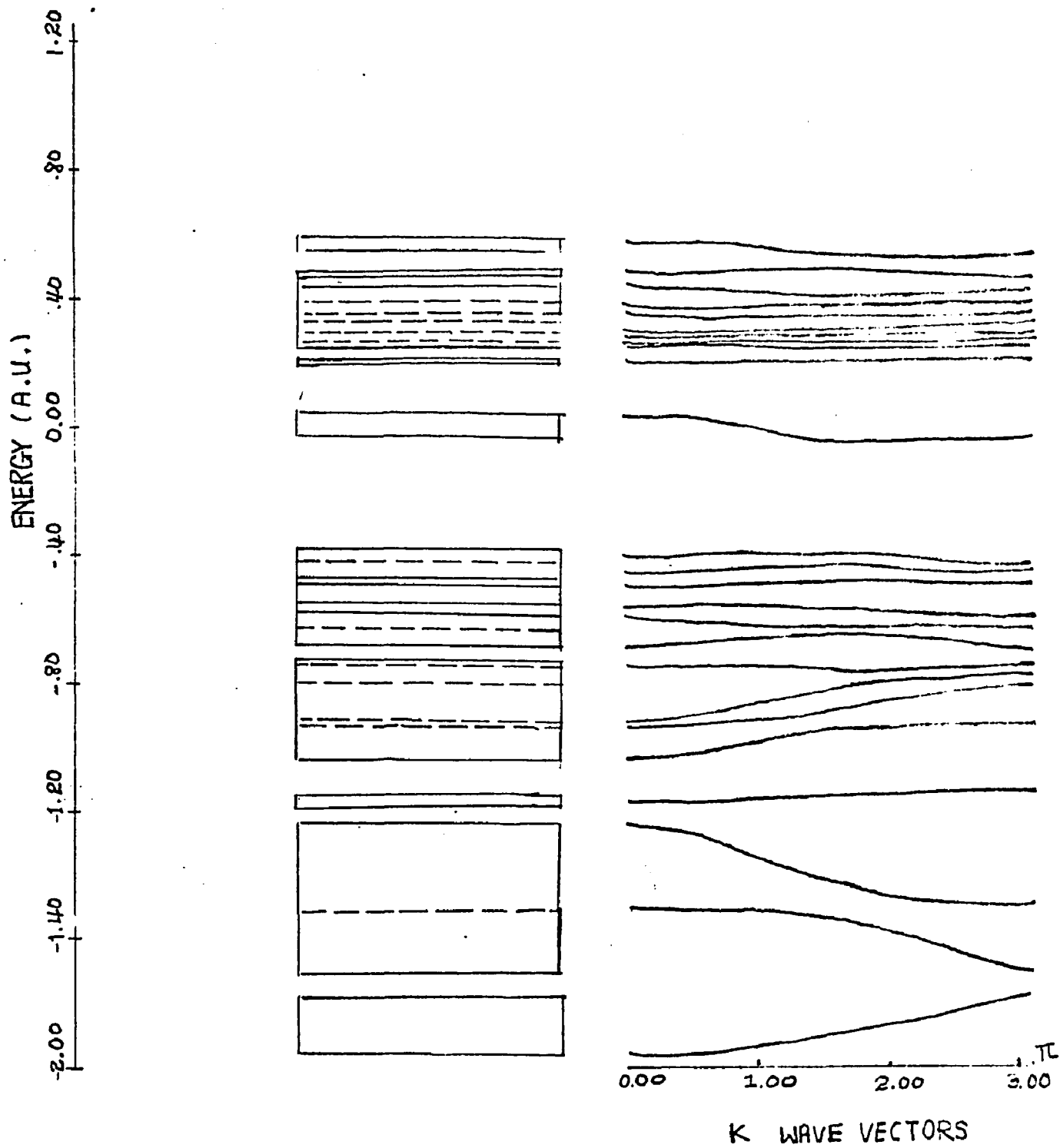
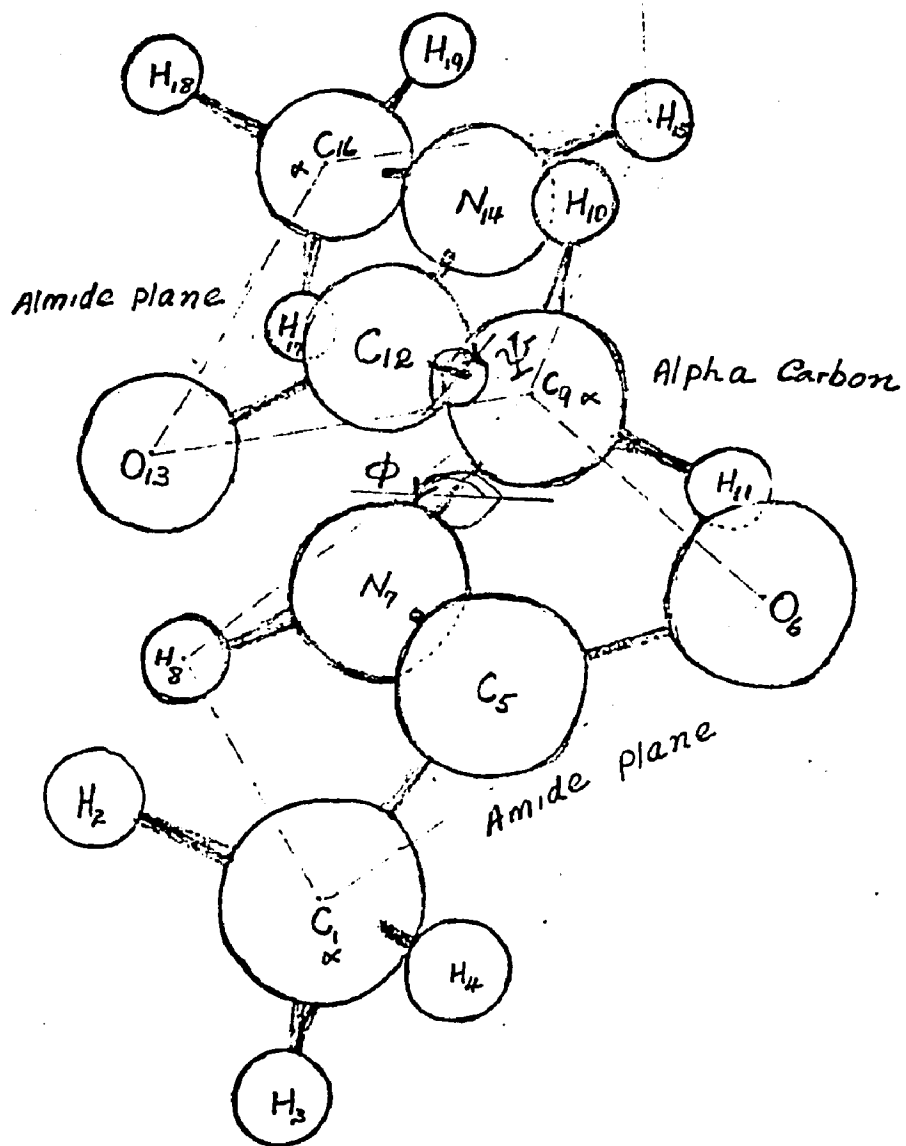
ENERGY BAND STRUCTURES OF
ALPHA POLYGLYCINE-ANILINE

Figure 32



planar dipeptide $\Phi = 0.00$ $\Psi = 0.00$

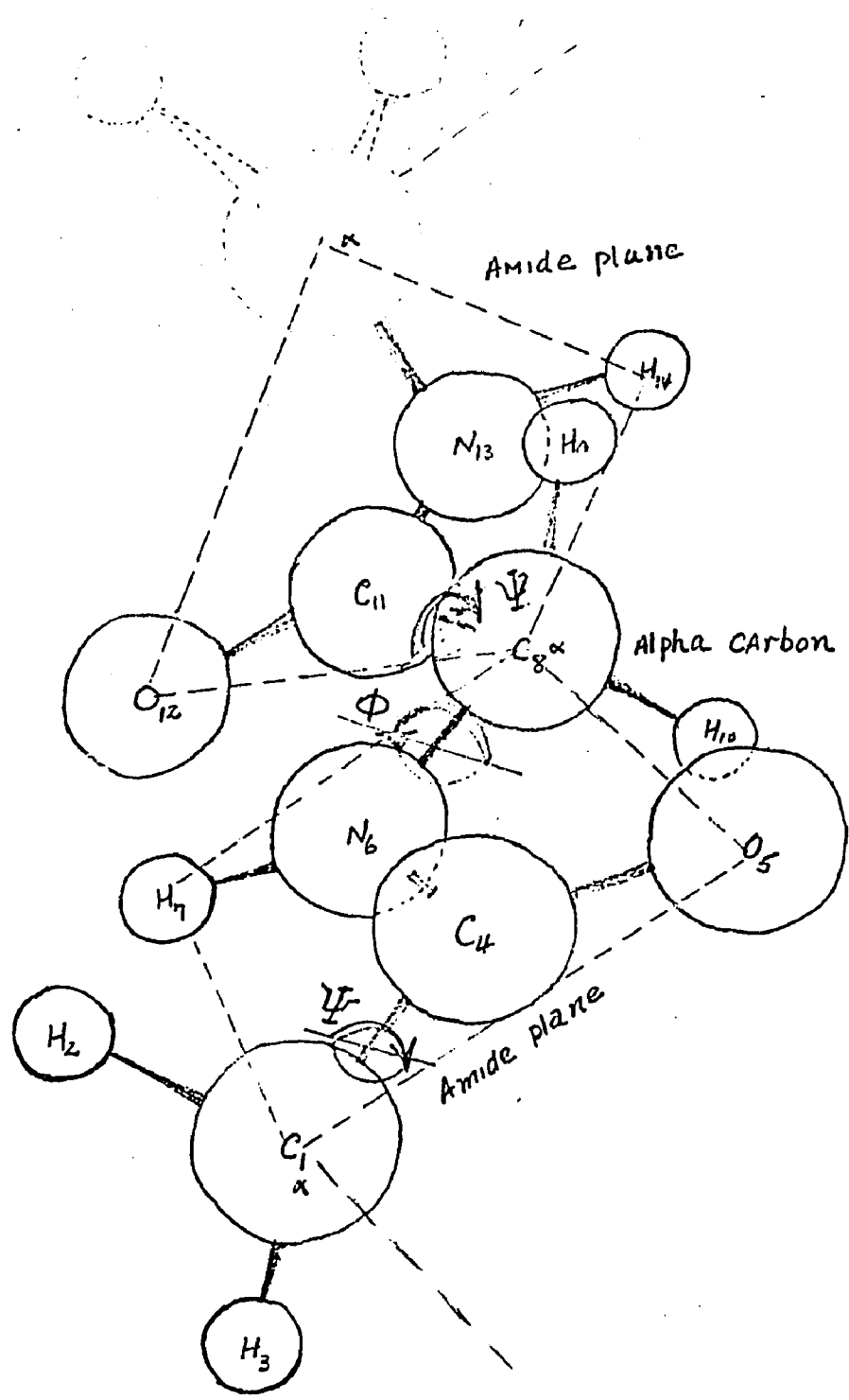


Fig. 33. Elementary cell geometry for polyglycine.

Figure 34

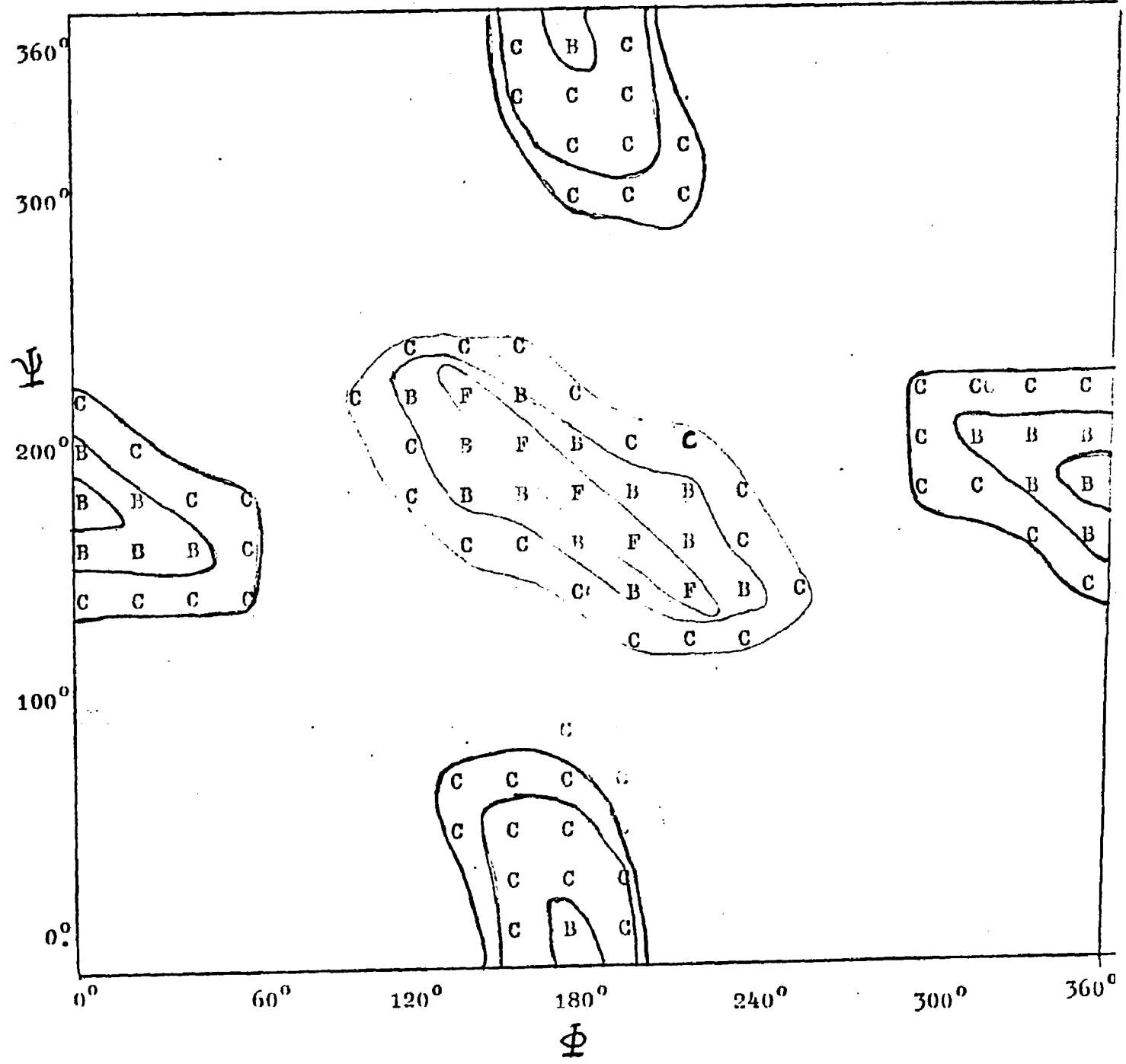


Figure 35

DIPEPTIDE GLYCYL-L-GLYCINE ENERGY SURFACE

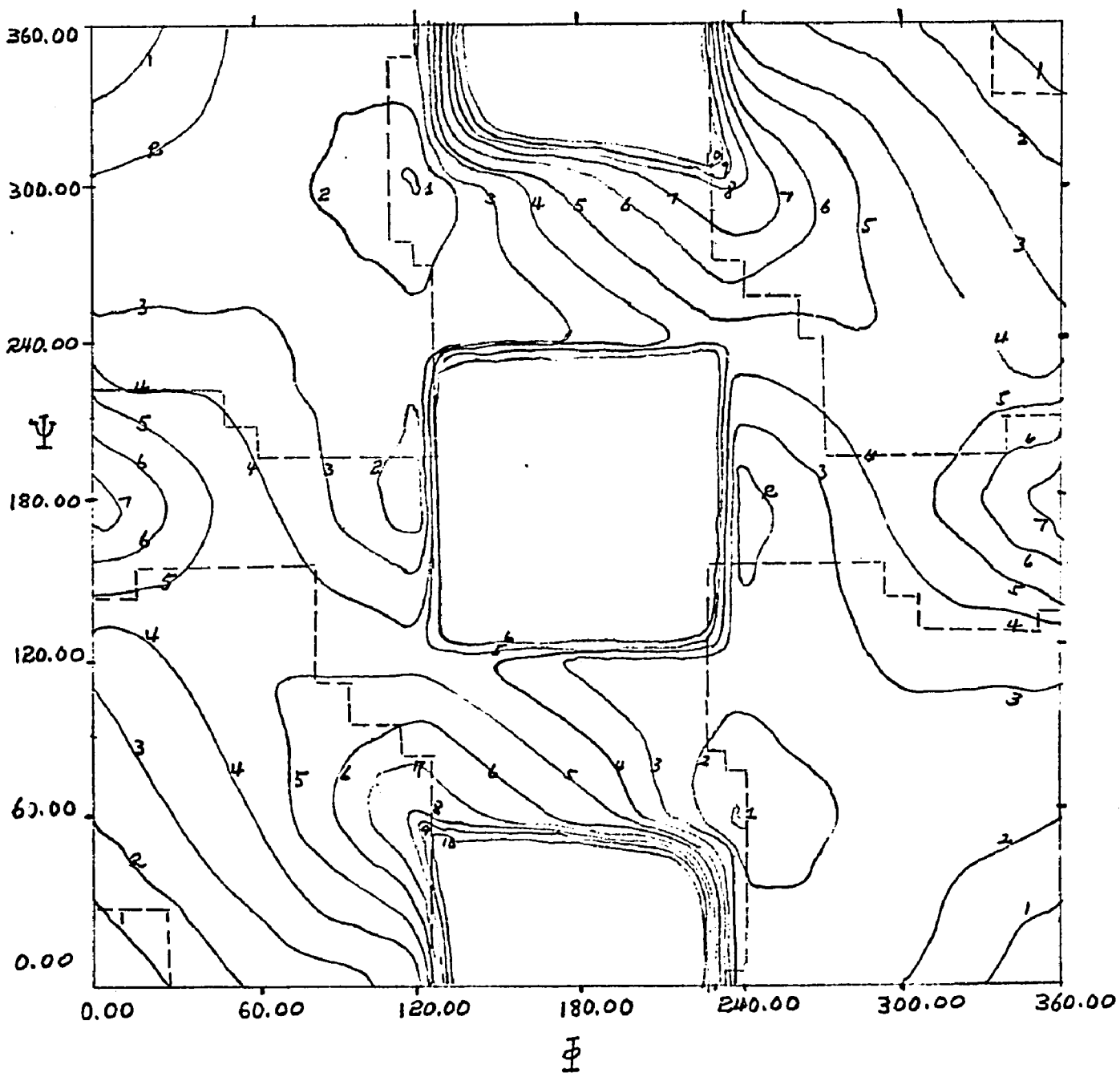


Figure 36

POLYPEPTIDE GLYCYL-L-GLYCINE ENERGY SURFACE

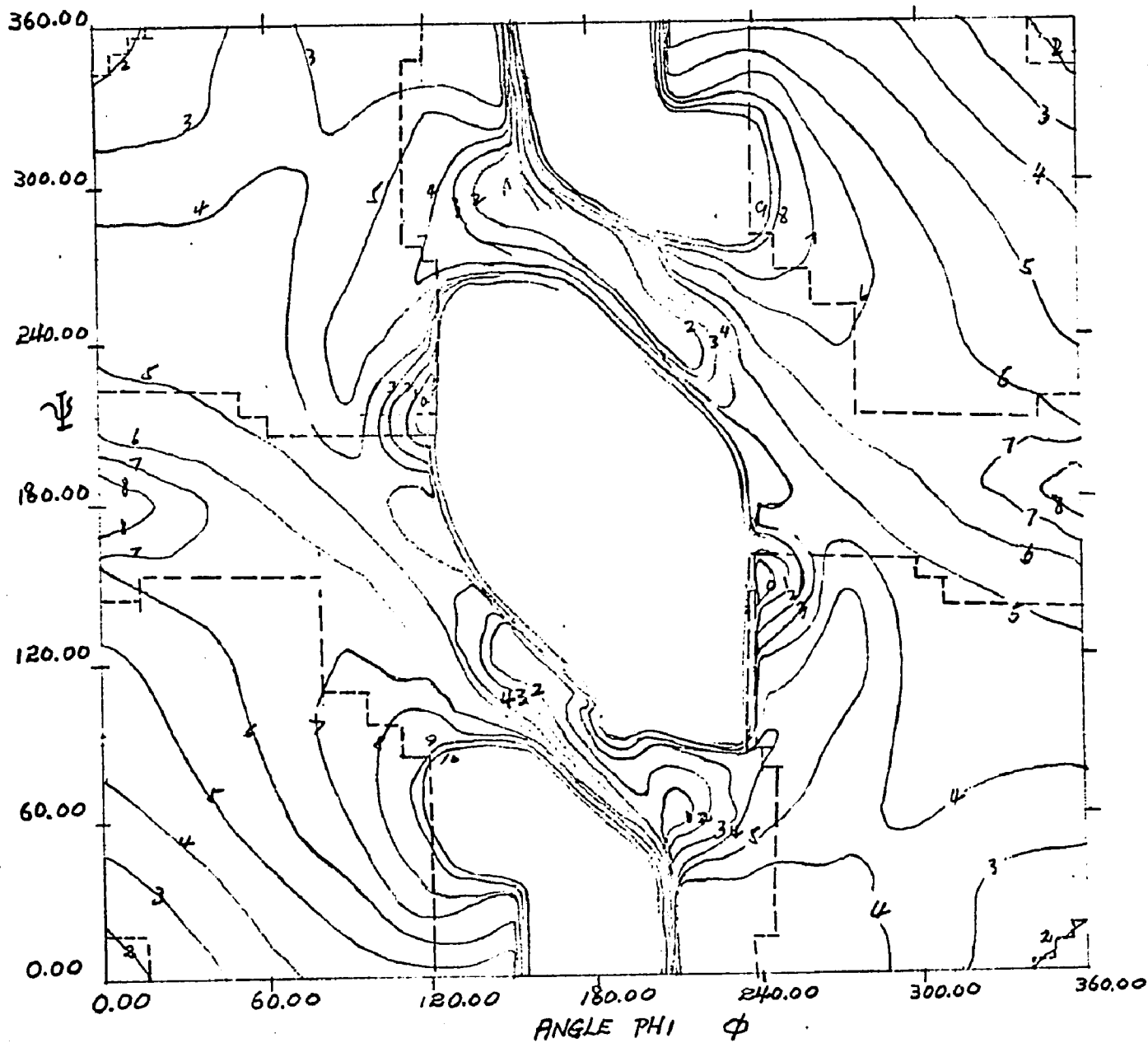


Figure 37

DIPEPTIDE GLYCYL-L-GLYCINE MOLECULE

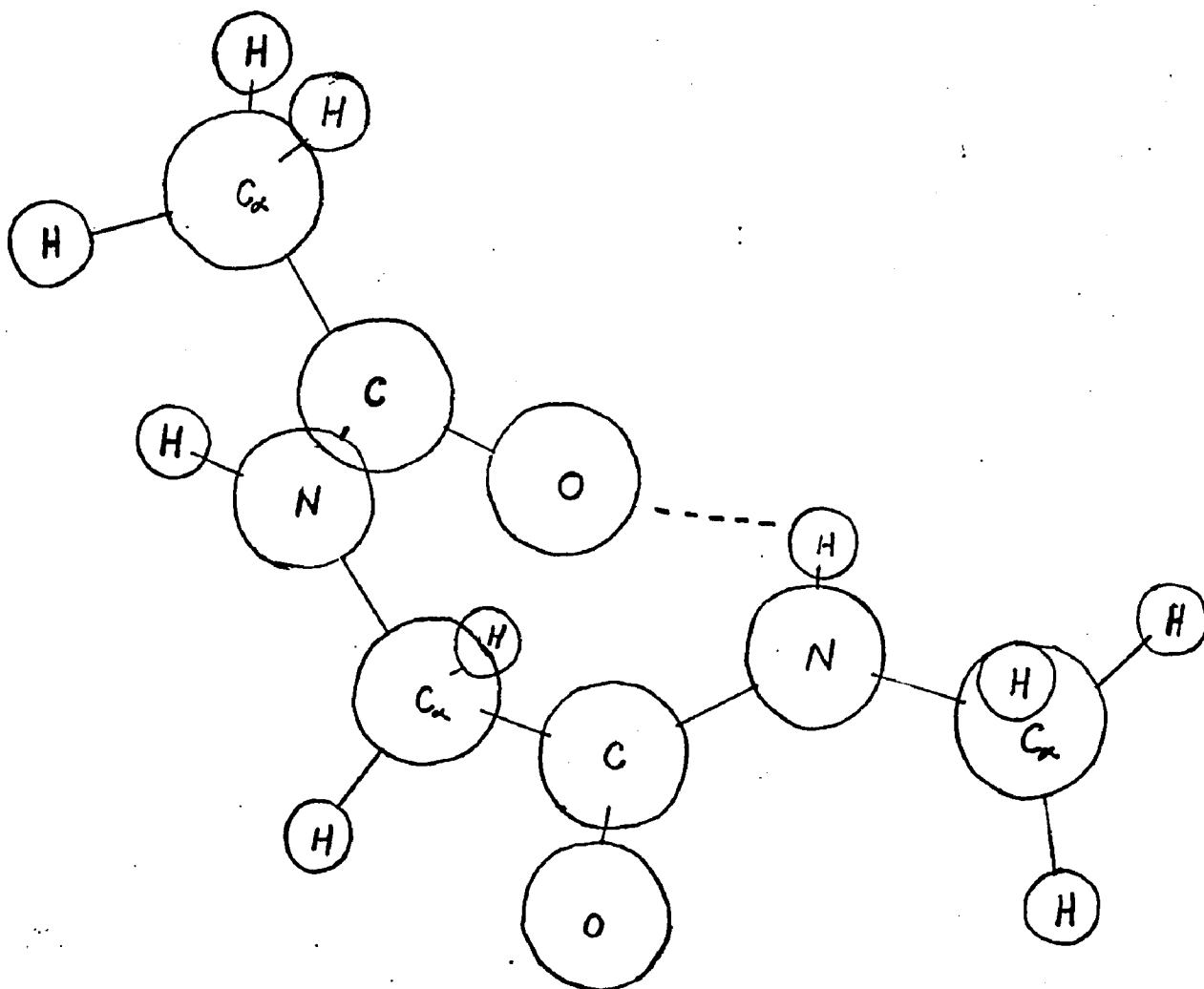


Figure 38

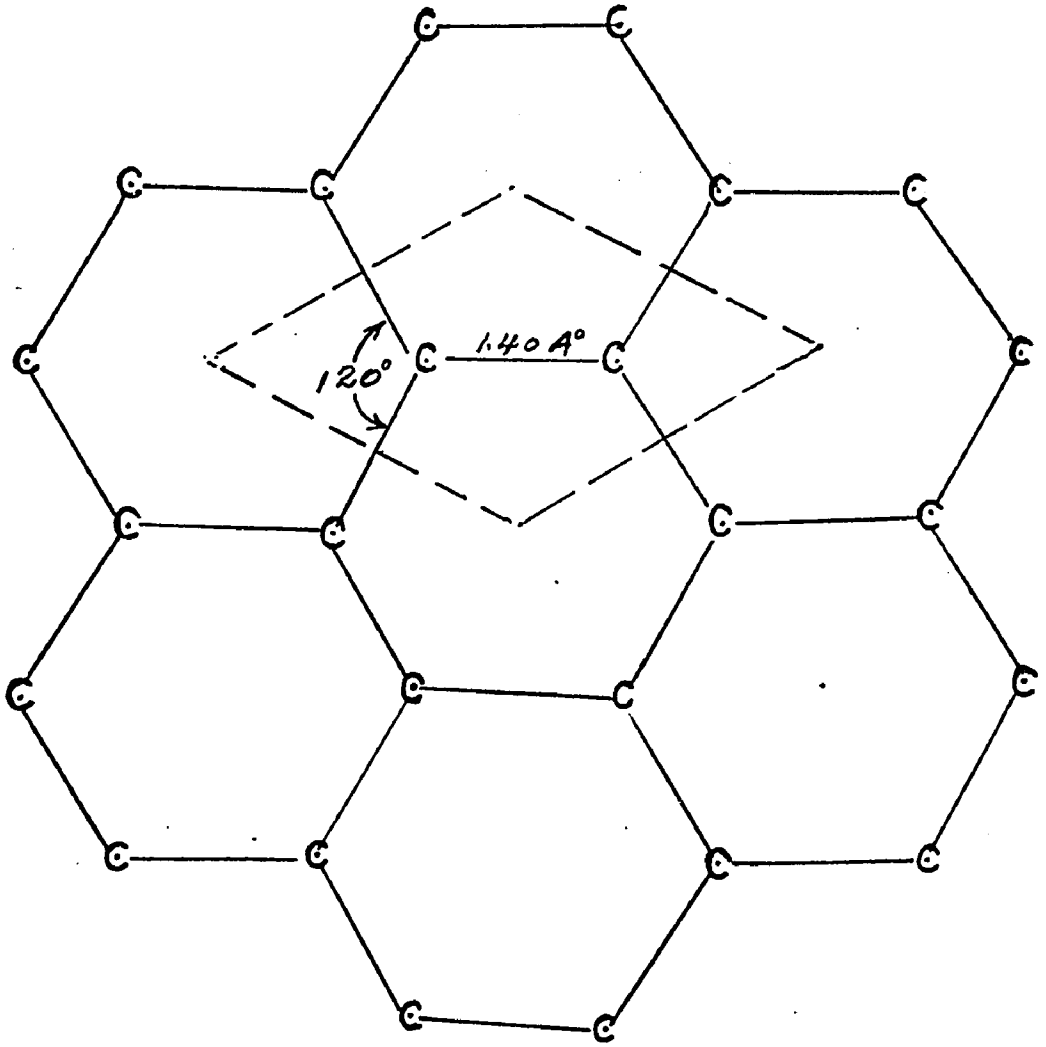


Figure 39

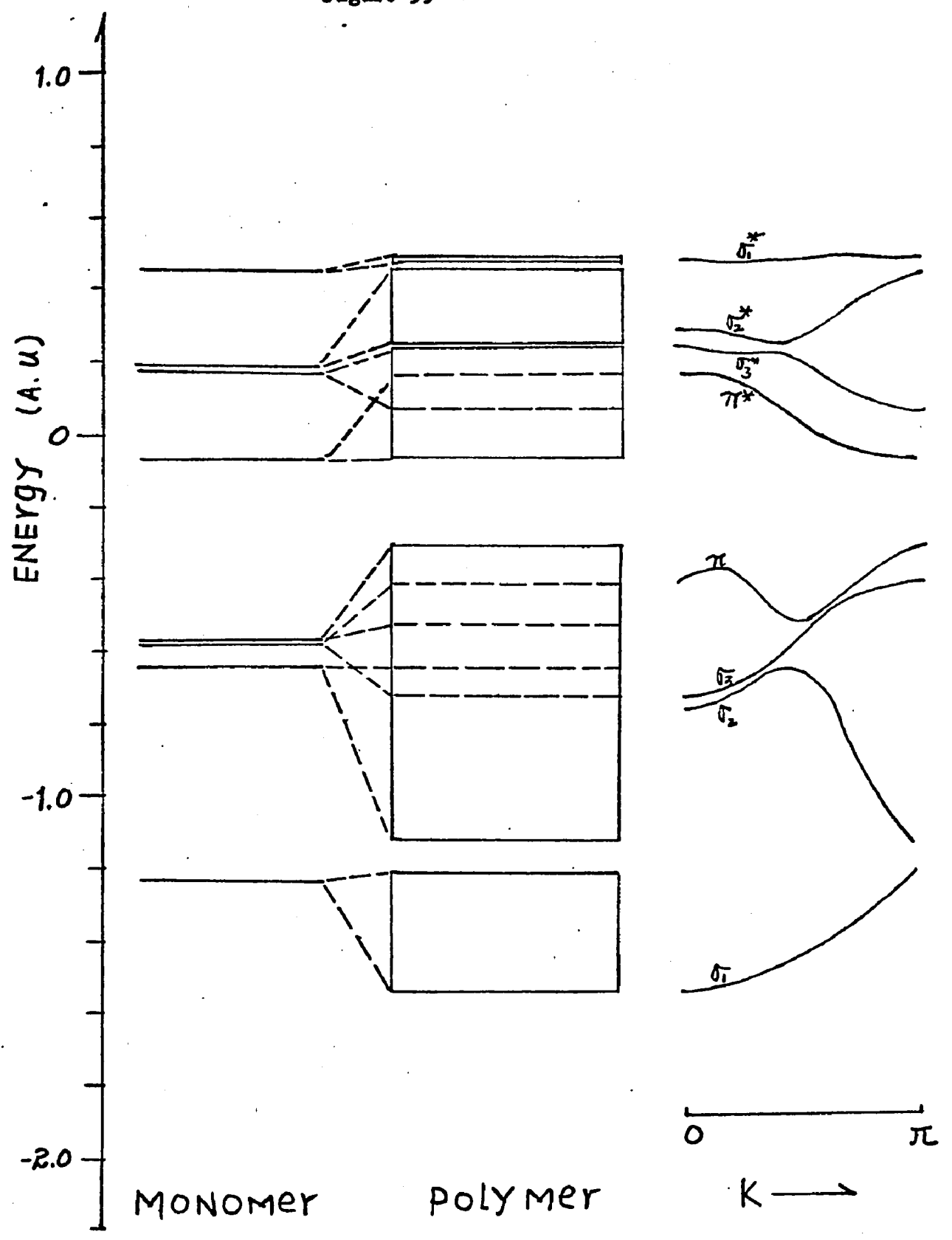


Figure 40

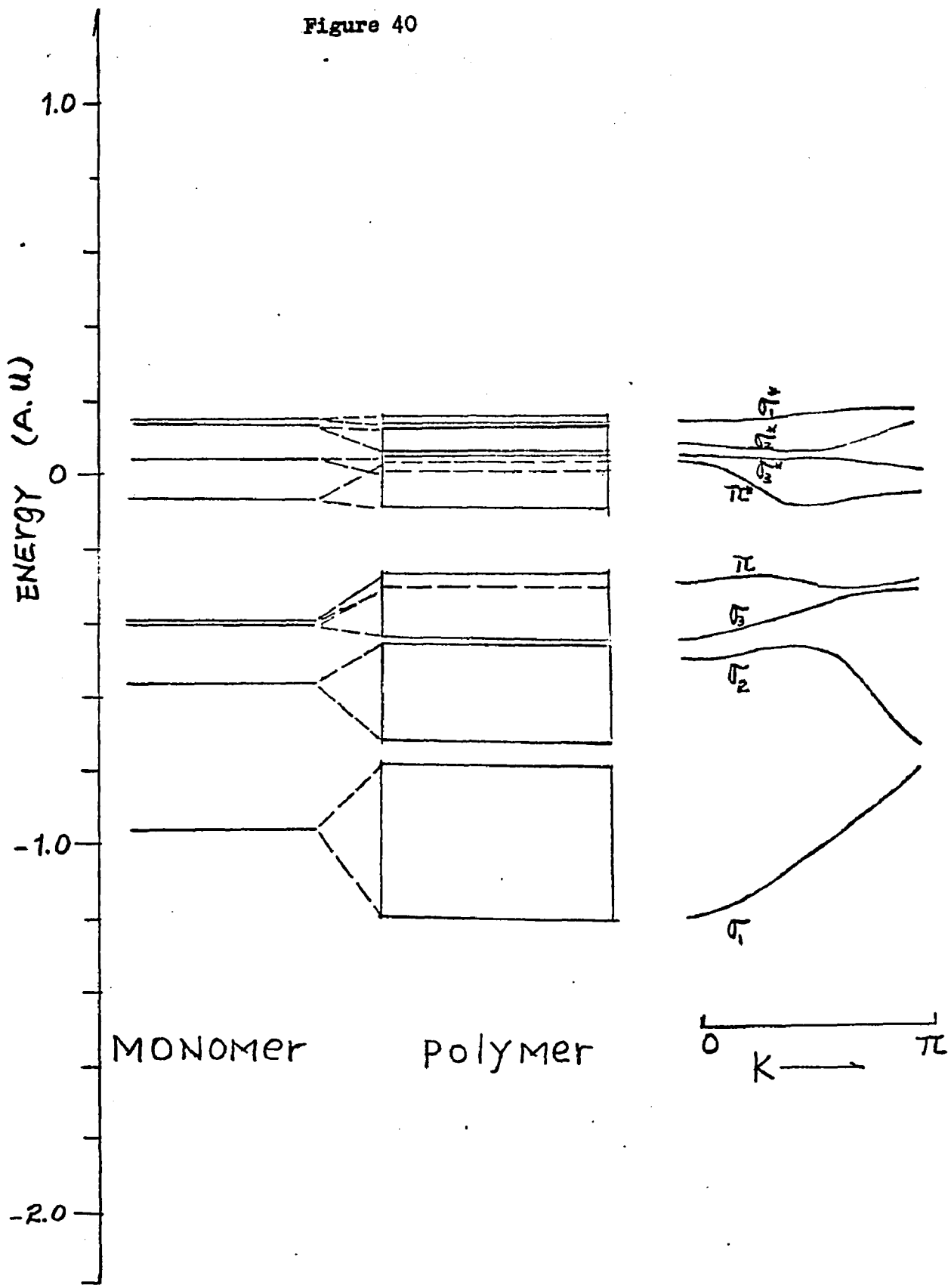


TABLE I
Flow Chart For Line Group Classification

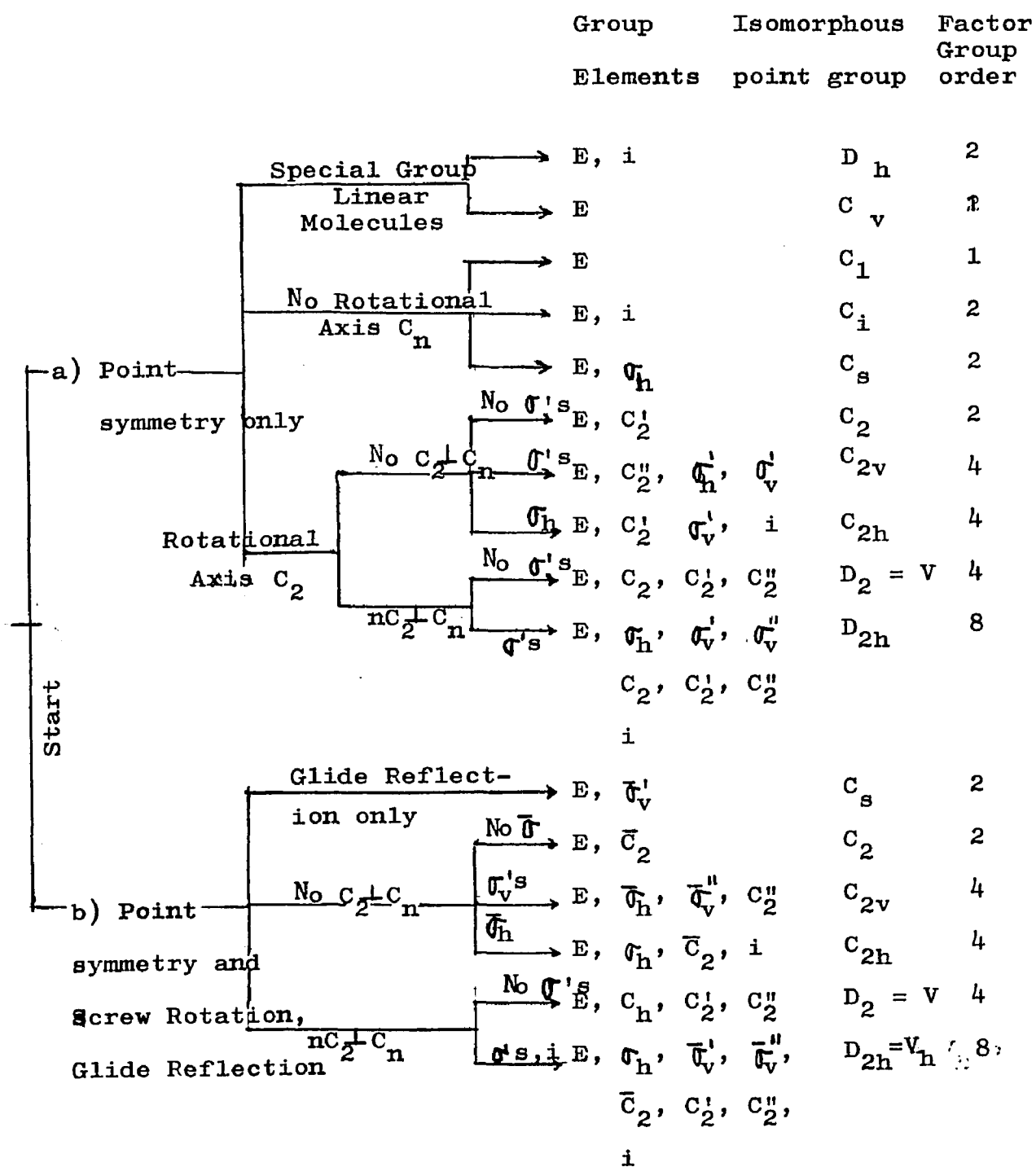


Figure 41

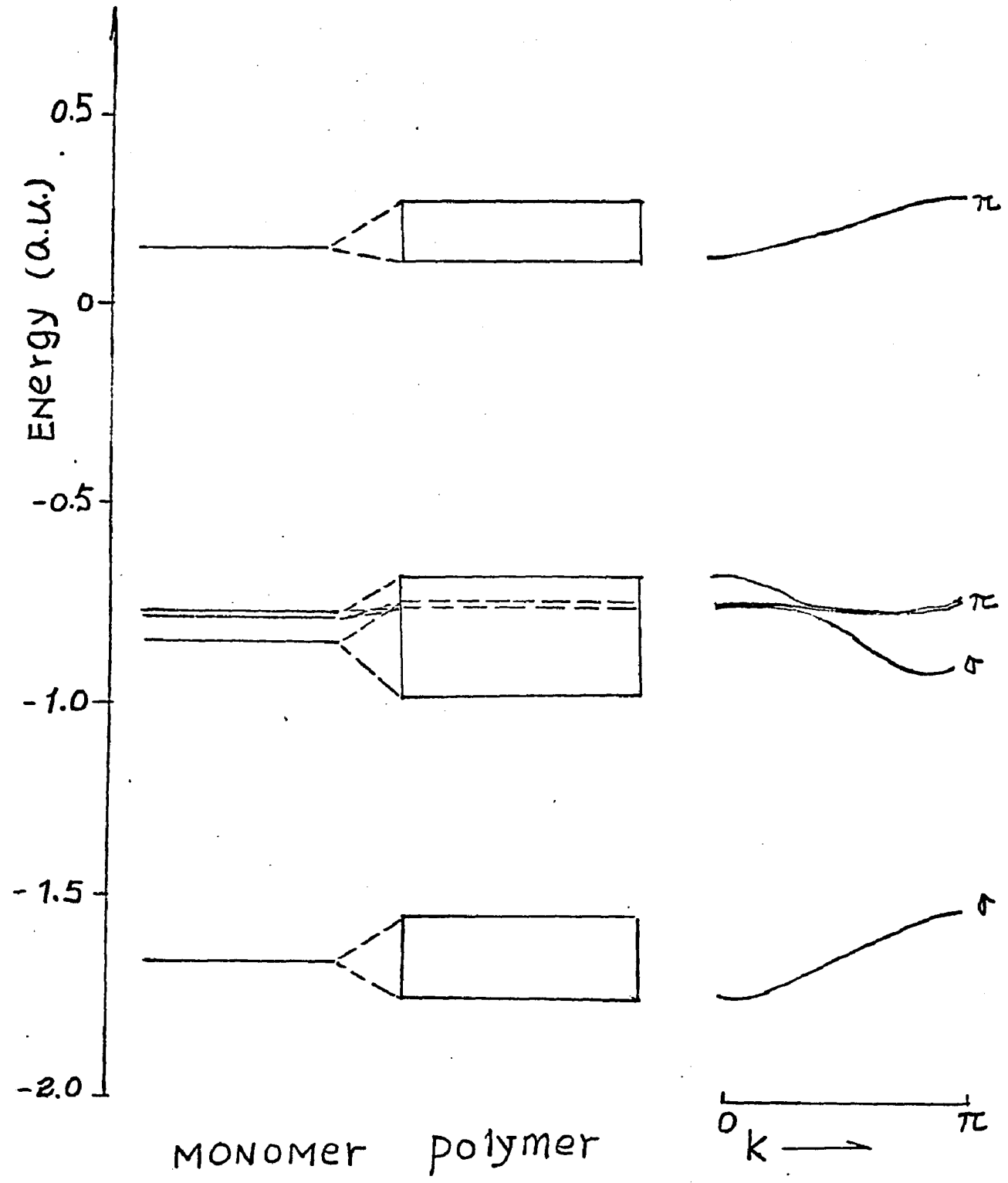


Table II INDO parameters for first-row elements (electron volts)

Elements	H	Li	Be	B	C	N	O	F
G^1		0.092012	0.1407	0.199265	0.267708	0.346029	0.43423	0.5323
F^2		0.049865	0.089125	0.13041	0.17372	0.21905	0.26415	-.3158
$-\beta_A^0$	9	9	13	17	21	25	31	39
$1/2(I_S + A_S)$	7.176	3.106	5.946	9.594	14.051	19.316	25.390	32.272
$1/2(I_P + A_P)$		1.258	2.563	4.001	5.5572	7.275	9.111	11.080

Table III \bar{B} . MINDO/2 parameters for first-row elements

Elements	HH	NO	CH	CC	HN	CN	NN	HO	CO	OO
B	.35869	.42679	.33382	.35410	.37556	.36137	.29963	.54268	.43562	.68733
(A ⁻¹)	.7535	2.1550	1.2475	1.7345	1.4204	1.8551	3.1459	.9073	1.8657	1.4547

Table IIIA. MINDO/2 parameters of one-center integrals (electron volts)

Elements	H	C	N	O
U _{ss}	-13.595	-49.659	-68.364	-90.837
U _{pp}	...	-41.159	-57.440	-77.670
F ⁰	12.845	11.089	12.106	13.599
G ¹	...	7.285	9.416	11.816
F ²	...	4.724	5.961	7.249
I _s	-13.595	-20.035	-26.217	-32.689
I _p	...	-10.430	-13.334	-16.340

Table 4. Summary of some electrical properties of some polymers

Polymers	Methods	Electron Effective Mass M_e^*	Hole Effective Mass M_h^*	Intrinsic Conductivity $\sigma_0 \Omega^{-1}/\text{cm}$	Energy Band Gap ΔE (eV)
Polyacetylene	INDO	.1952	-.7520	.7586	10.1439
	MINDO/2	.6214	-.7947	.8139	6.9603
Polyethylene	INDO	.6285	-.4703	.5403	13.6431
	MINDO/2	.2397	-.9630	1.4576	5.3114
F-Substituted Polyacetylene	INDO	.1781	-.5583	.3656	9.6187
-Substituted Polyacetylene	INDO	.2223	-.4814	.7034	9.2541

M*: Effective electron mass in units of electron rest mass (10^{-28} g)

Table 5. Summary of some electrical properties of polypeptide

Polypeptide	Methods	Electron Effective Mass M_e^*	Hole Effective Mass M_h^*	Intrinsic Conductivity $\sigma_0 \text{ } \Omega^{-1}/\text{cm}$	Energy Band Gap ΔE (eV)
Helix Polyglycine	INDO	.8364	-.9630	2.8091	8.51
	MINDO/2	.7066	-.8831	1.7297	5.70
Planar Polyglycine	INDO	.6810	-1.0580	2.4854	9.53
	MINDO/2	.7068	-.8979	1.8057	6.14
Helix Polyglycyl-aniline	INDO	.2079	-1.2660	2.9320	9.39

M^* : Effective electron mass in units of electron rest mass (10^{-28} g)

Table 6. Comparison of energy band structure of graphite by different methods

Band	Band widths of valence bands of graphite (ev)		
methods	ab initio	MINDO/2	INDO
π	7.35	1.36	5.44
σ_3	7.07	4.49	8.70
σ_2	8.43	7.62	13.06
σ_1	5.90	12.25	9.25
Total valence band width	19.30	23.40	31.56

Table 7. Comparison of allowed transition of graphite by different methods

Allowed Transitions	ab initio ¹	MINDO/2	INDO	Observed Results ²
$\pi \rightarrow \pi^*$	4.6	5.44	7.07	4.6
$\sigma_2 \rightarrow \pi^*$	16.50	10.34	15.78	No Data
$\sigma_3 \rightarrow \sigma_3^*$	16.30	8.07	12.52	14.50

Table 8. Energies of one-dimensional poly(hydrogenfluoride) crystal calculated by INDO-MO method.

Linear system	E_t au Total energy	Energy/FH	E kcal Energy gained/FH	E kcal Energy/H bond
FH	-27.1275	-27.1275		
2FH	-54.2766	-27.1383	6.7792	13.5584
3FH	-81.4308	-27.1436	10.1061	15.1592
4FH	-108.5865	-27.1466	11.9892	15.9856
5FH	-135.7428	-27.1486	13.2446	16.5244
6FH	-162.8994	-27.1499	14.0607	16.8728
7FH	-190.0562	-27.1509	14.6794	17.1260
8FH	-217.2130	-27.1516	15.1434	17.3070

Table 9. Energies of one-dimensional poly(hydrogenfluoride) crystal calculated by INDO-CMO method.

Linear system	E_t (au) Total energy	E (au) Energy/FH	ΔE kcal Energy gained/FH	ΔE kcal Energy/H bond
$(FH)_1$	-27.0604	-27.0604		
$(FH)_2$	-54.2167	-27.1083	10.0329	12.0394
$(FH)_3$	-81.3716	-27.1239	13.2795	14.9394
$(FH)_4$	-108.5260	-27.1315	14.8767	16.2290
$(FH)_5$	-135.6824	-27.1365	15.9187	17.0557
$(FH)_6$	-162.8390	-27.1398	16.6203	17.6000

Table 10. Inter and intramolecular density submatrices for HF chain calculated by crystal molecular orbital theory with the z-axis along the chain.

Molecule I	Molecule II			Molecule II		
	H1s	F2p _y	F2p _z	H1s	F2p _y	F2p _z
H1s	-.0465	-.0925	-.1389	1.8843	-.2140	.3714
F2p _y	.0255	.0787	-.1513	-.2140	1.4601	.8337
F2p _z	.0372	.04497	-.0323	.3714	.8337	.6557

* The intra molecular electronic density at F2p_x and F2s are both equal to 2.0

Table 11. Electron population for poly(hydrogenfluoride) one-dimensional crystal
calculated by INDO-MO method.

Number of Atom	Element	Net Charge							
		1	2	3	4	5	6	7	8
1	F	-.2685	-.3325	-.3457	-.3497	-.3512	-.3519	-.3522	-.3524
2	H	.2685	.2933	.3003	.3026	.3035	.3039	.3041	.3043
3	F		-.2628	-.3252	-.3375	-.3412	-.3425	-.3432	-.3435
4	H		.3019	.3259	.3329	.3352	.3361	.3365	.3368
5	F			-.2670	-.3294	-.3415	-.3450	-.3464	-.3470
6	H			.3118	.3348	.3416	.3438	.3448	.3452
7	F				-.2686	-.3309	-.3430	-.3466	-.3479
8	H				.3150	.3376	.3444	.3466	.3475
9	F					-.2693	.3316	-.3438	-.3473
10	H					.3162	.3387	.3477	.3455
11	F						-.2696	-.3320	-.3443
12	H						.3168	.3393	.3460
13	F							-.2698	-.3322
14	H							.3171	.3396
15	F								-.2690
16	H								.3173

Table 12. Electron population for poly(hydrogenfluoride) one-dimensional crystal calculated by INDO-CMO method.

Atom	Element	et Charge					
		1	2	3	4	5	6
1	F	-.3411	-.3616	-.3665	-.3717	-.3724	-.3728
2	H	.3411	.3417	.3443	.3481	.3485	.3487
3	F		-.3343	-.3484	-.3543	-.3552	-.3555
4	H		.3542	.3485	.3531	.3537	.3540
5	F			-.3362	-.3524	-.3549	-.3556
6	H			.3583	.3537	.3549	.3554
7	F				-.3398	-.3528	-.3552
8	H				.3632	.3544	.3555
9	F					-.3401	-.3530
10	H					.3638	-.3547
11	F						-.3402
12	H						.3641

References

1. D. Poland and H.A. Scheraga, "Theory of Helix-Coil Transitions in Biopolymers" (Academic Press, New York, and London 1970).
2. B. Pullman, The Jerusalem Simposia on Quantum Chemistry and Biochemistry, Vol. 5, Jerusalem 1973.
3. M. Tinkham, "Group Theory and Quantum Mechanics" (McGraw-Hill, New York 1964).
4. S.F. Edwards, Proc. Phys. Soc. (London) 85, 613 (1965).
5. M.E. Fisher, J. Chem. Phys. 44, 616 (1966).
6. P.J. Flory and S. Fisk, J. Chem. Phys. 44, 2243 (1966).
7. M.F. Sykes, J. Chem. Phys. 39, 410 (1963).
8. M. Kumbar and S. Winwer, J. Chem. Phys. 50, 5257 (1969).
9. K.K. Knaell and Roy A. Scott, J. Chem. Phys. 54, 566 (1970).
10. J.E. Lennard-Jones, Proc. Roy. Soc. (London) A158, 280 (1937)
11. J. Ooshika, J. Phys. Soc. Japan 12, 1238, 1246 (1957)
12. H.C. Longuet-Higgins and L. Salem, Proc. Roy. Soc. (London) A251, 172 (1959).
13. M. Tsuji, S. Huzinaga and T. Hasino, Rev. Mod. Phys. 32, 425 (1960).
14. W. Kutzelnigg, Theoret. Chem. Acta 4, 417 (1966).
15. F.P. Boer, M.D. Newton and W. N. Lipscomb, Proc. Acad. Sci. U.S. 52, 890 (1964).

16. R. Hoffman, J. Chem. Phys. 39, 1397 (1963).
17. L.C. Allen and J.D. Russell, J. Chem. Phys. 46, 1029 (1967).
18. R. Rein, N. Fukuda, H. Win, G.A. Clerke and F.E. Harris, J. Chem. Phys. 45, 4743 (1966).
19. A. Pullman, E. Kuchanski, M. Gillbert, and A. Davis, Theoret. Chim. Acta. (Berl.), 10, 231 (1968).
20. B.J. Duke, Theoret. Chim. Acta. (Berl.), 9, 260 (1968).
21. J.A. Pople, D.P. Santry, and G.A. Segal, J. Chem. Phys. 43, 5129 (1965).
22. J.A. Pople and G.A. Segal, J. Chem. Phys. 44, 3289 (1966).
23. G. Klopman and B. O'Leary, Topics in Current Chemistry 15, 447 (1970).
24. J.M. Sichel and M.A. Whitehead, Theoret. Chim Acta (Berl.) 7, 32 (1967).
25. J. Del Bene and H.H. Jaffe, J.Chem. Phys. 44, 759 (1966).
26. J.A. Pople, D.L. Beveridge, and P.A. Dobosh, J. Chem. Phys. 47, 2026 (1967).
27. N.C. Baird and M.J.S. Dewar, J. Chem. Phys. 50, 1262 (1969).
28. (a) J. Ladik, Acta. Phys. Acad. Sci. Hung 11, 239 (1960);
(b) J. Ladik and G. Biczó, J. Chem. Phys. 42, 1658 (1965);
(c) J. Ladik, D.K. Rai, and K. Appel, J. Mol. Spectry. 27, 72 (1968);
(d) J. Avery, J. Packer, J. Ladik, and G. Biczó, *ibid.* 29, 194 (1969); B.F. Rozsyai, F. Martino, and J. Ladik, J. Chem. Phys. 52, 5708 (1970).

29. J.M. Andre and G. Leroy, *Theoret. Chim. Acta* 9, 123 (1967).
30. K. Morakuma, *J. Chem. Phys.* 54, 962 (1971).
31. H. Fujita and I. Imamura, *J. Chem. Phys.* 53, 4555 (1970).
32. S. O'Shea and D.P. Santry, *J. Chem. Phys.* 54, 2667 (1971).
33. J.M. Andre, L. Gouverneur, and G. Leroy, *Intern. J. Quantum Chem.* 1, 427, 451 (1967).
34. D.L. Beveridge and I. Jano and J. Ladik, *J. Chem. Phys.* 56, 4744 (1972).
35. J.M. Andre, G.S. Kapsomenos and G. Leroy, *Chem. Phys. letters* 8, 195 (1971).
36. S. Suhai and J. Ladik, *Theoret. Chim. Acta (Berl.)* 28, 27-35 (1972).
37. M. Suard-Sender, *J. Chem. Phys.* 62, 79, 89 (1965).
38. M.E. Bernel, D.O. Eley and V. Subramanyan, *Ann. N.Y. Acad. Sci.* 158 191 (1969).
39. M.H. Wood, M. Barber, J.H. Hiller and J.M. Thomas, *J. Chem. Phys.* 56 (1972) 1788.
40. G. Del Re, J. Ladik, and G. Biczko, *Phys. Rev.* 155, 997 (1967).
41. C.C.J. Roothaan, *Rev. Mod. Phys.* 23, 69 (1951).
42. P. Henrici, *J. Soc. Appl. Math.* 6, 144 (1958).
43. R.S. Mulliken, *J. Chem. Phys.* 56, 792 (1952).
44. R.L. Flurry, Jr., and D.L. Breen, *Inter. J. Quan. Chem.* 6, 305 (1972).
45. J.C. Slater, "Insulators Semiconductor and Metals", *Quantum Theory of Molecules and Solids*, 3 (McGrand-Hill, New York, 1967).

46. A.D. Baker, *Accts. Chem. Rev.* 3, 17-25, Jan. 1970.
47. D. Betteridge and A.D. Baker, *Analy. Chem.* 42, 43A, Jan. 1970.
48. T. Koopmans, *Physica*, 1, 104 (1934).
49. R. Zbinden, "IR Spectroscopy of high polymers", Academic Press, N.Y. N.Y. 1094.
50. Cotton F.A. *Chemical Applications of Group Theory*, Wiley Interscience, New York, 1963.
51. J.A. Pople and D.L. Beveridge, "Approximate Molecular Orbital Theory" (McGraw-Hill, New York, 1970).
52. J.C. Slater, "Quantum Theory of Atomic Structure", McGraw-Hill, Vol. 1. p. 339-342, New York 1960.
53. K.J. Nielsen, *Methods in Numerical Analysis* (MacMillan, New York, 1956).
54. D.L. Beveridge and B.J. Bulkin, *J. Chem. Educ.* 48, 587 (1971).
55. W.D. Metz, *Science*, 180 398 April 1973.
56. B.E. Wigner and H.B. Huntington, *J. Chem. Phys.* 3, 764 (1929).
57. P. Henrici, *J. Soc. Appl. Math.* 6, 144 (1958).
58. W.L. McCubbin and R. Manne, *Chem. Phys. Letters* 2, 230, (1968).
59. A. Imamura, *J. Chem. Phys.* 54, 962 (1971).
60. J.M. Sichi and M.A. Whitehead, *Theoret. Chim. Acta* 11, 20 (1968).
61. D.L. Beveridge and W. Wun, *Chem. Phys. letter* 5, 507 (1973)
62. B. Rosenberg and A. Postow, *Ann. N.Y. Acad. Sci.* 158, 161 (1969).

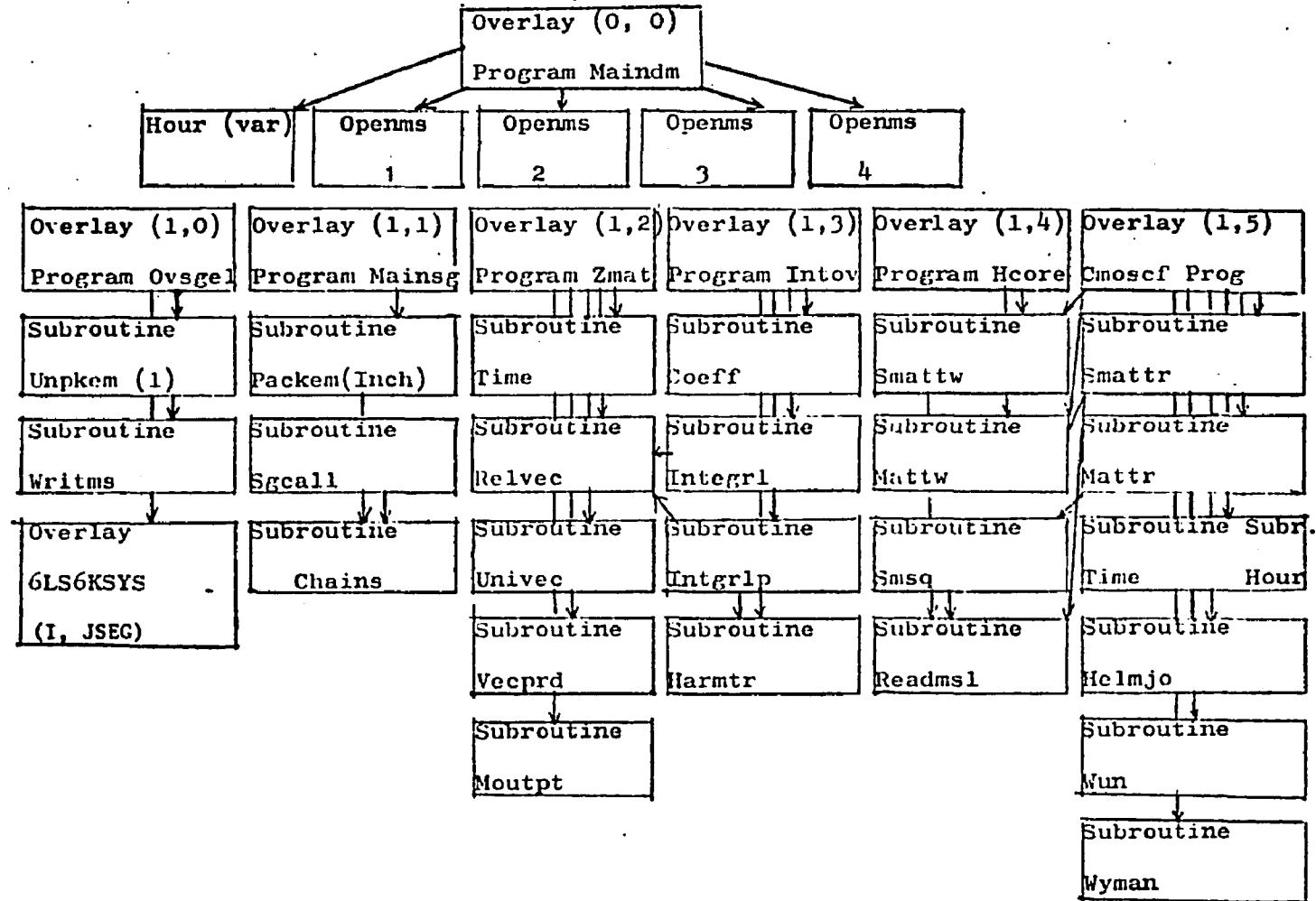
63. R.E. Dickerson and I. Geis, "The Structure and Action of Proteins", (Hurper and Row, Publishers: New York, Evenston, London).
64. P.R. Wallace, Phy. Rev. 71, 622 (1927).
65. D.L. Greenaway, G. Hanbeke, F. Bassani, and E. Tosatti, Phy. Rev. 178, 1340 (1969).
66. G.S. Painter and D.E. Ellis, Phy. Rev. 1, 4774 (1970).
67. P.A. Kollman and L.C. Allen, J. Am. Chem. Soc. 192:41 753, (1969).
68. J.R. Sabin, J. Chem. Phys. 56, 45 (1971).
69. J. Bacon and D.P. Santry, J. Chem. Phys. 56, 2011 (1971).
70. J. Bacon and F.P. Santry, J. Chem. Phys. 55, 3743 (1971).

Appendix: Computer Program Listings for INDO-CMO Calculations.

The digital computer program used in this study was originally written by D.L. Beveridge and I. Jano for the CDC 6600 computer. The original version was modified and added to by W. Wun and also transcribed to the IBM 370-168.

The following page contains a flow chart of the CDC version, followed by program listings. The results of the test calculation described in Chapter IV are included.

ENERGY BAND Calculation by INDO & MINDO



```

OVERLAY(S6KSYS,0,0)
PROGRAM MAINDM
* (INPLT,OUTPUT,TAPES=INPUT,TAPE6=OUTPUT,TAPE1,TAPE2,TAPE3,TAPE4)
C THIS SYSTEM IS FOR INDO SCF TIGHT BINDING LCAO CRYSTAL ORBITALS
C BASED ON DEL RE, LADIK AND BICZO, PHYS REV 155, 997(1977) AND
C POPLE, BEVERIDGE AND DOBOSH, J CHEM PHYS 47, 2026 (1967)
C CODED IN SCOPE FORTRAN FOR THE USAEC CDC 6600, COURANT INSTITUTE
C BY DAVID L BEVERIDGE, CHEMISTRY DEPARTMENT, HUNTER COLLEGE, CUNY
COMMON//TPOS(5),ADDRSS(50,5),NAET(5),IR,IW,IPUN,NAITCP,
1 NSTART,NCOUNT,SECNT,CONTRL(6),NCYCLE(50),X(50)
C THE FOLLOWING ARE LABELED COMMONS COMMON TO ALL SEGMENTS
COMMON/ARRAYS/ABC(30000)
COMMON/INFO/NATOMS,CHARGE,MULTIP,AN(50),C(50,3),N
COMMON/ELORB/EL(104),ORB(4,7)
COMMON/INFOC1/Z(2673)
COMMON/1/ZZ(6375)
COMMON/AUXINT/ZZZZ(34)
COMMON/OPTION/ZZZ(7)
COMMON/IDENT/IDENT(8)
DATA((EL(I),I=1,36)=4H H,4H HE,4H LI,4H BE,4H B,4H C,
14H N,4H O,4H F,4H NE,4H NA,4H MG,4H AL,4H SI,4H P,
24H S,4H CL,4H AR,4H K,4H CA,4H SC,4H TI,4H V,4H CR,
34H MN,4H FE,4H CO,4H NI,4H CU,4H ZN,4H GA,4H GE,4H AS,
44H SE,4H BR,4H KR)
DATA((EL(I),I=37,71)=4H RB,4H SR,4H Y,4H ZR,4H NR,4H MO,
14H TC,4H RV,4H RH,4H PD,4H AG,4H CD,4H IN,4H SN,4H SE,
24H TE,4H I,4H XE,4H CS,4H BA,4H LA,4H CE,4H PR,4H ND,
34H FM,4H SM,4H EU,4H GD,4H TB,4H DY,4H HO,4H ER,4H TM,
44H YB,4H LU)
DATA((EL(I),I=72,102)=4H HF,4H TA,4H W,4H RE,4H OS,4H IR,
14H FT,4H AU,4H HG,4H TL,4H PB,4H BI,4H PO,4H AT,4H RN,
24H FR,4H RA,4H AC,4H TH,4H PA,4H U,4H NP,4H PU,4H AM,
34H CM,4H BK,4H CF,4H ES,4H FM,4H MD,4H NO)
ORR(1,4)=GHS
ORR(2,3)=GHPY
ORR(2,4)=GHPZ
ORR(2,5)=GHPX
ORR(3,2)=GHDX2-Y2
ORR(3,3)=GHGYZ
ORR(3,4)=GHD72
ORR(3,5)=GHDXZ
ORR(3,6)=GHDXY
CALL HOUR (VAR)
IR = 5
IW = 6
WRITE(IW,1000)
1000 FORMAT(10H IN MAINDM)
NSTART = 0
CALL OPENMS(1,ADDRSS(1,1),50,0)
CALL OPENMS(2,ADDRSS(1,2),50,0)
CALL OPENMS(3,ADDRSS(1,3),50,0)
CALL OPENMS(4,ADDRSS(1,4),50,0)
CALL OVERLAY(6LS6KSYS,1,0)
END
SUBROUTINE MOUTPT(A,"N,MDIM,NDIM,NAME)
C OUTPUT OF M X N MATRIX DIMENSIONED TO MDIM X NDIM
DIMENSION A(MDIM,NDIM)
XMINOF(ISSAM,JANO)=MINO(ISSAM,JANO)
PRINT 1000,NAME

```

```

KITE = 0
20 LOW = KITE+1
KITE = KITE+14
KITE = XMINOF(KITE,N)
PRINT 19,(I,I=LOW,KITE)
19 FORMAT( // ,4X,14(6X,I2),/)
DO 32 I=1,M
32 PRINT 18,I,(A(I,J),J=LOW,KITE)
18 FORMAT(I4,2X,14F8.4)
IF(N-KITE) 40,40,20
40 RETURN
END
OVERLAY(S6KSYS,1,0)
PROGRAM OVSGCL
* (INPLT,OUTPUT,TAPES=INPUT,TAPEK=OUTPUT,PUNCH,TAPE1)
C THIS OVERLAY CALLS THE SEGMENTS IN THE ORDER SET UP BY THE MAINSEG
COMMON//TPOS(5),ADDRSS(50,5),NAET(5),IR,IW,IPUN,WAITOP,
1 NSTART,NCOUNT,SEGCNT,CONTRL(6),NCYCLE(50),X(50)
TYPE INTEGER TPOS,ADDRSS,WAITOP,SEGCNT,CONTRL
COMMON/FINAL/INFIN
COMMON/JSEG/JSEG
COMMON/IDENT/IDENT(3)
COMMON/ELORB/EL(104),ORB(4,7)
1 CONTINUE
WRITE(IW,1000)
1000 FORMAT(10H IN OVSGCL)
CALL OVERLAY(6LS6KSYS,1,1)
DO 10 I=1,INFIN
CALL UNPKEM(I)
WRITE(IW,1001)JSEG,NCOUNT
1001 FORMAT(///,22H PROCEEDING TO SEGMENT,I3,15H OF CART NUMBER,I3,///)
JSEG = JSEG+1
CALL OVERLAY(6LS6KSYS,1,JSEG)
10 CONTINUE
NSTART = 0
GO TO 1
END
SUBROUTINE UNPKEM(I)
COMMON//TPOS(5),ADDRSS(50,5),NAET(5),IR,IW,IPUN,WAITOP,
1 NSTART,NCOUNT,SEGCNT,CONTRL(6),NCYCLE(50),X(50)
TYPE INTEGER TPOS,ADDRSS,WAITOP,SEGCNT,CONTRL
COMMON/JSEG/JSEG
COMMON/TPRTE/NPKRF
COMMON/PACKED/IA(20),IP(20)
DIMENSION IDUM(5)
IF(I-1)1,2,1
2 CALL WRITMS(1,IA,40,NPKRF)
CALL READMS(1,IA,40,1)
NPKR = 1
1 II = I - 20*(NPKR-1) + (I/(20*(NPKR-1)+1))
KDUM = IA(II)/100000000
IDUM(1) = IA(II)/10000-10000*KDUM
IDUM(2) = IA(II) - 100000000*KDUM-10000*IDUM(1)
IDUM(3) = IP(II)/100000000
IDUM(4) = IP(II)/10000-10000*IDUM(3)
IDUM(5) = IP(II) - 100000000*IDUM(3) - 10000*IDUM(4)
JSEG = KDUM/100
NCOUNT = KDUM - 100*JSEG
DO 10 K=1,5
IF(IDUM(K).GT.999)11,12

```

```

11 CONTRL(K+1) = 1000 - IDUM(K)
   GO TO 13
12 CONTRL(K+1) = IDUM(K)
13 CONTINUE
10 CONTINUE
   IF(1/(20*NPKR)-1)3,4,3
   4 NPKR = NPKR+1
   CALL READMS(1,IA,40,NPKR)
3 CONTINUE
  RETURN
  END
  SUBROUTINE SMATTR(RLUN,A,NEL,RECN,NDIM,NDIMSQ)
  DIMENSION A(NDIMSQ)
  INTEGER RECN,RLUN
  COMMON//TPOS(5),ADDRSS(50,5),NAET(5),IR,IW,IPUN,WAITCP,
1  NSTART,NCOUNT,SEQCNT,CONTRL(6),NCYCLE(50),X(50)
  INTEGER TPOS,ADDRSS,WAITOP,SEQCNT,CONTRL
  WAITCP = 0
  NELSG = (NEL+(NEL+1))/2
  CALL READMS(RLUN,A,NELSG,RECN)
  CALL SMSQ(A,NEL,NDIM,NDIMSQ)
  RETURN
  END
  SUBROUTINE SMATTW(RLUN,A,NEL,RECN,NDIM,NDIMSQ)
  COMMON//TPOS(5),ADDRSS(50,5),NAET(5),IR,IW,IPUN,WAITCP,
1  NSTART,NCOUNT,SEQCNT,CONTRL(5),NCYCLE(50),XXX(50)
  TYPE INTEGER TPOS,ADDRSS,WAITOP,SEQCNT,CONTRL
  DIMENSION A(NDIMSQ)
  INTEGER RECN,RLUN
  INDEX = 0
  DO 10 J=1,NEL
  KJ = NDIM*(J-1)
  DO 10 I=1,J
  INDEX = INDEX + 1
  A(INDEX) = A(I+KJ)
10 CONTINUE
  NELSG = (NEL+(NEL+1))/2
  CALL WRITMS(RLUN,A,NELSG,RECN)
  RESTORE MATRIX TO ORIGINAL FORM
  CALL SMSQ(A,NEL,NDIM,NDIMSQ)
  RETURN
  END
  SUBROUTINE SMSQ(A,NEL,NDIM,NDIMSQ)
  DIMENSION A(NDIMSQ)
  INDEX = (NEL+(NEL+1))/2
  DO 10 JJ=1,NEL
  J = NEL - JJ + 1
  KJ = NDIM*(J-1)
  DO 10 II=1,J
  I = J-II+1
  A(I+KJ) = A(INDEX)
  INDEX = INDEX - 1
10 CONTINUE
  DO 11 J=1,NEL
  KJ = NDIM*(J-1)
  DO 11 I=1,J
  KI = NDIM*(I-1)
11 A(J+KI) = A(I+KJ)
  RETURN
  END

```

```

SURRCUTINE MATTR(RLUN,A,NEL,RECN,NDIM,NDIMSG)
DIMENSION A(NDIMSG)
INTEGER RECN,RLUN
COMMON//TPOS(5),ADDRSS(50,5),NAET(5),IR,IW,IPUN,WAITCP,
1NSTART,NCOUNT,SEQCNT,CONTRL(6),NCYCLE(50),X(50)
INTEGER TPOS,ADDRSS,WAITOP,SEQCNT,CONTRL
WAITCP = 0
NELSG = NEL*NEL
CALL READMS(RLUN,A,NELSG,RECN)
CALL AMSQ(A,NEL,NDIM,NDIMSG)
RETURN
END
SURRCUTINE WUN(XK,EIGS,N)
DIMENSION XK(8),EIGS(100,8),YENG(800),VEC(8),DX(30),DY(30)
COMMON/IDENT/IDENT(8)
CALL PLOTS(100,24H WUN I.D.NUMBER K562305.)
CALL PLOT(1.0,-11.0,3)
CALL PLOT(1.0,-9.5,-3)
CALL PLOT(1.0,-9.5,-3)
II=0
DO 222 I=1,N
DO 222 J=1,8
II=II+1
YENG(II)=EIGS(I,J)
222 CONTINUE
CALL SCALE (XK,3.08,8,1,X0,DX)
CALL SCALE (YENG,8.0,II,1,Y0,DY)
CALL AXIS(0,0,0.0,13H WAVE VECTORS,-13,3.08,0,0,X0,DX)
CALL AXIS(0,0,0.0,14H ENERGY (A,U.),+14,8.0,90,0,Y0,DY)
CALL SYMBOL(0.5,9.50,0.20,26H ENERGY BAND STRUCTURES OF,0,0,26)
CALL SYMBOL(1.0,9.00,0.20,IDENT,0,0,80)
MZ=0
K=0
DO 333 IJ=1,II
K=K+1
VEC(K)=YENG(IJ)
IF(K,EQ,8)44,333
44 MZ=MZ+1
K=0
CALL LINE(XK,VEC,8,1,-1,MZ,X0,DX,Y0,DY)
333 CONTINUE
CALL PLOT(12.0,0,0,999)
RETURN
END
SURRCUTINE MATTW(RLUN,A,NEL,RECN,NDIM,NDIMSG)
COMMON//TPOS(5),ADDRSS(50,5),NAET(5),IR,IW,IPUN,WAITCP,
1NSTART,NCOUNT,SEQCNT,CONTRL(6),NCYCLE(50),XXX(50)
TYPE INTEGER TPOS,ADDRSS,WAITOP,SEQCNT,CONTRL
DIMENSION A(NDIMSG)
INTEGER RECN,RLUN
INDEX = 0
DO 10 J=1,NEL
K = NDIM*(J-1)
DO 10 I=1,NEL
INDEX = INDEX + 1
A(INDEX) = A(I+K)
10 CONTINUE
NELSG = NEL*NEL
CALL WRITMS(RLUN,A,NELSG,RECN)
RESTICHE MATRIX TO ORIGINAL FORM

```

```

CALL AMSQ(A,NEL,NDIM,NDIMSQ)
RETURN
END
SUBROUTINE AMSQ(A,NEL,NDIM,NDIMSQ)
DIMENSION A(NDIMSQ)
INDEX = NEL*NEL
DO 10 JJ=1,NEL
J = NDIM+(NEL-JJ)
DO 10 KK=1,NEL
K = NEL - KK + 1
A(J+K) = A(INDEX)
INDEX = INDEX - 1
10 CONTINUE
RETURN
END
OVERLAY(SAKSYS,1,1)
PROGRAM MAINSG
*(INPLT,OUTPUT,TAPE5=INPUT,TAPE6=OUTPUT,PUNCH,TAPE1)
COMMON//TPOS(5),ADDRSS(50,5),NAET(5),IR,IW,IPUJ,WAITCP,
1 NSTART,ACOUNT,SEGCNT,CONTRL(6),NCYCLE(50),X(50)
TYPE INTEGER SEGCNT,CONTRL
TYPE INTEGER TPOS,ADDRSS,WAITCP
TYPE INTEGER SEGNC,OUTOP,OP1,OP2,SEGOP
TYPE INTEGER SFGNC
DIMENSION SEGNC(50),INOP(50),OUTOP(50),OP1(50),OP2(50),
1 SEGOP(50),SEGCN(50)
C THIS COMMON IS USED ONLY IN 1604 VERSION FOR PACKING ROUTES
COMMON/NPKR/PKR
TYPE INTEGER X
COMMON/ELORB/EL(104),ORB(4,7)
TYPE INTEGER EL,ORB
COMMON/FINAL/INFIN
ORB(1,4) = 6HS
ORB(2,3) = 6HPY
ORB(2,4) = 6HPZ
ORB(2,5) = 6HPX
ORB(3,2) = 6HDX2-Y2
ORB(3,3) = 6HDXZ
ORB(3,4) = 6HDZ2
ORB(3,5) = 6HDXZ
ORB(3,6) = 6HDXY
WRITE (IW,2000)
2000 FORMAT(10H IN MAINSG)
C IF FIRST TIME IN MAIN, INITIALIZE NECESSARY VARIABLES AND REAP ROUTE
IF(NSTART)2,1,2
1 CONTINUE
C INITIALIZE THE TAPE AREA OF BLANK COMMON
DO 111 I=1,5
TPOS(I) = 1
DO 102 J=1,50
ADDRESS(J,I) = 0
102 CONTINUE
111 CONTINUE
WAITCP = 0
C INITIALIZE THE ROUTE PACKAGE COUNTER (1604 VERSION ONLY)
NPKR = 1
C INITIALIZE THE DUMMY AREA OF BLANK COMMON
DO 31 I=1,50
31 X(I) = 0

```

```

C     AVAILABLE EQUIPMENT TABLE
      READ(IR,1000)(NAET(I),I=1,5)
1000  FORMAT(5I4)
      IF(NAET(1).EQ.0) 3,4
      3  WRITE(IW,1002)
1002  FORMAT(1H1,16H END OF THIS RUN)
      STOP
      4  CONTINUE
      WRITE(IW,999)
      999 FORMAT(1H1,17H TAFF ASSIGNMENTS,/)
      DO 99 I=1,5
      99  WRITE(IW,998)I,NAET(I)
      998 FORMAT(6H NAET(,I1,4H) = ,I3,/)
C     TAPE WRITE COMMON FLORP
      CALL WRITMS(2,EL(1),132,2)
C     READ THE ROUTE
      I = 1
      10  READ(IR,1001)SEQNC(I),SEGNO(I),INOP(I),OUTOP(I),OP1(I),OP2(I),
      1  SEGOF(I)
1001  FORMAT(7I4)
C     ZEROS FOR BOTH SEGNO AND SEQNO SIGNIFY THE END OF THE ROUTE
      IF(SEGNO(I).EQ.0.AND.SEQNO(I).EQ.0)5,6
      5  NSTART = I
      GO TO 11
      6  I = I + 1
      GO TO 10
      11  CONTINUE
      WRITE(IW,1004)
1004  FORMAT(///,50X,6H ROUTE,  //,10X,12H CARD NUMBER,3X,9H SEQUENCE,
      13X,8H SEGMENT,
      23X,5H INOP,3X,6H OUTOP,3X,4H OP1,3X,4H OP2,3X,6H SEGOF,/)
      NSTM1 = NSTART - 1
      DO 101 I=1,NSTM1
      101  WRITE(IW,1005)I,SEQNO(I),SEGNO(I),INOP(I),OUTOP(I),OP1(I),OP2(I),
      1  SEGOF(I)
1005  FORMAT(/, 9X,19,4X,19,3X,19,4X,15,4X,15,2X,15,2X,15,4X,15)
      WRITE(IW,1006)
1006  FORMAT(1H1)
C     BEFORE EXECUTING THE ROUTE, IT MUST BE SIFTED FOR THE CYCLE POINTS
C     MUST BE ASSIGNED
      DO 12 I= 1,NSTART
      IF(SEQNO(I))13,14,14
      13  NCYCLE(I) = SEQNO(I)
C     NCYCLE IS A COUNTER WHICH IS DECREMENTED DURING THE CYCLING PROCESS
C     WHEN NCYCLE IS ZERO, IT IS REINITIALIZED
      GO TO 12
      14  NCYCLE(I) = 0
      12  CONTINUE
C     SEQCNT IS A COUNTER THAT KEEPS TRACK OF SEGMENTS BEING EXECUTED
C     THAT ARE PART OF A STANDARD SEQUENCE OF SEGMENTS. HERE IT IS INITI
      SEQCNT = 0
C     NCOUNT IS A COUNTER THAT KEEPS TRACK OF WHICH CARD IS CURRENTLY BE
C     EXECUTED. IT IS ALSO INITIALIZED HERE
      NCOUNT = 0
      INCN = 0
      2  CONTINUE
C     AT THIS POINT, THE EXECUTION OF THE ROUTE BEGINS (OR CONTINUES).
C     FIRST CHECK TO SEE IF STANDARD SEQUENCE IS BEING EXECUTED
      IF(SEQCNT)16,15,16
      16  CONTINUE

```

```

C   SINCE STANDARD SEQUENCE IS BEING EXECUTED, CALL THE NEXT SEGMENT
C   THIS SEQUENCE
C   SEQCNT = SEQCNT + 1
C   CALL SGCALL
C   REMOVE THIS CARD IN THE CHAIN VERSION
C   IF(SEQCNT)26,15,26
15  CONTINUE
C   STANDARD SEQUENCE IS NOT BEING EXECUTED. CHECK TO SEE IF CURRENT
C   IS END OF ROUTE. IF SO, THEN ATTEMPT TO READ A NEW ROUTE, AFTER
C   REINITIALIZING
C   NCOUNT = NCOUNT + 1
C   IF(NCOUNT-NSTART)17,130,17
17  CONTINUE
C   NOW CHECK TO SEE IF CURRENT CARD IS A CYCLE CARD
C   IF(SEGNO(NCOUNT))18,19,19
18  CONTINUE
C   THIS IS A CYCLE CARD. CHECK TO SEE IF THIS CYCLE IS SATISFIED.
C   IF SO, GO TO THE NEXT CARD. IF NOT, THEN DECREMENT NCYCLE, REASSI
C   NCOUNT AND PROCEED
C   IF(NCYCLE(NCOUNT))20,21,20
20  NCYCLE(NCOUNT) = NCYCLE(NCOUNT)-1
C   NCOUNT = NCOUNT+SEGNO(NCOUNT)
C   IF(NCOUNT=1)24,25,25
24  WRITE(IW,1007)
1007 FORMAT(//,52H ATTEMPTING TO CYCLE PAST THE BEGINNING OF THE ROUTE,
1 //12H ERROR FATAL)
C   STOP
25  IF(SEGNO(NCOUNT))22,19,19
22  WRITE(IR,1003)
1003 FORMAT(///,48H FIRST CARD IN ANY CYCLE CAN NOT BE A CYCLE CARD,//
1,12H ERROR FATAL)
C   STOP
21  NCYCLE(NCOUNT) = SEGNO(NCOUNT)
C   GO TO 15
19  CONTINUE
C   BEFORE CALLING THE APPROPRIATE SEGMENT OR SEQUENCE OF SEGMENTS,
C   LOAD THE OPTIONS INTO THE CONTROL BUFFER
C   CONTRL(1) = 10000*SEGNO(NCOUNT) + SEGNO(NCOUNT)
C   CONTRL(2) = INOP(NCOUNT)
C   CONTRL(3) = OUTOP(NCOUNT)
C   CONTRL(4) = OP1(NCOUNT)
C   CONTRL(5) = OP2(NCOUNT)
C   CONTRL(6) = SEGOP(NCOUNT)
C   CALL SGCALL
26  CONTINUE
C   INCN = INCN + 1
C   CALL PACKEM(INCN)
C   GO TO 2
130 CONTINUE
C   INFIA = INCN
C   END
C   SUBROUTINE SGCALL
C   COMMON//TPOS(5),ADDRSS(50,5),NAET(5),IR,IW,IPUJ,WAITOP,
1 NSTART,NCOUNT,SEQCNT,CONTRL(6),NCYCLE(50),X(50)
C   COMMON/JSEG/J
C   TYPE INTEGER TPOS,ADDRSS,WAITOP

```

```

C     THIS SUBROUTINE IS THE CALLING PROGRAM FOR THE VARIOUS SEGMENTS
C     IN ADDITION TO JUST CALLING AN ISOLATED SEGMENT, A STANDARD SEQUENCE
C     OF SEGMENTS CAN BE CALLED, ALL OF WHICH MUST SHARE THE SAME SET OF
C     OPTIONS, WHATEVER ACTION IS TO BE TAKEN IS DETERMINED BY THE EIGHT
C     DIGIT INTEGER SEGNO, IF THE LEFTMOST FOUR DIGITS OF SEGNO ARE ZERO
C     THEN ONLY THE SEGMENT IDENTIFIED BY THE RIGHTMOST FOUR DIGITS IS CALLED
C     IF THE LEFTMOST FOUR DIGITS ARE NOT ZERO, THEN THE STANDARD SEQUENCE
C     OF SEGMENTS REPRESENTED BY THE LEFTMOST DIGITS IS CALLED. IN THIS
C     THE RIGHTMOST FOUR DIGITS ARE MEANINGLESS. VARIOUS ORDERINGS OF THE
C     SEQUENCE CAN BE DETERMINED BY SEGOP
      SEGN0 = CONTRL(1)
      SEGOP = CONTRL(6)
      NSEQ = SEGN0/10000
      NSEGF = SEGN0-10000*NSEQ
C     CHECK TO SEE IF STANDARD SEQUENCE IS DESIRED
      IF(NSEQ)1,2,1
1     IF(SEQCNT)4,3,4
3     SEQCNT = 1
4     CONTINUE
C     PROCEED TO THE DESIRED STANDARD SEQUENCE
      GO TO (10,20,30,40,50,60,70)NSEQ
10    CONTINUE
C     STANDARD SEQUENCES FOR MODEL BUILDER
      IF(CONTRL(2).EQ.2)12,11
C     ROUTE FOR MBLD FORMULA MATRIX INPUT
11    N=2
      SEG(1) = 2
      SEG(2) = 3
      GO TO 13
C     ROUTE FOR MBLD ZED MATRIX INPUT
12    N= 1
      SEG(1) = 3
13    CONTINUE
      GO TO 1000
20    CONTINUE
C     STANDARD SEQUENCE FOR SLATER OVERLAP AND S COULOMB INTEGRALS
      N = 5
      SEG(1) = 5
      SEG(2) = 6
      SEG(3) = 7
      SEG(4) = 8
      SEG(5) = 9
      GO TO 1000
30    CONTINUE
      GO TO 1000
40    CONTINUE
      GO TO 1000
50    CONTINUE
C     THIS IS A SAMPLE ONLY
      GO TO (51,52,53)SEGOP
51    CONTINUE
      N=3
      SEG(1) = 4
      SEG(2) = 5
      SEG(3) = 6
      GO TO 59
52    CONTINUE
      N=3
      SEG(1) = 35
      SEG(2) = 33

```

```

      SEG(3) = 34.
      GO TC 59
53 CONTINUE
      N=2
      SEG(1) = 34
      SEG(2) = 36
59 CONTINUE
C   END OF SAMPLE
      GO TC 1000
60 CONTINUE
      GO TC 1000
70 CONTINUE
1000 CONTINUE
C   N IS THE TOTAL NUMBER OF SEGMENTS IN A STANDARD SEQUENCE
      IF(SEQCNT=N-1)6,5,6
      5 CONTINUE
C   THE LAST SEGMENT IN THIS SEQUENCE HAS ALREADY BEEN CALLED.
C   RESET SEQCNT AND RETURN TO MAIN PROGRAM
      SEQCNT = 0
      RETURN
      6 J = SEG(SEQCNT)
      GO TC 7
      2 J = NSEGF
      7 CONTINUE
C   CALL CHAIN(J)
      RETURN
      END
      SUBROUTINE PACKEM(I)
C   THIS SUBROUTINE GOES WITH MAINSEG (1604 VERSION ONLY)
      COMMON//TPOS(5),ADDRSS(50,5),NAET(5),IR,IW,IPUN,WAITCP,
      1 NSTART,NCOUNT,SEQCNT,CONTRL(6),NCYCLE(50),X(50)
      TYPE INTEGER TPOS,ADDRSS,WAITOP,SEQCNT,CONTRL
      COMMON/JSEG/JSEGF
      COMMON/NPKR/NPKR
      COMMON/IPRTE/NPKRF
      COMMON/PAKED/IA(20),IB(20)
      DIMENSION IDUM(5)
      NPKRF = NPKR
      DO 10 K=1,5
      IF(CONTRL(K+1).LT.0)11,12
11 IDUM(K) = -CONTRL(K+1)+1000
      GO TC 13
12 IDUM(K) = CONTRL(K+1)
13 CONTINUE
10 CONTINUE
      II = I - 20*(NPKR-1)+(I/(20*(NPKR-1)+1))
      IA(II) = 10000000000*JSEGF+1000000000*NCOUNT+1000*IDUM(1)+IDUM(2)
      IB(II) = 100000000*IDUM(3)+10000*IDUM(4)+IDUM(5)
      IF(I/(20*NPKR)-1)1,2,1
      2 CALL WRITMS(1,IA,40,NPKR)
      NPKR = NPKR + 1
      1 CONTINUE
      RETURN
      END
      OVERLAY(S6KSYS,1,2)
      PROGRAM ZMAT
      * (INPUT,OUTPUT,TAPE5=INPUT,TAPE6=OUTPUT,PUNCH)
C   THIS PROGRAM ACCEPTS A DEFINITION OF A MOLECULE IN TERMS OF
C   ATOMIC NUMBERS, BOND LENGTHS, BOND ANGLES AND DIHEDRAL ANGLES
C   AND CALCULATES THE CARTESIAN COORDINATES IN ANGSTROMS

```

```

C      ADAPTED FROM MARK GORDON'S MBLD SYSTEM BY D L BEVERIDGE
C      CODED IN CDC SCOPE 3.1 LEVEL FORTRAN FOR THE CIMS CDC 4600
COMMON//TPCS(5),ADDRS(50,5),NAET(5),IR,IW,IPUT,NAITCP,
1  NSTART,NCOUNT,SEQCNT,CONTRL(6),NCYCLE(50),X(50)
   DIMENSION Z(50,4),BL(50),ALPHA(50),BETA(50)
   DIMENSION V1(3),V2(3),V3(3),VJ(3),VP(3),L1(3),L2(3),L3(3),L4(3),
*  A(50),B(50),D(50)
COMMON/INFO/NATOMS,CHARGE,MULTIP,AN(50),C(50,3),N
   TYPE REAL L1,L2,L3,L4
   TYPE INTEGER AN,CHARGE,Z,PUNCH
   DIMENSION R(50,50)
COMMON/IDENT/IDENT(8)
COMMON/ELORB/EL(104),ORB(4,7)
   TYPE INTEGER ORB
   COSF(QSAD)=COS(QSAD)
   SINF(QSAD)=SIN(QSAD)
   ABSF(QSAD)=ABS(QSAD)
   SIGNF(QSAD,QRAD)=SIGN(QSAD,QRAD)
   ATANF(QSAD)=ATAN(QSAD)
   SQRTF(QSAD)=SQRT(QSAD)
   FLOATF(ISSAM)=FLOAT(ISSAM)
   XMAXOF(ISSAM,JANO)=MAXO(ISSAM,JANO)
C      *****
C      INPUT AND OUTPUT OF INPUT
999  CONTINUE
   PUNCH = 8HPUNCH
   READ 1000,(IDENT(I),I=1,8)
   IF(ECF,5) 1,2
   1  STOP
   2  CONTINUE
   PRINT 998
998  FORMAT(1H1)
   PRINT 2006
2006 FORMAT(/,14H INPUT DATA.../)
   PRINT1000,(IDENT(I),I=1,8)
1000 FORMAT(8A10)
   IF(IDENT(8) .EQ. PUNCH)3,4
   3  PRINT 2008
2008 FORMAT(/,16H PUNCH OPTION ON./)
   PUNCH 1000,(IDENT(I),I=1,8)
   4  CONTINUE
   READ 1001, NATOMS,CHARGE,MULTIP
1001  FORMAT(3I2)
   PRINT1002, NATOMS,CHARGE,MULTIP
1002  FORMAT(/,10H NATOMS = ,I4,2X,10H CHARGE = ,I4,2X,10H MULTIP = ,I4,2X,10H)
   IF(IDENT(8) .EQ. 8HPUNCH)5,6
   5  PUNCH 8,NATOMS,CHARGE,MULTIP
   6  FORMAT(3I4)
   6  CONTINUE
   PRINT 1004
1004  FORMAT(/,9H Z MATRIX,/)
C      *****
C      SPECIAL FOR INDC SCF LOAD CMO SYSTEM
C      THE FIRST NATOMS CARDS SPECIFY THE ATOMS OF THE ZEROth CELL AND
C      THE SECOND NATOMS CARDS SPECIFY THE ATOMS OF THE PLUS CELL
C      M = 2*NATOMS
C      CALCULATION OF COORDINATES
DO 6969 I=1,M
   READ 1003, AN(I),Z(I,1),BL(I),Z(I,2),ALPHA(I),Z(I,3),BETA(I),

```

```

1Z(I,4)
1003 FORMAT(13,I4,F7,4,I4,F11,5,I4,F11,6,I4,F10,5)
6969 PRINT 1003, AN(I),7(I,1),BL(I),Z(I,2),ALPHA(I),Z(I,3),BETA(I),
1Z(I,4)
DO 502 J=1,M
502 ALPHA(J) = ALPHA(J)+3.141592654/180.
DO 503 J=1,M
503 BETA(J) = BETA(J)+3.141592654/180.
DO 504 J= 1,3
504 C(1,J)=0.0
C(2,1)=0.0
C(2,2)=0.0
C(2,3)=BL(2)
C(3,1)=BL(3)*SINF(ALPHA(3))
C(3,2)=0.0
C *****
C THE FOLLOWING IS AN ADDITION TO COORD FINDER PROGRAM TO BE USED
C IF THE MOLECULE UNDER CONSIDERATION HAS ONLY ONE HEAVY ATOM OR FOR
C A MOLECULE SUCH AS NEOPENTANE IN WHICH THE CENTRAL ATOM HAS NO
C HYDROGENS BONDED TO IT
IF(Z(3,1),EQ.1) 505,506
505 C(3,3) = BL(3)*COSF(ALPHA(3))
GO TO 507
506 C(3,3) = C(2,3)-BL(3)*COSF(ALPHA(3))
507 I=3
IF(ABSF(C(3,1)),LT.,.00001) 550,510
550 DO 509 I = 4,1000
IF(I,LE,M,AND,ABSF(C(I-1,1)),LT.,.00001) 508,510
508 C(I,1) = BL(I)*SINF(ALPHA(I))
C(I,2) = 0.0
ITEMP = Z(I,1)
JTEMP = Z(I,2)
OC(I,3) = C(ITEMP,3)-BL(I)*COSF(ALPHA(I))*SIGNF(1.,C(ITEMP,3)-C(JTE
MP,3))
509 CONTINUE
510 CONTINUE
IF(I,EQ,3) 511,512
511 K=4
GO TO 513
512 K=I
513 CONTINUE
IF(K,GT,M) 601,600
600 CONTINUE
DO 533 J = K,M
IF(Z(J,4),EQ.0) 514,517
C *****
C THIS PART IS USED IF THE ATOM IS BEING DEFINED BY A DIHEDRAL ANGLE
514 CALL RELVEC(V1,Z(J,2),Z(J,3))
CALL UNIVVEC(L1,V1)
C V1 IS A VECTOR FROM ATOM Z(J,3) TO ATOM Z(J,2)
C L1 IS A UNIT VECTOR OF V1. BL(Z(J,2)) IS BONDLENGTH OF ATOM Z(J,2)
CALL RELVEC(V2,Z(J,1),Z(J,2))
CALL UNIVVEC(L2,V2)
C V2 IS THE VECTOR FROM ATOM Z(J,2) TO ATOM Z(J,1)
C L2 IS THE UNIT VECTOR OF V2. BL(Z(J,1)) IS BONDLENGTH DEFINING
C ATOM Z(J,1)
CALL VECPRD(VP,L1,L2)
DO 515 I = 1,3
515 L3(I) = VP(I)/SQRTF(1.-(L1(1)*L2(1)+L1(2)*L2(2)+L1(3)*L2(3))*2)
C L3 IS THE UNIT VECTOR OF VP. ALPHA(Z(J,1)) IS THE ANGLE DEFINING

```

```

C     ATOM Z(J,1)
      CALL VECPRD(L4,L3,L2)
C     L4,L3,L2 ARE A NEW SET OF MUTUALLY ORTHOGONAL AXES. WE WILL NOW
C     OBTAIN COORD OF ATOM J IN TERMS OF THESE AXES RELATIVE TO ATOM Z(J
      DO 516 I=1,3
      OVJ(I) = RL(J)*(-L2(I)*COSF(ALPHA(J))+L4(I)*SINF(ALPHA(J))*COSF(BET
      1A(J))+L3(I)*SINF(ALPHA(J))*SINF(BETA(J)))
C     VJ IS THE VECTOR FROM ATOM Z(J,1) TO ATOM J
      ITEMP = Z(J,1)
      C(J,I) = VJ(I) + C(ITEMP,I)
516  CONTINUE
      GO TO 533
517  IF(Z(J,4).EQ.1.OR.Z(J,4).EQ.-1) 549,528.
C     *****
C     THIS PART IS USED IF ATOM IS DEFINED BY TWO BONDANGLES
549  CALL RELVEC(V1,Z(J,1),7(J,3))
      CALL UNIVVEC(L1,V1)
      CALL RELVEC(V2,Z(J,2),Z(J,1))
      CALL UNIVVEC(L2,V2)
      ZETA = -(L1(1)+L2(1)+L1(2)+L2(2)+L1(3)+L2(3))
      A(J) = (-COSF(BETA(J))+ZETA*COSF(ALPHA(J)))/(1.-ZETA**2)
      B(J) = (COSF(ALPHA(J))-ZETA*COSF(BETA(J)))/(1.-ZETA**2)
      PI = 3.141592654
      IF(ZETA.LT.0) 518,519
518  TEMP = PI
      GO TO 520
519  TEMP = 0.0
520  CONTINUE
      IF(ZETA.EQ.0) 521,522
521  GAMMA = PI/2.
      GO TO 523
522  GAMMA = ATANF(SQRTF(1.-ZETA**2)/ZETA) +TEMP
523  CONTINUE
      IF (ABSF(GAMMA+ALPHA(J)+BETA(J)-2.*PI).LT..00000001) 524,525
524  D(J) = 0.0
      GO TO 526
525  D(J) = Z(J,4)*(SQRTF(1.+A(J)*COSF(BETA(J))-B(J)*COSF(ALPHA(J)))/S
      1SQRTF(1.-ZETA**2))
526  CONTINUE
      CALL VECPRD(V3,L1,L2)
      DO 527 I = 1,3
      L3(I) = A(J)*L1(I)+B(J)*L2(I)+D(J)*V3(I)
      VJ(I) = RL(J)*L3(I)
      ITEMP = Z(J,1)
      C(J,I) = VJ(I)+C(ITEMP,I)
527  CONTINUE
      GO TO 533
C     *****
C     THIS PART IS USED IF ATOM IS DEFINED BY ONE BONDANGLE AND BY THE
C     ANGLE WHICH BOND Z(J,1)-J MAKES WITH THE PLANE OF Z(J,1),Z(J,2)
C     AND Z(J,3)
528  CALL RELVEC(V1,Z(J,1),Z(J,3))
      CALL UNIVVEC(L1,V1)
      CALL RELVEC(V2,Z(J,2),Z(J,1))
      CALL UNIVVEC(L2,V2)
      ZETA = -(L1(1)+L2(1)+L1(2)+L2(2)+L1(3)+L2(3))
      CALL VECPRD(V3,L1,L2)
C     BETA(J) HERE REFERS TO 90-ANGLE WHICH BOND Z(J,1)-J MAKES WITH THE
C     AFOREMENTIONED PLANE
      A(J) = COSF(BETA(J))/(1.-ZETA**2)

```

```

      IF(Z(J,4),EQ,2) 530,529
529 P(J)= -SQRTF((1,-COSF(ALPHA(J))*2-A(J)+COSF(BETA(J)))/(1.-ZETA**
      1))
      GO TO 531
530 B(J)=SQRTF((1.-COSF(ALPHA(J))*2-A(J)+COSF(BETA(J)))/(1.-ZETA**2)
531 CONTINUE
      P(J) = B(J)*ZETA+COSF(ALPHA(J))
      DO 532 I=1,3
      L3(I) = B(J)*L1(I)+D(J)*L2(I)+A(J)*V3(I)
      VJ(I) = BL(J)*L3(I)
      ITEMP = Z(J,1)
      C(J,I) = VJ(I) + C(ITEMP,I)
532 CONTINUE
533 CONTINUE
601 CONTINUE
C *****
C   OUTPUT SECTION
      PRINT 2007
2007 FORMAT(/,15H OUTPUT DATA...,/)
      PRINT 1998
1998 FORMAT (//,20X,11HCOORDINATES,//4X,10HNO OF ATOM,3X,6HSYMBOL,10X,
      11HX,10X,1HY,10X,1HZ,/)
      DO 900 J=1,M
      IF(M,EQ,NATOMS+1) 12,13
      12 PRINT 1997
1997 FORMAT(/,10X,22H NEAREST NEIGHBOR CELL,/)
      13 IND1=AN(J)
      900 PRINT 1999      ,J,EL(IND1),( C(J,I),I=1,3)
1999 FORMAT(8X,12,5X,A4,4X,3F12.8)
      IF(IDENT(10).EQ.PUNCH) 7,11
      7 PUNCH 9,(AN(I),(C(I,J),J=1,3),I=1,M)
      9 FORMAT(14,3(3X,F12.7))
      11 CONTINUE
      DO 10 I=1,M
      DO 10 J=1,M
      10 P(I,J) = SQRT((C(I,1)-C(J,1))**2+(C(I,2)- C(J,2))**2+(C(I,3)-C(J,3)
      *)**2)
      CALL MOUTPT(R,M,M,50,50,10H DISTANCES)
      DO 290 I=1,M
      DO 290 J=1,3
290 C(I,J) = C(I,J)/0.529167
      END
      SURRCUTINE TIME
      CALL HOUR(VAR)
      PRINT 1000, VAR
1000 FORMAT(/,8H TIME = ,A10,/)
      RETURN
      END
      SURRCUTINE RFLVEC(R,J,K)
      COMMON/INFO/NATOMS,CHARGE,MULTIP,AN(50),C(50,3),N
      DIMENSION R(3)
      TYPE REAL C,R
      TYPE INTEGER J,K,I
      DO 1 I=1,3
      1 R(I)=C(J,1)-C(K,I)
C   R IS THE RELATIVE VECTOR FROM ATOM K TO ATOM J
      RETURN
      END
      SURRCUTINE UNIVVEC(L,R)
      DIMENSION L(3),R(3)

```

```

      TYPE REAL L,R
      TYPE INTEGER I
      SQRTF(QSAD)=SQRT(GSAD)
      DO 2 I=1,3
2      L(I)=R(I)/SQRTF(R(1)**2 + R(2)**2 + R(3)**2)
C      L IS THE UNITVECTOR OF R
      RETURN
      END
      SUBROUTINE VECPRD(VP,X,Y)
      DIMENSION VP(3),X(3),Y(3)
      TYPE REAL VP,X,Y
      VP(1)=X(2)*Y(3)-X(3)*Y(2)
      VP(2)=X(3)*Y(1)-X(1)*Y(3)
      VP(3)=X(1)*Y(2)-X(2)*Y(1)
C      VP IS THE VECTOR PRODUCT OF X CROSSED Y
      RETURN
      END
      OVERLAY(S&KSYS,1,3)
      PROGRAM INTOV
      COMMON//TPOS(5),ADDRSS(50,5),NAET(5),IR,IW,IPUN,WAITCP,
1  INSTART,NCOUNT,SEQCNT,CONTRL(6),NCYCLE(50),XX(50)
      COMMON/INFO/NATOMS,CHARGE,MULTIP,AN(50),C(50,3),N
      COMMON/ARRAYS/S(100,100),Y(9.5,203),Z(17.45),GAMMA(50,50),X(760)
      COMMON/AUXINT/A(17),R(17)
      COMMON/NLM/MU(18),NC(18),LC(9),MC(9)
      COMMON/INFO1/CZ(50),U(100),ULIM(50),LLIM(50),NELECS,CCCA,CCCC
      COMMON/OPTION/OPTION,OPNCLO,HUCKEL,CNDO,INDO,CLOSEP,CPFN
      TYPE INTEGER OPTION,OPNCLO,HUCKEL,CNDO,INDO,CLOSEP,CPFN
      PRINT 1000
1000 FORMAT(9H IN INTOV)
      CALL COEFF
      CALL INTGRL
      CALL INTGRPL
C      LEAVING THIS SEGMENT WITH S IN MATRIX A, SP IN MATRIX B
C      GAMMA AND GAMMAP FILLED
      END
      SUBROUTINE COEFF
      COMMON/ARRAYS/S(100,100),Y(9.5,203),Z(17.45),X(10100)
      PRINT 1000
1000 FORMAT(9H IN COEFF)
      DO 1 I=1,9135
1      Y(I)=0.0
      DO 2 I=1,765
2      Z(I)=0.0
C      LOAD NON-ZERO Y CCOEFFICIENTS
      Y(7039)= 64.
      Y(7040)= 64.
      Y(7049)= -64.
      Y(7032)= -128.
      Y(7041)= -64.
      Y(7033)= -128.
      Y(7042)= 128.
      Y(7025)= 64.
      Y(7034)= 128.
      Y(7026)= 64.
      Y(7035)= -64.
      Y(7027)= -64.
      Y(6904)= -96.
      Y(6913)= 32.
      Y(6896)= -192.

```

Y(6905)= 192.
Y(6906)= 288.
Y(6915)= -96.
Y(6889)= 192.
Y(6907)= -192.
Y(6890)= 96.
Y(6899)= -288.
Y(6891)= -192.
Y(6900)= 192.
Y(6892)= -32.
Y(6901)= 96.
Y(2854)= -16.
Y(2863)= 16.
Y(2847)= 32.
Y(2856)= -16.
Y(2865)= -16.
Y(2840)= -16.
Y(2849)= -16.
Y(2858)= 32.
Y(2842)= 16.
Y(2851)= -16.
Y(2710)= 48.
Y(2719)= -48.
Y(2711)= 48.
Y(2720)= -96.
Y(2729)= 48.
Y(2703)= -48.
Y(2712)= -48.
Y(2721)= 96.
Y(2704)= -48.
Y(2713)= 48.
Y(2722)= 48.
Y(2731)= -48.
Y(2705)= 96.
Y(2714)= -48.
Y(2723)= -48.
Y(2706)= 48.
Y(2715)= -96.
Y(2724)= 48.
Y(2707)= -48.
Y(2716)= 48.
Y(5329)= 64.
Y(5322)= -128.
Y(5340)= -64.
Y(5315)= 64.
Y(5333)= 128.
Y(5326)= -64.
Y(5185)= -96.
Y(5194)= 32.
Y(5186)= -96.
Y(5195)= 64.
Y(5204)= 32.
Y(5178)= 96.
Y(5187)= 32.
Y(5196)= 64.
Y(5179)= 96.
Y(5188)= -32.
Y(5197)= 32.
Y(5206)= -96.
Y(5180)= -64.

Y(5189)= -32.
Y(5198)= -96.
Y(5181)= -32.
Y(5190)= -64.
Y(5199)= 96.
Y(5182)= -32.
Y(5191)= 96.
Y(4375)= -144.
Y(4384)= 96.
Y(4393)= -16.
Y(4368)= 144.
Y(4386)= -48.
Y(4395)= 96.
Y(4370)= -96.
Y(4379)= 48.
Y(4397)= -144.
Y(4372)= 16.
Y(4381)= -96.
Y(4390)= 144.
Y(1900)= 144.
Y(1909)= -144.
Y(1893)= -144.
Y(1920)= 144.
Y(1895)= 144.
Y(1922)= -144.
Y(1906)= -144.
Y(1915)= 144.
Y(955)= -16.
Y(964)= 32.
Y(973)= -16.
Y(948)= 16.
Y(966)= -48.
Y(975)= 32.
Y(950)= -32.
Y(959)= 48.
Y(977)= -16.
Y(952)= 16.
Y(961)= -32.
Y(970)= 16.
Y(8155)= 64.
Y(8156)= -64.
Y(8165)= -64.
Y(8148)= -64.
Y(8157)= 64.
Y(8149)= 64.
Y(8158)= 64.
Y(8150)= -64.
Y(8020)= -96.
Y(8029)= 32.
Y(8021)= 128.
Y(8013)= 96.
Y(8031)= -96.
Y(8014)= -128.
Y(8015)= -32.
Y(8024)= 96.
Y(7084)= -64.
Y(7076)= -128.
Y(7085)= 64.
Y(7086)= 128.
Y(7069)= 128.

Y(7070)= 64.
Y(7079)= -128.
Y(7071)= -64.
Y(3205)= -16.
Y(3214)= 16.
Y(3206)= 16.
Y(3215)= -16.
Y(3198)= 16.
Y(3216)= -16.
Y(3199)= -16.
Y(3217)= 16.
Y(3200)= -16.
Y(3209)= 16.
Y(3201)= 16.
Y(3210)= -16.
Y(7579)= 64.
Y(7580)= -64.
Y(7572)= -128.
Y(7573)= 128.
Y(7565)= 64.
Y(7566)= -64.
Y(5680)= 64.
Y(5681)= -64.
Y(5673)= -64.
Y(5691)= -64.
Y(5674)= 64.
Y(5692)= 64.
Y(5684)= 64.
Y(5685)= -64.
Y(7435)= -96.
Y(7444)= 32.
Y(7436)= -96.
Y(7445)= 160.
Y(7428)= 96.
Y(7437)= 128.
Y(7446)= -96.
Y(7429)= 96.
Y(7438)= -128.
Y(7447)= -96.
Y(7430)= -160.
Y(7439)= 96.
Y(7431)= -32.
Y(7440)= 96.
Y(5545)= -96.
Y(5554)= 32.
Y(5546)= 32.
Y(5555)= 32.
Y(5538)= 96.
Y(5556)= 32.
Y(5539)= -32.
Y(5557)= -96.
Y(5540)= -32.
Y(5549)= -32.
Y(5541)= -32.
Y(5550)= 96.
Y(3070)= 48.
Y(3079)= -48.
Y(3071)= -48.
Y(3080)= 48.
Y(3063)= -48.

Y(3081)= 48.
Y(3064)= 48.
Y(3082)= -48.
Y(3065)= 48.
Y(3074)= -48.
Y(3066)= -48.
Y(3075)= 48.
Y(8200)= -64.
Y(8201)= 64.
Y(8193)= 64.
Y(8194)= -64.
Y(7615)= -64.
Y(7616)= -64.
Y(7625)= 64.
Y(7608)= 64.
Y(7617)= 64.
Y(7609)= 64.
Y(7618)= -64.
Y(7610)= -64.
Y(3250)= 16.
Y(3259)= -16.
Y(3243)= -16.
Y(3261)= 16.
Y(3245)= 16.
Y(3254)= -16.
Y(5725)= -64.
Y(5718)= 64.
Y(5736)= 64.
Y(5729)= -64.

C LOAD NON-ZERO Z COEFFICIENTS

Z(341)= -1.
Z(343)= 3.
Z(345)= -3.
Z(347)= 1.
Z(664)= -1.
Z(665)= 5.
Z(666)= -10.
Z(667)= 10.
Z(668)= -5.
Z(669)= 1.
Z(154)= -1.
Z(156)= 5.
Z(158)= -10.
Z(160)= 10.
Z(162)= -5.
Z(164)= 1.
Z(222)= -1.
Z(223)= 1.
Z(224)= 4.
Z(225)= -4.
Z(226)= -6.
Z(227)= 6.
Z(228)= 4.
Z(229)= -4.
Z(230)= -1.
Z(231)= 1.
Z(307)= -1.
Z(308)= 2.
Z(309)= 2.
Z(310)= -6.

Z(312)= 6.
Z(313)= -2.
Z(314)= -2.
Z(315)= 1.
Z(409)= -1.
Z(410)= 3.
Z(411)= -1.
Z(412)= -5.
Z(413)= 5.
Z(414)= 1.
Z(415)= -3.
Z(416)= 1.
Z(528)= -1.
Z(529)= 4.
Z(530)= -5.
Z(532)= 5.
Z(533)= -4.
Z(534)= 1.
Z(562)= -1.
Z(563)= 2.
Z(565)= -2.
Z(566)= 1.
Z(732)= -1.
Z(733)= 1.
Z(545)= 1.
Z(546)= -3.
Z(547)= 2.
Z(548)= 2.
Z(549)= -3.
Z(550)= 1.
Z(579)= 1.
Z(580)= -1.
Z(581)= -1.
Z(582)= 1.
Z(596)= -1.
Z(598)= 1.
Z(443)= -1.
Z(444)= 1.
Z(445)= 2.
Z(446)= -2.
Z(447)= -1.
Z(448)= 1.
Z(698)= -1.
Z(699)= 3.
Z(700)= -3.
Z(701)= 1.
Z(324)= 1.
Z(325)= -1.
Z(326)= -3.
Z(327)= 3.
Z(328)= 3.
Z(329)= -3.
Z(330)= -1.
Z(331)= 1.
Z(460)= 1.
Z(462)= -2.
Z(464)= 1.

RETURN

END

SUBROUTINE INTGRL

```

C   INTRACELL ATOMIC INTEGRALS FOR INDO SCF LCAO MO CALCULATION
TYPE INTEGER AN,ULIM,ULK,ULL,CZ,U,CHARGE,ANL,ANK
TYPE REAL MU,NUM,K1,K2
COMMON/ARRAYS/S(100,100),Y(9,5,203),Z(17,45),XX(100),SP(100,100)
C   ARRAYS Y AND Z TOGETHER TAKE UP 9900 WORDS OF CORE
COMMON/NLM/MU(18),NC(18),LC(9),MC(9)
DIMENSION E(3)
DIMENSION P(100,100)
EQUIVALENCE(P,Y)
COMMON/INFO/NATOMS,CHARGE,MULTIP,AN(50),C(50,3),N
COMMON/INFO1/CZ(50),U(100),ULIM(50),LLIM(50),NELECS,CCCA,CCCC
COMMON/1/XXX(500),GAMMA(50,50),T(9,9),PAIRS(9,9),TEMP(9,9),C1(3),
1   C2(3),YYY(526),GAMMAP(50,50)
COMMON/AUXINT/A(17),R(17)
COMMON/OPTION/OPTION,OPNCLO,HUCKEL,CNDO,INDO,CLOSED,CPEN
TYPE INTEGER OPTION,OPNCLO,HUCKEL,CNDO,INDO,CLOSED,CPEN
FLOATF(ISSAM)=FLOAT(ISSAM)
SQRTF(GSAD)=SQRT(GSAD)
XMAXOF(ISSAM,JANO)=MAX0(ISSAM,JANO)
C   *****
C   INITIALIZATION AND ASSIGNMENT OF ATOM AND ORBITAL VECTORS
PRINT 1000
1000 FORMAT(10H IN INTGRL)
N=0
DO 60 I=1,NATOMS
LLIM(I) = N+1
K=1
IF (AN(I),GT.10) 10,20
10 N=N+9
CZ(I)=AN(I)-10
GO TO 50
20 IF (AN(I),LT.3) 40,30
30 N=N+4
CZ(I) = AN(I)-2
GO TO 50
40 N=N+1
CZ(I)= AN(I)
50 CONTINUE
ULIM(I) = N
60 CONTINUE
C   FILL U ARRAY---U(J) IDENTIFIES THE ATOM TO WHICH ORBITAL J IS
C   ATTACHED E.G. ORBITAL 32 ATTACHED TO ATOM 7. ETC.
DO 70 K=1,NATOMS
LLK = LLIM(K)
ULK = ULIM(K)
LIM = ULK+1-LLK
DO 70 I=1,LIM
J = LLK+I-1
70 U(J) = K
C   ASSIGNMENT OF ORBITAL EXPONENTS TO ATOMS BY SLATERS RULES
MU(1)=1,2
MU(2)=1,7
LC(1)=1
NC(2)=1
DO 80 I=3,10
NC(I)=2
80 MU(I)=.325*FLOATF(I-1)
DO 90 I=11,18
NC(I)=3
90 MU(I)=(.65*FLOATF(I)-4.95)/3.

```

```

C      ASSIGNMENT OF ANGLLAR MOMENTUM QUANTUM NOS. TO ATOMIC ORBITALS
      LC(1)=0
      LC(2)=1
      LC(3)=1
      LC(4)=1
      LC(5)=2
      LC(6)=2
      LC(7)=2
      LC(8)=2
      LC(9)=2
      MC(1)=0
      MC(2)=1
      MC(3)=-1
      MC(4)=0
      MC(5)=0
      MC(6)=1
      MC(7)=-1
      MC(8)=2
      MC(9)=-2

C      STEP THRU PAIRS OF ATOMS
      DO 320 K=1,NATOMS
      DO 320 L=K,NATOMS
      DO 100 I=1,3
      C1(I) = C(K,I)
100    C2(I) = C(L,I)
C      CALCULATE UNIT VECTOR ALONG INTERATOM AXIS.E
      CALL RELVEC(R,E,C1,C2)
      LLK = LLIM(K)
      LLL = LLIM(L)
      ULK = ULIM(K)
      ULL = ULIM(L)
      NORBK=ULK-LLK+1
      NORBL=ULL-LLL+1
      ANK=AN(K)
      ANL=AN(L)

C      LOOP THRU PAIRS OF BASIS FUNCTIONS, ONE ON EACH ATOM
      DO 200 I=1,NORBK
      DO 200 J=1,NORBL
      IF(K,EQ,L)160,110
110    IF(MC(I).NE,MC(J)) 150,120
120    IF(MC(I).LT,0) 140,130
130    CONTINUE
      PAIRS(I,J)=SQRTF((MU(ANK)*R)**(2*NC(ANK)+1)*(MU(ANL)*R)**(2*NC(ANL)
1) + 1)/(FACT(2*NC(ANK))*FACT(2*NC(ANL)))*(-1.)**(LC(J)+MC(J))
      2*SS(NC(ANK),LC(I),MC(I),NC(ANL),LC(J),MU(ANK)*R,MU(ANL)*R)
      GO TC 190
140    PAIRS(I,J)=PAIRS(I-1,J-1)
      GO TC 190
150    PAIRS(I,J)=0.0
      GO TC 190
160    IF (I,EQ,J) 170,180
170    PAIRS(I,J)=1.0
      GO TC 190
180    PAIRS(I,J)=0.0
190    CONTINUE
200    CONTINUE
      LCULK=LC(NORBK)
      LCULL=LC(NORBL)
      MAXL = XMAXOF(LCULK,LCULL)
      IF(R,GT,0,000001) 220,210

```

```

210 GO TO 250
C ROTATE INTEGRALS FROM DIATOMIC BASIS TO MOLECULAR BASIS
220 CALL HARMTR(T,MAXL,E)
DO 230 I=1,NORBK
DO 230 J=1,NORBL
TEMP(I,J) = 0.
DO 230 KK=1,NORBL
TEMP(I,J) = TEMP(I,J)+T(J,KK)+PAIRS(I,KK)
230 CONTINUE
DO 240 I=1,NORBK
DO 240 J=1,NORBL
PAIRS(I,J) = 0.
DO 240 KK=1,NORBK
PAIRS(I,J) = PAIRS(I,J)+T(I,KK)*TEMP(KK,J)
240 CONTINUE
C FILL S MATRIX
250 CONTINUE
DO 260 I=1,NORBK
DO 260 J=1,NORBL
260 S(LLK+I-1,LLL+J-1) = PAIRS(I,J)
C COMPUTATION OF 1-CENTER COULOMB INTEGRALS OVER SLATER S FUNCTIONS
N1=NC(ANK)
N2=NC(ANL)
K1=ML(ANK)
K2=ML(ANL)
IF(K,NE,L) 290,270
270 TERM1 = FACT(2*N1-1)/((2*K2)**(2*N1))
TERM2 = 0.
LIM = 2*N1
DO 280 J=1,LIM
NUM = FLOATF(J)*(2.*K1)**(2*N1-J)*FACT(4*N1-J-1)
DEN = FACT(2*N1-J)*2.*FLOATF(N1)*(2.*(K1+K2))**(4*N1-1-J)
TERM2 = TERM2 + NUM/DEN
280 CONTINUE
GO TO 310
C COMPUTATION OF 2-CENTER COULOMB INTEGRALS OVER SLATER S FUNCTIONS
290 TERM1 = (R/2.)**(2*N2)*SS(0,0,0,2*N2-1,0,0,2.*K2*R)
TERM2 = 0.
LIM = 2*N1
DO 300 J=1,LIM
300 TERM2 = TERM2+ (FLOATF(J)*(2*K1)**(2*N1-J)*(R/2.)**(2*N1-J+2*N2))
1 (FACT(2*N1-J)*2.*FLOATF(N1))*SS(2*N1-J,0,0,2*N2-1,0,2.*K1*R)
2 2*K2*R)
310 GAMMA(K,L) = ((2.*K2)**(2*N2+1)/FACT(2*N2))*(TERM1-TERM2)
320 CONTINUE
C SYMMETRIZATION OF OVERLAP AND COULOMB INTEGRAL MATRICES
DO 330 I=1,N
DO 330 J=1,N
330 S(J,I) = S(I,J)
DO 340 I=1,NATOMS
DO 340 J=1,NATOMS
340 GAMMA(J,I) = GAMMA(I,J)
RETURN
END
SUBROUTINE INTGRLF
C INTERCELL ATOMIC INTEGRALS FOR INDO SCF LCAO MO CALCULATIONS
TYPE INTEGER AN,ULIM,ULK,ULL,C7,U,CHARGE,ANL,ANK
TYPE REAL MU,NUM,K1,K2
COMMON/NUM/MU(16),NC(16),LC(9),MC(9)
DIMENSION E(3)

```

```

COMMON/ARRAYS/S(100,100),Y(9,5,203),Z(17,45),XX(100),SP(100,100)
DIMENSION P(100,100)
EQUIVALENCE(P,Y)
COMMON/INFO/NATOMS,CHARGE,MULTIP,AN(50),C(50,3),N
COMMON/INFO1/CZ(50),U(100),ULIM(50),LLIM(50),NELECS,CCCA,CCCF
COMMON/1/XXX(500),GAMMA(50,50),T(9,9),PAIRS(9,9),TEMP(9,9),C1(3),
1  C2(3),YYY(526),GAMMAP(50,50)
COMMON/AUXINT/A(17),R(17)
COMMON/OPTION/OPTION,OPNCLO,HUCKEL,CNDO,INDO,CLOSEP,CPFN
TYPE INTEGER OPTION,OPNCLO,HUCKEL,CNDO,INDO,CLOSEP,CPFN
SQRTF(OSAD)=SQRT(GSAD)
XMAXOF(ISSAM,JANO)=MAXO(ISSAM,JANO)
FLOATF(ISSAM)=FLOAT(ISSAM)
PRINT 1000
1000 FORMAT(11H IN INTERLP)
C *****
C STEP THROUGH ATOM PAIRS, ONE IN ZEROth CELL AND ONE IN PLUS CELL
DO 320 K=1,NATOMS
DO 320 L=1,NATOMS
LTEMP = L+NATOMS
DO 100 I=1,3
C1(I) = C(K,I)
100 C2(I) = C(LTEMP,I)
C CALCULATE UNIT VECTOR ALONG INTERATOM AXIS,E
CALL RELVEC(R,E,C1,C2)
LLK = LLIM(K)
LLL = LLIM(L)
ULK = ULIM(K)
ULL = ULIM(L)
NORBK=ULK-LLK+1
NORBL=ULL-LLL+1
ANK=AN(K)
ANL=AN(L)
C LOOP THRU PAIRS OF BASIS FUNCTIONS, ONE ON EACH ATOM
DO 200 I=1,NORBK
DO 200 J=1,NORBL
110 IF(MC(I).NE.MC(J)) 150,120
120 IF(MC(I).LT.0) 140,130
130 CONTINUE
PAIRS(I,J)=SQRTF((MU(ANK)*R)**(2*NC(ANK)+1)*(MU(ANL)*R)**(2*NC(ANL)
1)+1)/(FACT(2*NC(ANK))*FACT(2*NC(ANL)))*(-1.)**(LC(J)+MC(J))
2*SS(NC(ANK),LC(I),MC(I),NC(ANL),LC(J),MU(ANK)*R,MU(ANL)*R)
GO TO 190
140 PAIRS(I,J)=PAIRS(I-1,J-1)
GO TO 190
150 PAIRS(I,J)=0.0
190 CONTINUE
200 CONTINUE
LCULK=LC(NORBK)
LCULL=LC(NORBL)
MAXL = XMAXOF(LCULK,LCULL)
IF(R,GT,0,000001) 220,210
210 GO TO 250
C ROTATE INTEGRALS FROM DIATOMIC BASIS TO MOLECULAR BASIS
220 CALL HARRTR(T,MAXL,E)
DO 230 I=1,NORBK
DO 230 J=1,NORBL
TEMP(I,J) = 0.
DO 230 KK=1,NORBL
TEMP(I,J) = TEMP(I,J)+T(J,KK)*PAIRS(I,KK)

```

```

230 CONTINUE
    DO 240 I=1,NORBK
    DO 240 J=1,NORBL
    PAIRS(I,J) = 0.
    DO 240 KK=1,NORBK
    PAIRS(I,J) = PAIRS(I,J)+T(I,KK)*TEMP(KK,J)
240 CONTINUE
C   FILL S MATRIX
250 CONTINUE
    DO 260 I=1,NORBK
    DO 260 J=1,NORBL
260 SP(LLK+I-1,LLL+J-1) = PAIRS(I,J)
C   COMPLETATION OF 1-CENTER COULOMB INTEGRALS OVER SLATER S FUNCTI
    N1=NC(ANK)
    N2=NC(ANL)
    K1=ML(ANK)
    K2=ML(ANL)
C   COMPLETATION OF 2-CENTER COULOMB INTEGRALS OVER SLATER S FUNCTI
290 TERM1 = (R/2.)**(2*N2)*SS(0,0,0,2*N2-1,0,0,2.*K2*R)
    TERM2 = 0.
    LIM = 2*N1
    DO 300 J=1,LIM
300 TERM2 = TERM2+ (FLOATF(J)*(2*K1)**(2*N1-J)*(R/2.)**(2*N1-J+2*K2))
    1 (FACT(2*N1-J)+2.*FLOATF(N1))*SS(2*N1-J,0,0,2*N2-1,0,2.*K1*R)
    2 2*K2*R)
310 GAMMAP(K,L) = ((2.*K2)**(2*N2+1)/FACT(2*N2))*(TERM1-TERM2)
320 CONTINUE
    RETURN
    END
C   FUNCTION SS(NN1,LL1,MM,NN2,LL2,ALPHA,BETA)
    PROCEDURE FOR CALCULATING REDUCED OVERLAP INTEGRALS
    COMMON/ARRAYS/S(100,100),Y(9,5,203),Z(17,45),XX(10100)
    COMMON/AUXINT/A(17),R(17)
    TYPE INTEGER ULIM
    XARSF(ISSAM)=IABS(ISSAM)
    XMODF(ISSAM,JANO)=MOD(ISSAM,JANO)
    SORTF(QSAD)=SORT(QSAD)
    N1=NN1
    L1=LL1
    M=MM
    N2=NN2
    L2=LL2
    P=(ALPHA + BETA)/2.
    PT=(ALPHA - BETA)/2.
    X = 0
    M=XARSF(M)
C   REVERSE QUANTUM NUMBERS IF NECESSARY
    IF((L2.LT.L1).OR.((L2.EQ.L1).AND.(N2.LT.N1))) 20,10
10 GO TO 30
20 K = N1
    N1= N2
    N2= K
    K= L1
    L1= L2
    L2= K
    PT=-PT
30 CONTINUE
    K = XMODF((N1+N2-L1-L2),2)
C   FIND A AND B INTEGRALS
    CALL AINTGS(P,N1+N2)

```

```

CALL BINTGS(PT,N1+N2)
IF((L1.GT.0).OR.(L2.GT.0)) 60,40
C BEGIN SECTION USED FOR OVERLAP INTEGRALS INVOLVING S FUNCTIO.
C FIND Z TABLE NUMBER L
40 L = (90-17*N1+N1**2-2*N2)/2
   ULIM = N1+N2
   LLIM = 0
   DO 50 I=LLIM,ULIM
   X=X+Z(I+1,L)*A(I+1)*B(N1+N2-I+1)/2.
50 CONTINUE
   SS=X
   GO TC 80
C BEGIN SECTION USED FOR OVERLAPS INVOLVING NON-S FUNCTIONS
C FIND Y TABLE NUMBER L
60 L=(5-M)*(24-10*M+M**2)*(83-30*M+3*M**2)/120+
   1 (30-9*L1+L1**2-2*N1)*(28-9*L1+L1**2-2*N1)/8+
   2 (30-9*L2+L2**2-2*N2)/2
   LLIM = 0
   DO 70 I=LLIM,8
   ULIM = 4-MOD(K+I,2)
   DO 70 J=LLIM,ULIM
   ITEMP = 2*J+MOD(K+I,2)+1
70 X = X + Y(I+1,J+1,L)*A(I+1)*R(ITEMP)
   SS = X*(FACT(M+1)/8)**2*SQRTF((2*L1+1)*FACT(L1-M)*
   1 (2*L2+1)*FACT(L2-M)/(4*FACT(L1+M)*FACT(L2+M)))
80 CONTINUE
   RETURN
   END
   SUBRCUTINE HARMTR(T,MAXL,E)
   DIMENSION T(9,9),E(3)
   SQRTF(QSAD)=SQRT(GSAD)
   COST = E(3)
   IF((1,-COST**2).GT.0.000000001) 20,10
10 SINT = 0.
   GO TC 30
20 SINT = SQRTF(1.-COST**2)
30 CONTINUE
   IF(SINT.GT.0.000001) 50,40
40 COSP = 1.
   SINP = 0.
   GO TC 70
50 COSP = E(1)/SINT
60 SINP = E(2)/SINT
70 CONTINUE
   DO 80 I=1,9
   DO 80 J=1,9
80 T(I,J) = 0.
   T(1,1) = 1.
   IF (MAXL.GT.1) 100,90
90 IF (MAXL.GT.0) 110,120
100 COS2T = COST**2-SINT**2
   SIN2T = 2.*SINT*COST
   COS2F = COSP**2-SIMP**2
   SIN2F = 2.*SIMP*COSP
C TRANSFORMATION MATRIX ELEMENTS FOR D FUNCTIONS
T(5,5) = (3.*COST**2-1.)/2.
T(5,6) = -SQRTF(3.)*SIN2T/2.
T(5,8) = SQRTF(3.)*SINT**2/2.
T(6,5) = SQRTF(3.)*SIN2T*COSP/2.
T(6,6) = COS2T*COSP

```

```

T(6,7) = -COST*SINP
T(6,8) = T(6,5)/(-SQRTF(3.))
T(6,9) = SINT*SINP
T(7,5) = SGRTF(3.)*SIN2T*SINP/2.
T(7,6) = COS2T*SINP
T(7,7) = COST*COSP
T(7,8) = -T(7,5)/SQRTF(3.)
T(7,9) = -SINT*COSP
T(8,5) = SGRTF(3.)*SINT**2*COS2P/2.
T(8,6) = SIN2T*COS2P/2.
T(8,7) = -SINT*SIN2P
T(8,8) = (1.+COST**2)*COS2P/2.
T(8,9) = -COST*SIN2P
T(9,5) = SQRTF(3.)*SINT**2*SIN2P/2.
T(9,6) = SIN2T*SIN2P/2.
T(9,7) = SINT*COS2P
T(9,8) = (1.+COST**2)*SIN2P/2.
T(9,9) = COST*COS2P
110 CONTINUE
C TRANSFORMATION MATRIX ELEMENTS FOR P FUNCTIONS
T(2,2) = COST*COSF
T(2,3) = -SINP
T(2,4) = SINT*COSF
T(3,2) = COST*SINP
T(3,3) = COSP
T(3,4) = SINT*SINP
T(4,2) = -SINT
T(4,3) = 0.
T(4,4) = COST
120 CONTINUE
RETURN
END
SUBROUTINE RELVEC(R,E,C1,C2)
DIMENSION E(3),C1(3),C2(3)
SQRTF(QSAD)=SQRT(QSAD)
X = 0.
DO 10 I=1,3
E(I) = C2(I)-C1(I)
X = X+E(I)**2
10 CONTINUE
R = SQRTF(X)
DO 40 I=1,3
IF (R,GT.,.000001) 30,20
20 GO TO 40
30 E(I) = E(I)/R
40 CONTINUE
RETURN
END
FUNCTION FACT(N)
TYPE INTEGER N,I,PRODT
FLOATF(ISSAM)=FLOAT(ISSAM)
PRODT = 1
IF (N,EQ.0) 10,20
10 GO TO 40
20 DO 30 I=1,N
30 PRODT = PRODT*I
40 FACT=FLOATF(PRODT)
RETURN
END
SUBROUTINE BINTGS(X,K)

```

```

C      FILLS ARRAY OF B-INTEGRALS. NOTE THAT B(I) IS B(I-1) IN THE
C      USUAL NOTATION
C      FOR X,GT,3                                EXPONENTIAL FORMULA IS USED
C      FOR 2,LT,X,LE,3 AND K,LE,10              EXPONENTIAL FORMULA IS USED
C      FOR 2,LT,X,LE,3 AND K,GT,10              15 TERM SERIES IS USED
C      FOR 1,LT,X,LE,2 AND K,LE,7              EXPONENTIAL FORMULA IS USED
C      FOR 1,LT,X,LE,2 AND K,GT,7              12 TERM SERIES IS USED
C      FOR ,5,LT,X,LE,1 AND K,LE,5             EXPONENTIAL FORMULA IS USED
C      FOR ,5,LT,X,LE,1 AND K,GT,5             7 TERM SERIES IS USED
C      FOR X,LE,,5                               6 TERM SERIES IS USED
C      *****
C      COMMON/AUXINT/A(17),R(17)
C      ABSF(QSAD)=ABS(QSAD)
C      FXPF(QSAD)=EXP(QSAD)
C      FLOATF(ISSAM)=FLOAT(ISSAM)
C      IO=0
C      ABSX=ABSF(X)
C      IF(AESX,GT,3.) 120,10
10  IF(AESX,GT,2.) 20,40
20  IF(K,LE,10) 120,30
30  LAST=15
C      GO TC 140
40  IF(AESX,GT,1.) 50,70
50  IF(K,LE,7) 120,60
60  LAST=12
C      GO TC 140
70  IF(AESX,GT,.5) 80,100
80  IF(K,LE,5) 120,90
90  LAST=7
C      GO TC 140
100 IF(AESX,GT,.000001) 110,170
110 LAST=6
C      GO TC 140

120 EXPX=EXPF(X)
C      EXPMX=1./EXPX
C      B(1)=(EXPX-EXPMX)/X
C      DO 130 I=1,K
130 B(I+1) = (FLOAT(I)*B(I)+(-1.)**I*EXPX-EXPMX)/X
C      GO TC 190

140 DO 160 I=10,K
C      Y=0.
C      DO 150 M=10, LAST
150 Y=Y+(-X)**M*(1.-(-1.)**(M+I+1))/(FACT(M)*FLOAT(M+I+1))
160 B(I+1)=Y
C      GO TC 190

170 DO 180 I=10,K
C      FNUM = 1.-(-1.)**(I+1)
C      FDEN = FLOAT(I)+1.
C      B(I+1) = FNUM/FDEN
180 CONTINUE
190 RETURN
C      END
C      SUBROUTINE AINTGS(X,K)
C      COMMON/AUXINT/A(17),R(17)
C      FXPF(QSAD)=EXP(QSAD)
C      A(1)= EXPF(-X)/X
C      DO 10 I=1,K

```

```

10 A(I+1) = (A(I)+I+EXPF(-X))/X
   RETURN
   END
   OVERLAY(S6KSYS,1,4)
   PROGRAM HCCRE
   *(INPLT,OUTPUT,TAPE5=INPUT,TAPE6=OUTPUT,PUNCH,TAPE1)
   COMMON//TPCS(5),ADDRSS(50,5),NAET(5),IR,IW,IPUN,WAITCP,
1 INSTART,NCOUNT,SEOCNT,CONTRL(6),NCYCLE(50),X(50)
C   FORMATION OF H AND H+ CORE HAMILTONIANS IN INDO SCF LCAO CMF
C   ENTERING THIS SEGMENT, A CONTAINS S MATRIX, D CONTAINS SP
   COMMON/ARRAYS/A(100,100),B(100,100),D(100,100)
   COMMON/INFO/NATOMS,CHARGE,MULTIP,AN(50),C(50,3),N
   COMMON/1/XXX(500),G(50,50),Q(100),YYY(100),ENERGY,XXY(574),
   * GP(50,50)
   COMMON/INFO1/CZ(50),U(100),ULIM(50),LLIM(50),NELECS,CCCA,OCCE
   COMMON/OPTION/OPTION,OPNCLO,HUCKEL,CNDO,INDO,CLOSEP,CPEN
   DIMENSION ENEG(18,3),BETA0(18)
   DIMENSION G1(18),F2(18)
   TYPE INTEGER OPTION,OPNCLO,HUCKEL,CNDO,INDO,CLOSEP,CPEN
   TYPE INTEGER CHARGE,CCCA,OCCE,UL,AN,CZ,U,LLIM,ANI
   FLOAT(1SSAM)=FLOAT(1SSAM)
   PRINT 1000
1000 FORMAT(10H IN HUCKCL)
C   *****
C   SLATER-CONDON PARAMETERS FOR INDO MATRIX ELEMENTS, IN AU
   G1(3)=,092012
   G1(4)=,1407
   G1(5)=,199265
   G1(6)=,267708
   G1(7)=,346029
   G1(8)=,43423
   G1(9)=,532305

   F2(3)=,049865
   F2(4)=,089125
   F2(5)=,13041
   F2(6)=,17372
   F2(7)=,219055
   F2(8)=,266415
   F2(9)=,31580
C   CNDC/2 ELECTRONEGATIVITIES AND BONDING PARAMETERS, IN EV
   ENEG(1,1)=7,1761
   FNEG(3,1)=3,1055
   ENEG(3,2)=1,258
   ENEG(4,1)=5,94557
   ENEG(4,2)=2,563
   ENEG(5,1)=9,59407
   FNEG(5,2)=4,001
   FNEG(6,1)=14,051
   ENEG(6,2)=5,572
   ENEG(7,1)=19,31637
   ENEG(7,2)=7,275
   FNEG(8,1)=25,39017
   FNEG(8,2)=9,111
   FNEG(9,1)=32,2724
   ENEG(9,2)=11,08
   FNEG(11,1)=2,804
   ENEG(11,2)=1,302
   ENEG(11,3)=0,150
   ENEG(12,1)=5,1254

```

```

ENE(12,2)=2.0516
FNEG(12,3)=0.16195
ENE(13,1)=7.7706
ENE(13,2)=2.9951
ENE(13,3)=0.22425
ENFG(14,1)=10.0327
ENE(14,2)=4.1325
ENE(14,3)=0.337
ENE(15,1)=14.0327
ENE(15,2)=5.4638
ENE(15,3)=0.500
ENE(16,1)=17.6496
ENE(16,2)=6.989
FNEG(16,3)=0.71325
ENE(17,1)=21.5906
FNEG(17,2)=8.7081
FNEG(17,3)=0.97695
BETA(1)=-9.
BETA(3)=-9.
BETA(4)=-13.
BETA(5)=-17.
BETA(6)=-21.
BETA(7)=-25.
BETA(8)=-31.
BETA(9)=-39.
BETA(11)=-7.7203
BETA(12)=-9.4471
BETA(13)=-11.3011
BETA(14)=-13.065
BETA(15)=-15.070
BETA(16)=-18.150
BETA(17)=-22.330

```

C
C
C

```

*****
FORMATION OF CORE HAMILTONIAN, HZERO
FIND NELECS AND FILL H CORE(DIAGONAL) WITH (I+A)/2
NELECS=0
DO 60 I=1,NATOMS
NELECS=NELECS+CZ(I)
LL=LLIM(I)
UL=LLIM(I)
ANI=AN(I)
L=0
DO 50 J=LL,UL
L=L+1
IF (L, EQ, 1) 10, 20
10 A(J, J) =-FNEG(ANI, 1)/27.21
GO TO 50
20 IF (L, LT, 5) 40, 30
30 A(J, J)=-ENE(ANI, 3)/27.21
GO TO 50
40 A(J, J)=-ENE(ANI, 2)/27.21
50 CONTINUE
60 CONTINUE
NELECS=NELECS-CHARGE
OCCA=NELECS/2
PRINT 322, NELECS, OCCA
322 FORMAT(/, 6H NELECS=, I4, 2X, 6H OCCA=, I4, /)
FORM HUCKEL HAMILTONIAN IN A (OFF DIAGONAL TWO CENTER TERMS)
DO 90 I=2, N
K=U(I)

```

```

L=AN(K)
UL=I-1
DO 90 J=1,UL
KK=U(J)
LL=AN(KK)
IF ((L.GT.9).OR.(LL.GT.9)) 70,80
70 A(J,I)=A(I,J)=0.75+A(I,J)*(BETA0(L)+BETA0(LL))/54.42
GO TC 90
80 A(J,I)=A(I,J)=A(I,J)*(BETA0(L)+BETA0(LL))/54.42
90 CONTINUE
DO 100 I=1,N
100 Q(I)=A(I,I)
C ADD V(AB) TO HCORE--CNDO
DO 170 I=1,K
J=U(I)
Q(I)=Q(I) +0.5*G(J,J)
DO 160 K=1,NATOMS
160 Q(I)=Q(I)-FLOATF(CZ(K))*G(J,K)
170 CONTINUE
C EXIT SEGMENT IF ONLY CNDO APPROXIMATIONS ARE DESIRED
C INDO MODIFICATION (CORRECTION TO U(I,I) )
180 DO 280 I=1,NATOMS
K=AN(I)
J=LLIM(I)
IF ((K.GT.1).AND.(K.LT.10)) 190,280
190 IF (K.GT.3) 200,210
200 Q(J)=Q(J) +(FLCATF(CZ(I))-1.5)*G1(K)/6.
210 IF(K,EQ,3) 220,230
220 TEMP=G1(K)/12.
GO TC 260
230 IF(K,EQ,4) 240,250
240 TEMP=G1(K)/4.
GO TC 260
250 TEMP= G1(K)/3.+(FLOATF(CZ(I))-2.5)*2.*F2(K)/25.
260 CONTINUE
DO 270 L=1,3
270 Q(J+L)=Q(J+L)+TEMP
280 CONTINUE
290 CONTINUE
DO 310 I=1,N
DO 300 J=I,N
300 A(J,I)=A(I,J)
310 A(I,I)=Q(I)
PRINT 320
320 FORMAT(18H CORE HAMILTONIAN //)
C MODIFICATION OF HZERO FOR ATOMS IN PLUS AND MINUS CELLS
DO 400 I=1,N
J = L(I)
DO 61 K=1,NATOMS
Q(I) = Q(I)-FLOATF(CZ(K))*(GP(J,K)+GP(K,J))
61 CONTINUE
400 A(I,I) = Q(I)
C *****
C FORMATION OF CORE HAMILTONIAN, HPLUS
DO 91 I=1,N
K = L(I)
L = AN(K)
DO 91 J=1,N
KK = U(J)
LL=AN(KK)

```

```

91 D(I,J) = D(I,J)*(BETA0(L)+BETA0(LL))/54.42
CALL SMATTW(2,A(1,1),N,1,100,10000)
CALL MATTW(2,D(1,1),N,2,100,10000)
C LEAVING THIS SEGMENT, A CONTAINS CMO HZERO AND D CONTAINS HPLU
END
OVERLAY(S6KSYS,1,5)
PROGRAM CMCSOF
*(INPUT,OUTPUT,TAPE5=INPUT,TAPE6=OUTPUT,PUNCH,TAPE1)
COMMON//TPCS(5),ADDRS(50,5),NAET(5),IR,IW,IPUN,WAITCP,
1 INSTART,NCOUNT,SEQCNT,CONTRL(6),NCYCLE(50),X(50)
C CLOSED SHELL HF CIRCUITRY FOR INDO SCF LCAO CMO CALCULATION
C LUN = 2 HAS HZERO AND HPLUS ON RECORDS 1 AND 2 RESPECTIVELY
C LUN=2 HAS FZERO AND FPLUS ON RECORDS 3 AND 4 RESPECTIVELY
C LUN = 3 HAS PZERO AND PPLUS ON RECORDS 1 AND 2 RESPECTIVELY
C LUN = 4 HAS CREAL(K) AND CINAG(K) ON RECS 1 TO 16
COMMON/ARRAYS/A(100,100),B(100,100),C(100,100)
COMMON/INFO/ATOMS,CHARGE,MULTIP,AN(50),D(50,3),N
COMMON/EXTRA/FR(5050),FI(5050)
COMMON/INFO1/CZ(50),U(100),ULIM(50),LLIM(50),NELECS,CCCA,CCCF
COMMON/IDENT/IDENT(8)
COMMON/ELORB/EL(104),ORB(4,7)
COMMON/1/XXX(500),G(50,50),Q(100),YYY(100),ENERGY,XXY(574),
* GP(50,50)
COMMON/OPTION/OPTION,OPNCLO,HUCKEL,CNDO,INDO,CLOSEC,COPEN
DIMENSION G1(18),F2(18)
TYPE INTEGER OPTION,OPNCLO,HUCKEL,CNDO,INDO,CLOSEC,COPEN
TYPE INTEGER CHARGE,CCCA,CCCF,UL,ULIM,U,AN,CZ,Z
DIMENSION V(4),GG(4),FV(8),WT(8),COSK(8),SINK(8),PP(100,100),
* EIGS(100,8),IA(100)
EQUIVALENCE(PP,FR)
COSF(QSAD)=COS(QSAD)
SINF(QSAD)=SIN(QSAD)
ABSF(QSAD)=ABS(QSAD)
SQRTF(QSAD)=SQRT(QSAD)
PRINT 1000
1000 FORMAT(9H IN SCFCL)
C *****
C SLATER COMMON MATRIX ELEMENTS FOR INDO MATRIX ELEMENTS
G1(3)=.092012
G1(4)=.1407
G1(5)=.199265
G1(6)=.267708
G1(7)=.346829
G1(8)=.43423
G1(9)=.532305
F2(3)=.049865
F2(4)=.069125
F2(5)=.13041
F2(6)=.17372
F2(7)=.219055
F2(8)=.266415
F2(9)=.31580
C MISCELLANEOUS INITIALIZATION
OPTICN = 4*INDO
NEL = (N+1)*N/2
PI = 3.141592654
IA(1) = 0
DO 198 I=2,100
198 IA(I) = I-1+IA(I-1)
RHO = 1.0E-13

```

```

C *****
C   INITIALIZATION OF PARAMETERS FOR GAUSSIAN INTEGRATION
C   ASSIGN V(I) AND G(I) FOR 8-POINT GRID
C   K J NIELSEN, METHODS IN NUMERICAL ANAL., MACMILLAN CO., NY (1966)
C   V(1) = 0.1834346425 $ GG(1) = 0.3626837834
C   V(2) = 0.5255324099 $ GG(2) = 0.3137066459
C   V(3) = 0.7966664774 $ GG(3) = 0.2223810345
C   V(4) = 0.9602898565 $ GG(4) = 0.1012285363
C   GENERATE WAVE NUMBER GRID POINTS, -4 TO +4 IN ELEMENTS 1 TO 8
C   K = 5
C   DO 199 I=1,4
C   K = K-1
C   FV(I) = (-V(K)+1)*PI/2.
C   WT(I) = GG(K)
C   IP4 = I+4
C   FV(IP4) = (V(I)+1)*PI/2.
C   WT(IP4) = GG(I)
199 CONTINUE
C   DO 200 I=1,8
C   COSK(I) = COSF(FV(I))
200 SINK(I) = SINF(FV(I))
C   NINT = 8
C   Z = 0
C   IT = 40
C *****
C   GRAND ITERATION CYCLE BEGINS AT THIS POINT
C   10 CONTINUE
C   Z = Z+1
C   IND=0
C *****
C   IF(Z,EO.1) 110,111
C   FIRST PASS THROUGH CIRCUITRY MUST SET UP P MATRICES
110 CONTINUE
C   FNUM = 2+UCCA
C   FDEN=N
C   EDENS=FNUM/FDEN
C   DO 113 I=1,N
C   FORM INITIAL GUESS AT PPLUS AND LEAVE IN PLACE
C   DO 112 J=1,N
112 B(I,J) = 0.
113 B(I,I)=EDENS
C   GO TO 114
C   ROUTE FOR ALL SUBSEQUENT ITERATIONS
111 CONTINUE
C   BRING PZERO INTO E, HZERO INTO A AND HPLUS INTO C
C   CALL SMATTR(3,B(1,1),N,1,100,10000)
114 CONTINUE
C   CALL SMATTR(2,A(1,1),N,1,100,10000)
C   CALL MATTR(2,C(1,1),N,2,100,10000)
C   FORM CHO FZERO
C   DO 40 I=1,N
C   II=U(I)
C   A(I,I)=A(I,I)-B(I,I)+G(II,II)*0.5
C   DO 30 K=1,N
C   JJ=U(K)
30 A(I,I)=A(I,I)+B(K,K)+(G(II,JJ)+GP(II,JJ)+GP(JJ,II))
C   LL=I+1
C   IF(LL,GT,N) 40,31
31 CONTINUE
C   DO 41 J=LL,N

```

```

      JJ=U(J)
      A(J,I)=A(J,I)-B(J,I)+G(II,JJ)*0.5
41  CONTINUE
40  CONTINUE
C   INDO MODIFICATION
50  DO 80 II=1,NATOMS
      K=AN(II)
      I=LLIM(II)
      IF (K, EQ, 1) 80, 60
60  PAA=B(I,I)+B(I+1,I+1)+B(I+2,I+2)+B(I+3,I+3)
      A(I,I)=A(I,I)-(PAA-B(I,I))*G1(K)/6.
      DO 70 J=1,3
      A(I+J,I+J)=A(I+J,I+J)-B(I,I)+G1(K)/6.-(PAA-B(I,I))+7.*F2(K)/50.
1   +B(I+J,I+J)+11.*F2(K)/50.
      A(I+J,I)=A(I+J,I)+R(I,I+J)*G1(K)/2.
      JJ=J-1
      IF(JJ, EQ, 0) 70, 71
71  CONTINUE
      DO 72 L=1, JJ
      A(I+J,I+L)=A(I+J,I+L)+R(I+J,I+L)+11.*F2(K)/50.
72  CONTINUE
70  CONTINUE
80  CONTINUE
90  CONTINUE
      DO 108 I=1,N
      LJ=I+1
      DO 108 J=LJ,N
108 A(I,J)=A(J,I)
C   MATRIX A NOW CONTAINS CMO FZERO
C   FORM FPLUS IN MATRIX C
      IF(Z, EQ, 1) 100, 101
C   ZERO PPLUS ON ENTIRE FIRST ITERATION OF GRAND CYCLE
100 DO 102 I=1,N
      DO 102 J=1,N
102 B(I,J) = 0.
      GO TO 103
C   BRING PPLUS IN FROM LUN 3 ON SUBSEQUENT ITERATIONS
101 CALL MATTR(3,B(1,1),N,2,100,10000)
103 CONTINUE
      DO 104 I=1,N
      DO 104 J=1,N
      II=U(I)
      JJ=U(J)
104 C(I,J)=C(I,J)-0.5*R(I,J)+GP(II,JJ)
C   STORE FZERO AND FPLUS ON LUN2
      CALL SMATW(2,A(1,1),N,3,100,10000)
      CALL MATW(2,C(1,1),N,4,100,10000)
C   LOOP OVER WAVE NUMBER GRID
      DO 99 IK=1,NINT
      CALL SMATTR(2,A(1,1),N,3,100,10000)
      CALL MATTR(2,C(1,1),N,4,100,10000)
C   FORM FREAL AND FIMAG AND DIAGONALIZE
      DO 105 I=1,N
      DO 105 J=1,I
      IJ = IA(I)+J
      FR(I,J) = A(I,J)+(C(I,J)+C(J,I))*COSK(IK)
      FI(I,J)=(C(I,J)-C(J,I))*SINK(IK)
      A(J,I)=FI(IJ)
      A(I,J)=FR(IJ)
105 CONTINUE

```

```

CALL HELMJC(FR,FI,A,C,YYY,N,RHO,IA)
DO 115 IL=1,N
115 EIGS(IL,IK)=YYY(IL)
C CONVERT EIGENVECTORS MATRICES FROM LINEAR TO SQUARE ARRAYS
DO 106 J=1,N
DO 106 I=1,N
IJ = I+(J-1)*N
B(I,J) = C(IJ)
106 CONTINUE
DO 107 I=1,N
DO 107 J=1,N
IJ=I+(J-1)*N
107 C(I,J)=A(IJ)
C STORE C MATRICES ON RECORD IND OF FILE 4
IND = IND+1
CALL MATTW(4,C(1,1),N,IND,100,10000)
IND = IND+1
CALL MATTW(4,B(1,1),N,IND,100,10000)
99 CONTINUE
C END OF LOOP OVER WAVE NUMBER
C *****
C GAUSSIAN INTEGRATION OVER K FOR NEW DENSITY MATRICES
IND = 0
DO 209 I=1,N
DO 209 J=1,N
209 B(I,J)=PP(I,J)=0.0
DO 210 IK=1,8
C BRING REAL AND IMAGINARY EIGENVECTORS INTO A AND C RESPECTIVELY
IND = IND+1
CALL MATTR(4,A(1,1),N,IND,100,10000)
IND = IND+1
CALL MATTR(4,C(1,1),N,IND,100,10000)
C FORM PZERO IN P AND PPLUS IN PP
DO 211 I=1,N
DO 211 J=1,N
PRIJ = PIIJ = 0.
DO 212 K=1,8
PRIJ=A(I,K)*A(J,K)+C(I,K)*C(J,K)
PIIJ=A(I,K)*C(J,K)-C(I,K)*A(J,K)
R(I,J) = B(I,J)+PRIJ*WT(IK)
PP(I,J) = PP(I,J)+(PRIJ*COSK(IK)-PIIJ*SINK(IK))*WT(IK)
212 CONTINUE
211 CONTINUE
210 CONTINUE
C B AND PP NOW CONTAIN NEW PZERO AND PPLUS, RESPECTIVELY
IF(Z,EQ,1) 224,225
224 CALL SMATTW(3,P(1,1),N,1,100,10000)
CALL MATTW(3,PP(1,1),N,2,100,10000)
IF(Z,EQ,18) GO TO 218
GO TO 10
225 CONTINUE
C CONVERGENCE TEST ON DENSITY MATRICES
CALL SMATTR(3,A(1,1),N,1,100,10000)
C FORM SUM OF ABSOLUTE VALUES OF DIFFERENCES
SUM=0.
DO 213 I=1,N
DO 213 J=1,N
213 SUM=SUM+ABS(B(I,J)-A(I,J))
SUM = SUM/NEI.
PRINT 1002, SUM

```

```

1002 FORMAT(12H SUMPZERO = ,F15.10)
      IF(SLM,LT,0.001) 215,401
C     THE FOLLOWING SEGMENT CONTROLS THE CONVERGENCE WHEN CALCULATIO
C     TO DIVERGE
401 IF(Z,LT,3) 405,403
405 OLDSUM=SUM
      GO TO 224
403 IF(SLM,GE,OLDSUM) 407,405
407 OLDSUM=SUM
      DO 411 I=1,N
      DO 411 J=1,N
411 B(I,J)=(B(I,J)+A(I,J))*0.5
      CALL MATTR(3,A(1,1),N,2,100,10000)
      DO 413 I=1,N
      DO 413 J=1,N
413 PP(I,J)=(PP(I,J)+A(I,J))*0.5
      GO TO 224
C     ROUTE FOR PZERO CONVERGED, NOW TEST PPLUS
215 CALL MATTR(3,A(1,1),N,2,100,10000)
      SUM=0,
      DO 216 I=1,N
216 SUM=SUM+ABSF(PP(I,J)-A(I,J))
      SUM = SUM/NEL
      PRINT 1003, SUM
1003 FORMAT(12H SUMPPLUS = ,F15.10)
      IF(SLM,LT,0.001) 218,224
C     *****
C     PROBLEM CONVERGED, OUTPUT RESULTS
218 CONTINUE
      PRINT 223
223 FORMAT(/,22H ENERGY BAND STRUCTURE,/)
      PRINT 222,(FV(IK),IK=1,8)
222 FORMAT(/,4X,8F14.10,/)
      DO 300 I=1,N
300 PRINT 221,I,(EIGS(I,IK),IK=1,8)
221 FORMAT(I4,8F14.10)
      CALL WUN(FV,EIGS,N)
      PRINT 283
283 FORMAT(/,5H ATOM,2X,10H ATOMIC NO,2X,7H SYMBOL,2X,7H CHARGE,2X,10H
1 NET CHARGE,/)
      DO 289 LI=1,NATOMS
      RO=0,
      L1=LLIM(LI)
      L2=ULIM(LI)
      DO 281 LK=L1,L2
281 PO=RC+B(LK,LK)
      LJ=AN(LI)
      RON=CZ(LI)-RO
      PRINT 282,LI,AN(LI),EL(LJ),RO,RON
282 FORMAT(I4,7X,I2,6X,A5,F12.5,2X,F10.7,/)
289 CONTINUE
      IND=0
      DO 284 IK=1,8
      IND=IND+1
      CALL MATTR(4,A(1,1),N,IND,100,10000)
      PRINT 285,FV(IK)
285 FORMAT(/,3H K=,F14.8,/)
      CALL MOUTPT(A,N,N,100,100,3H CR)
      IND=IND+1
      CALL MATTR(4,A(1,1),N,IND,100,10000)

```

```

CALL MOUTPT(C,N,N,100,100,3H CI)
284 CONTINUE
C CALCULATION OF ELECTRONIC ENERGY EZERO
C BRING HZERO IN A AND FZERO IN B AND PZERO IN C
CALL SMATTR(2,A(1,1),N,1,100,10000)
CALL SMATTR(2,B(1,1),N,3,100,10000)
CALL SMATTR(3,C(1,1),N,1,100,10000)
CALL MOUTPT(C,N,N,100,100,3H P0)
EELCTR=0.
DO 230 I=1,N
DO 230 J=1,N
230 EELCTR=EELCTR+(A(I,J)+B(I,J))*C(I,J)+0.5
PRINT 241
241 FORMAT(//,24H ELECTRONIC ENERGY EZERO,')
PRINT 246 ,EELCTR
246 FORMAT(F16,8)
C FORM EPLUS
C BRING HPLUS IN A, FPLUS IN B, AND PPLUS IN C
CALL MATTR(2,A(1,1),N,2,100,10000)
CALL MATTR(2,B(1,1),N,4,100,10000)
CALL MATTR(3,C(1,1),N,2,100,10000)
CALL MOUTPT(C,N,N,100,100,3H PP)
EPLUS=0.
DO 251 I=1,N
DO 251 J=1,N
251 EPLUS=EPLUS+(A(I,J)+B(I,J))*C(I,J)+0.5
PRINT 261
261 FORMAT(//,6H EPLUS,/)
PRINT 246,EPLUS
EELCTR=EELCTR+EPLUS*2.
PRINT 267
267 FORMAT(//,18H ELECTRONIC ENERGY,/)
PRINT 246 ,EELCTR
C CALCULATE NUCLEAR REPULSION ENERGY EZERO
FREP=0.
NAT=NATOMS-1
DO 269 I=1,NAT
LAT=I+1
DO 268 J=LAT,NATOMS
SRAB=(D(I,1)-D(J,1))**2+(D(I,2)-D(J,2))**2+(D(I,3)-D(J,3))**2
RAR=SQRT(SRAB)
268 EREP=EREP+CZ(I)*CZ(J)/RAR
269 CONTINUE
PRINT 272
272 FORMAT(//,31H NUCLEAR REPULSION ENERGY EZERO,/)
PRINT 246,EREP
C CALCULATE REPULSION ENERGY EPLUS
ERPP=0.
NAT2=2*NATOMS
NAT1=1+NATOMS
DO 270 I=1,NATOMS
DO 270 J=NAT1,NAT2
SRAB=(D(I,1)-D(J,1))**2+(D(I,2)-D(J,2))**2+(D(I,3)-D(J,3))**2
RAR=SQRT(SRAB)
JTEMP=J-NATOMS
CZ(J)=CZ(JTEMP)
270 ERPP=ERPP+CZ(I)*CZ(J)/RAR
PRINT 273
273 FORMAT(//,31H NUCLEAR REPULSION ENERGY EPLUS,/)
PRINT 246 ,ERPP

```

```

      EREP=EREP+FRPP
      PRINT 276
276  FORMAT(/,31H TOTAL NUCLEAR REPULSION ENERGY,/)
      PRINT 246,EREP
      EREP=EREP+EELCTR
      PRINT 275
275  FORMAT(/,13H TOTAL ENRGY,/)
      PRINT 246,EREP
      END
      SUBROUTINE HELMJO(FR,FI,CR,CI,EIGS,N,RO,IA)
      DIMENSION FR(5050),FI(5050),CR(10000),CI(10000),EIGS(100),IA(
C      THIS ROUTINE FINDS THE EIGENVALUES AND EIGENVECTORS
C      OF A HERMITIAN MATRIX WHICH IS CONTAINED IN LINEAR FORM
C      IN FR AND FI, THE EIGENVALUES ARE STORED IN EIGS AND THE
C      EIGENVECTORS COME BACK IN THE LINEAR ARRAYS CI AND CR
C      NOTE,.. THE NOTATION IN THIS SUBROUTINE IS OPPOSITE OF WHAT
C      WE HAVE BEEN STICKING TO IN THE OTHER ROUTINES
C
      N IS THE DIMENSION OF THE INPUT MATRICES
      RC IS THE ACCURACY REQUIRED
C
      TYPE REAL MU
      SIGNF(QSAD,QRAD)=SIGN(QSAD,QRAD)
      SQRTF(QSAD)=SQRT(QSAD)
      FLOATF(ISSAM)=FLOAT(ISSAM)
      COSF(QSAD)=COS(QSAD)
      SINF(QSAD)=SIN(QSAD)
      ABSF(QSAD)=ABS(QSAD)
      NX=IA(N+1)
      MN=N+N
      DO 201 I=1,NN
      CR(I)=0,0
201  CI(I)=0,0
      DO 202 I=1,N
      ISA = I + (I-1)*N
202  CR(ISA) = 1,0
      TN=0,0
      DO 1 I=2,N
      II=I-1
      DO 1 J=1,II
      IJ=IA(I)+J
      1  TN=TN+2,*FR(IJ)*FR(IJ)+2,*FI(IJ)*FI(IJ)
      IF(TN,EQ,0.0)100,101
100  DO 102 J=1,N
      IJ=IA(J+1)
      I=J+(J-1)*N
102  EIGS(J)=CR(I)=FR(IJ)
      RETURN
101  R1=SQRTF(TN)
      P2=RC/FLOATF(N)*R1
      THR=R1
      IND=0
10  THR=THR/FLOATF(N)
11  DO 6 I=2,N
      II=I-1
      DO 6 J=1,II
      IJ=IA(I)+J
      W=SQRTF(FR(IJ)*FR(IJ)+FI(IJ)*FI(IJ))
      IF(W,GE,THR)7,6
      7  IND=1

```

```

ISA = IA(J+1)
V1 = FR(ISA)
ISA = IA(I) + J
V2 = FR(ISA)
ISA = IA(I+1)
V3 = FR(ISA)
ISA = IA(I) + J
V4 = FI(ISA)
MU=V3-V1
IF(ML, EQ, 0, 0) 3, 2
2 T1=SCRTF(MU*MU+4, *W*W)
Y=(ML+SIGNF(T1, MU))/(2.*V*W)
GO TC 4
3 Y=1./W
4 OMEGA=V2*Y
TAU=V4*Y
DUP=SQRTF(OMEGA*OMEGA+TAU*TAU+1.)
DO 5 K=1, N
IF(J, GE, K) 21, 22
21 KJ=IA(J)+K
ZI=+1,
GO TC 23
22 KJ=IA(K)+J
ZI=-1,
23 IF(I, GE, K) 24, 25
24 KI=IA(I)+K
XI=+1,
GO TC 26
25 KI=IA(K)+I
XI=-1,
26 CONTINUE
TRI=(-(FR(KJ)*OMEGA-FI(KJ)*ZI*TAU)+FR(KI))/DUP
TII=(-(FR(KJ)*TAU+FI(KJ)*ZI*OMEGA)+FI(KI)*XI)/DUP
TRJ=(FR(KJ)+FR(KI)*OMEGA+FI(KI)*XI*TAU)/DUP
TIJ=(FI(KJ)*ZI+FI(KI)*XI*OMEGA-FR(KI)*TAU)/DUP
IF(J, GT, K) 51, 52
51 KJ=IA(J)+K
FR(KJ)=TRJ
FI(KJ)=TIJ
GO TC 60
52 KJ=IA(K)+J
IF(J, LT, K) 53, 54
53 FR(KJ)=TRJ
FI(KJ)=-TIJ
GO TC 60
54 FR(KJ)=TRJ
60 IF(I, GT, K) 61, 62
61 KI=IA(I)+K
FR(KI)=TRI
FI(KI)=TII
GO TC 70
62 KI=IA(K)+I
IF(I, LT, K) 63, 64
63 FR(KI)=TRI
FI(KI)=-TII
GO TC 70
64 FR(KI)=TRI
70 CONTINUE
JK=K+(J-1)*N
IK=K+(I-1)*N

```

```

TRJ  =(CR(JK)+CR(IK)*OMEGA+CI(IK)*TAU)/DUP
TRI  =(CR(IK)-(CR(JK)+OMEGA-CI(JK)*TAU))/DUP
TIJ  =(CI(JK)+CI(IK)*OMEGA-CR(IK)*TAU)/DUP
TII  =(CI(IK)-(CI(JK)*OMEGA+CR(JK)*TAU))/DUP
CR(JK)=TRJ
CR(IK)=TRI
CI(JK)=TIJ
CI(IK)=TII
5  CONTINUE
V5=(1,+Y*MU-Y*Y*W+W)/(DUP+DUP)
FR(I)=V2*V5
FI(I)=V4*V5
ISA = IA(J+1)
FR(ISA) = V3+1./Y
ISA = IA(I+1)
FR(ISA) = V1-1./Y
6  CONTINUE
IF(IND,EQ,1)44,41
41 IF(THR,GT,R2)10,42
44 IND=0
GO TC 11
42 DO 45 I=1,N
ISA = IA(I+1)
45 FIGS(I) = FR(ISA)
DO 460 I=1,N
II=I+1
IF (II,GT,N) GO TC 460
DO 46 J=II,N
IF(EIGS(J).LT.EIGS(I))47,46
47 T=EIGS(J)
EIGS(J)=EIGS(I)
EIGS(I)=T
DO 48 K=1,N
KJ=K+(J-1)*N
KI=K+(I-1)*N
T=CR(KJ)
CR(KJ)=CR(KI)
CR(KI)=T
T=CI(KJ)
CI(KJ)=CI(KI)
CI(KI)=T
48 CONTINUE
46 CONTINUE
460 CONTINUE
RETURN
END

```

SUBROUTINE WYMAN(EIGS,N,OCCA,MRIJ)

C CURVB IS THE CURVATURE OF THE HIGHEST VALENCE BAND
 C CURVC IS THE CURVATURE OF THE LOWEST CONDUCTING BAND
 C EMASS IS THE EFFECTIVE MASS OF ELECTRON (HMASS IS THE EFFECTIVE
 C MASS OF THE HOLES ,COTY IS THE CONDUCTIVITY ,LCONT IS THE NATURAL
 C LOG OF THE CONDUCTIVITY ,LEIGS IS THE LOWEST ENERGY POINT IN THE
 C CONDUCTING BAND ,MEIGS IS THE HIGHEST ENERGY POINT IN VALENCE
 C BAND ,BGAP IS THE ENERGY BAND GAP IN A.U
 000007 INTEGER OCCA,OCCB
 000007 DIMENSION EIGS(100,8)
 000007 REAL MRIJ
 000007 REAL MEIGS,LEIGS
 000007 A=50.4537
 000010 B=-110.1330
 000012 C=100.4546
 000013 D=-76.8840
 000015 E=92.1648
 000016 F=-43.3753
 000020 G=24.2567
 000021 H=-6.9653
 000023 HBAR=1.0544E-27
 000024 COND=60.8228E+26
 000026 OCCB=OCCA*1
 000030 DO 1 I=1,N
 000031 IF(I.EQ.OCCA)3,5
 000035 3 CURVB=A+EIGS(I,1)+B*EIGS(I,2)+C*EIGS(I,3)+D*EIGS(I,4)+E*EIGS(I,5)+
 1F*EIGS(I,6)+G*EIGS(I,7)+H*EIGS(I,8)
 000066 EMASS=HBAR**2/(CURVB*27.21*1.6321E-28)
 000071 MEIGS=EIGS(I,1)
 000073 DO 33 IK=1,8
 000074 MEIGS=AMAX1(EIGS(I,IK),MEIGS)
 000102 33 CONTINUE
 000104 GO TO 1
 000104 5 IF(I.EQ.OCCB)4,1
 000111 4 CURVC=A*EIGS(I,1)+B*EIGS(I,2)+C*EIGS(I,3)+D*EIGS(I,4)+E*EIGS(I,5)+
 1F*EIGS(I,6)+G*EIGS(I,7)+H*EIGS(I,8)
 000142 HMASS=HBAR**2/(CURVC*27.21*1.6321E-28)
 000145 LEIGS=EIGS(I,1)
 000147 DO 44 IK=1,8
 000150 LEIGS=AMIN1(EIGS(I,IK),LEIGS)
 000156 44 CONTINUE
 000160 1 CONTINUE
 000163 BGAP=LEIGS-MEIGS
 000165 EA=SQRT(SQRT(ABS(EMASS)))
 000173 HB=SQRT(SQRT(ABS(HMASS)))
 000201 COTY=COND*(EA*HB**3.+EA**3*HB)*MRIJ
 000213 FCONT=ALOG(COTY)
 000216 PRINT 20, CURVB,CURVC
 000225 PRINT 30, EMASS ,HMASS
 000235 PRINT 50, COTY ,FCONT
 000245 PRINT 60, LEIGS,MEIGS
 000255 PRINT 70, BGAP
 000263 10 FORMAT(8F8,4)
 000263 20 FORMAT(//,8H CURVB= ,E15,4,2X,8H CURVC= ,E15.4)
 000263 22 FORMAT(3X,5I6)
 000263 30 FORMAT(//,8H EMASS= ,E15,4,2X,8H HMASS= ,E15.4)
 000263 50 FORMAT(//,8H COTY= ,E15,4,2X,8H FCONT= ,E15.4)

```

000463 60 FORMAT(//,8H LEIGS= ,E15,4.2X,8H MEIGS= ,E15.4)
000263 66 FORMAT(6X,5I2)
000463 70 FORMAT(//,8H BGAP= ,E15,4)
000463 RETURN
000464 END

```

```

SUBROUTINE WUN(XK,EIGS,N)
DIMENSION XK(8),EIGS(100,8),YENG(800),VEC(8),DX(30),DY(30)
COMMON/IDENT/IDENT(8)
CALL PLOTS(100,24H WUN I,D.NUMBER K562305.)
CALL PLOT(1.0,-11.0, 3)
CALL PLOT(1.0,-9.5,-3)
CALL PLOT(1.0,-9.5,-3)
II=0
DO 222 I=1,N
DO 222 J=1,8
II=II+1
YENG(II)=EIGS(I,J)
222 CONTINUE
CALL SCALE (XK,3,08,8,1,X0,DX)
CALL SCALE (YENG,8,0,II,1,Y0,DY)
CALL AXIS(0.0,0.0,13H WAVE VECTORS,-13,3.08,0.0,X0,DX)
CALL AXIS(0.0,0.0,14H ENERGY (A.U.),+14,8.0,90.0,Y0,DY)
CALL SYMBOL(0.5,9.50,0,20,26H ENERGY BAND STRUCTURES OF,0.0,26)
CALL SYMBOL(1.0,9.00,0,20,IDENT,0.0,80)
MZ=0
K=0
DO 333 IJ=1,II
K=K+1
VEC(K)=YENG(IJ)
IF(K.EQ.8)44,333
44 MZ=MZ+1
K=0
CALL LINE(XK,VEC,8,1,-1,MZ.X0,DX,Y0,DY)
333 CONTINUE
CALL PLOT(12,0,0,0,999)
RETURN
END

```

INPUT DATA...

POLYETHYLENE 1C ATOM PER CELL

NATOMS = 3 CHARGE = 0 MULTIP = 1

Z MATRIX

6	-0	-0.0000	-0	-0.000000	-0	-0.000000	-0
1	1	1.1000	-0	-0.000000	-0	-0.000000	-0
1	1	1.1000	2	109.471221	-0	-0.000000	-0
6	1	1.5400	2	109.471221	3	109.471221	-1
1	4	1.1000	1	109.471221	2	109.471221	-0
1	4	1.1000	1	109.471221	5	109.471221	-0

OUTPUT DATA...

COORDINATES

NO OF ATOM	SYMBOL	X	Y	Z
1	C	0.00000000	0.00000000	0.00000000
2	H	0.00000000	0.00000000	1.10000000
3	H	1.03708994	0.00000000	-.36666667
4	C	-.72596298	-1.25740472	-.51333334
5	H	-1.68797558	-.96610387	-.96148150
6	H	-.19985346	-1.64956001	-1.39604939

DISTANCES

	1	2	3	4	5	6
1	0.0000	1.1000	1.1000	1.5400	2.1705	2.1705
2	1.1000	0.0000	1.7963	2.1705	2.3348	2.9987
3	1.1000	1.7963	0.0000	2.1705	2.9525	2.3047
4	1.5400	2.1705	2.1705	0.0000	1.1000	1.1000
5	2.1705	2.3348	2.9525	1.1000	0.0000	1.6936
6	2.1705	2.9987	2.3047	1.1000	1.6936	0.0000

PROCEEDING TO SEGMENT 2 OF CARD NUMBER 2

IN INTOV
 IN COEFF
 IN INTGRL
 IN INTGRLP

PROCEEDING TO SEGMENT 3 OF CARD NUMBER 3

IN HUCKCL

NELECS= 6 OCCA= 3

CORE HAMILTONIAN

PROCEEDING TO SEGMENT 4 OF CARD NUMBER 4

IN SCFCL

SUMZERO =	.0184822992	2.3963007062	2.8221971035	3.0792161064
SUMPZERO =	.0024644322			
SUMPZERO =	.0016446739	-1.0162645347	-.9333384463	-.9110316313
SUMPZERO =	.0008059441	-.5646649263	-.5716164052	-.5977217436
SUMPLUS =	.0001538202	-.4427501722	-.5106098085	-.5070451039

ENERGY BAND STRUCTURE

	.0903738206	.1704016728	.1886327798		
	.3805874197	.4120628829	.4204253979		
	.4132375702	.4508675611	.4601520168		
	.0623765476	.3193955505	.7452919478		
			1.2826578643		
			1.8589347897		
1	-1.6330263665	-1.6141868828	-1.5323305242	-1.3669706866	-1.1701693018
2	-.9904454938	-.9759190949	-.9132694410	-.7899340570	-.6532558013
3	-.7616341146	-.7405801474	-.6478257962	-.4586623842	-.3133667223
4	.1562209920	.1552125545	.1464959420	.0832451202	-.0218884969
5	.2529093744	.2548693076	.2647500856	.2933910402	.3394561656
6	.5662900872	.5465690007	.4653802511	.3525101915	.3493761267

CURVB= -5.2092E+00 CURCB= -4.0140E+00

EMASS= -4.8058E-29 HMASS= -6.2368E-29

CONIF= 1.1988E+00 FCONT= 1.8135E-01

LEIGS= -2.1888E-02 MEIGS= -3.1337E-01

BGAP= 2.9148E-01

ATOM	ATOMIC NO	SYMBOL	CHARGE	NET CHARGE
------	-----------	--------	--------	------------

1	6	C	3.93764	.0623553
---	---	---	---------	----------

2	1	H	1.02390	-.0239035
---	---	---	---------	-----------

3 1 H 1,03845 -,0384518

K= :06237655

CR

	1	2	3	4	5	6
1	.7177	-.0055	.2673	.3492	-.0169	-.0996
2	.0766	.0636	-.5745	.0581	-.1143	-.4787
3	-.0276	-.0041	.4881	-.3439	.0240	-.7284
4	.0384	-.0797	-.5175	.1247	.1412	-.3308
5	.2960	-.0522	-.2112	-.5223	-.1436	.1698
6	.3094	.0568	-.1625	-.3720	.1913	.1767

CI

	1	2	3	4	5	6
1	.4604	.0472	-.0442	-.2488	.0555	.0087
2	.0593	-.5080	.0869	-.0341	.3601	.1200
3	-.0062	.0418	-.0704	.2494	-.0824	.1895
4	.0325	.6012	.0740	-.0810	-.4450	.0828
5	.1916	.4055	.0302	.3628	.4554	-.0421
6	.2003	-.4423	.0241	.2573	-.6033	-.0437

K= .31939555

CR

	1	2	3	4	5	6
1	.2530	-.0267	.0202	.2245	.0511	.0869
2	-.0124	.3154	-.0806	.0070	.3668	.4813
3	-.0564	-.0193	.0864	-.2486	-.0788	.7298
4	-.0167	-.3964	-.0920	.0461	-.4584	.3318
5	.0986	-.2643	-.0379	-.2956	.4648	-.1776
6	.1031	.2851	-.0259	-.2100	-.6060	-.1849

CI

	1	2	3	4	5	6
1	.8086	.0362	-.2790	.3600	-.0169	.1046
2	.1080	-.3948	.5775	.0714	-.0936	.1128
3	-.0125	.0334	-.4849	-.3646	.0310	.1347
4	.0602	.4603	.5073	.1379	.1170	.0784
5	.3408	.3188	.2090	-.5525	-.1235	-.0455
6	.3559	-.3456	.1660	-.4021	.1558	-.0479

CR

	1	2	3	4	5	6
1	.6282	.0330	-.2904	-.2589	.0051	-.1872
2	.0188	-.4656	.5649	-.0946	-.6419	.0381
3	-.1067	.0252	-.4811	.3179	-.1171	.1514
4	-.0021	.5809	.4758	-.1324	.0550	.0250
5	.2667	.4222	.2070	.4631	-.0432	.0048
6	.2768	-.4433	.1801	.3695	.0628	.0075

CI

	1	2	3	4	5	6
1	.5289	.0045	.1264	.2978	.0331	.1799
2	.1505	-.1059	-.1661	-.0315	.3725	.4959
3	.0687	-.0065	.0834	-.4227	-.0763	.6604
4	.1015	.1789	-.0967	.0132	-.4991	.3378
5	.2489	.1118	-.0410	-.3436	.4944	-.2297
6	.2580	-.1163	-.0433	-.2605	-.5877	-.2423

K= 1.28265786

CR

	1	2	3	4	5	6
1	.7479	-.0080	.0102	.2564	-.0171	-.2866
2	.1077	.4008	.0628	-.1542	-.1400	.0203
3	-.0795	-.0056	-.2209	-.7056	-.0241	.2384
4	.0678	-.5383	.0930	-.1056	.2090	.0183
5	.3753	-.4508	.0609	-.2432	-.1722	.0520
6	.3815	.4520	.0575	-.2063	.1852	.0733

CI

	1	2	3	4	5	6
1	.1005	-.0012	.3795	-.0221	-.0136	.3707
2	.1945	.1395	-.5812	.1608	.3538	.4837
3	.2174	.0174	.4208	-.2236	-.0525	.3350
4	.1457	-.2438	-.4135	.1444	-.5286	.2989
5	.0868	-.1754	-.2228	-.3291	.4920	-.3499
6	.0881	.1775	-.2282	-.3070	-.4715	-.3959

K= 1.85893479

CR

	1	2	3	4	5	6
1	-.4841	.0078	.0648	.3458	.2976	.1425
2	.0549	.2272	-.2233	-.2271	.2386	-.2316
3	.2709	.0416	.5221	.6438	-.1969	-.0538
4	.0415	-.3582	-.1424	-.1376	.1699	.5727
5	-.2613	-.3410	-.2870	.1290	-.1850	-.4668
6	-.2549	.3329	-.3285	.1164	-.3004	.2536

CI

	1	2	3	4	5	6
1	-.4114	-.0184	-.2777	.3244	-.3327	-.0276
2	-.2991	-.2810	.4309	-.3345	.4837	.1827
3	-.2486	.0027	.2309	-.2782	-.0333	-.0506
4	-.2228	.4090	.2595	-.2620	-.0993	-.3676
5	-.3070	.4252	.1919	.0290	.2273	.3159
6	-.2999	-.4046	.2062	.0355	.4577	-.2033

K= 2.39630071

CR

	1	2	3	4	5	6
1	-.0646	-.0185	.2588	-.4059	.1445	-.0868
2	-.3708	.2701	-.1347	.2999	.0571	.2022
3	-.5155	.1295	-.6258	-.0688	-.1224	.0375
4	-.2737	-.3795	-.1579	.2125	.0203	-.5198
5	-.1573	-.5014	.1589	.0463	-.0442	.3790
6	-.1471	.4048	.2810	.0607	-.0758	-.1852

CI

	1	2	3	4	5	6
1	.4627	-.0191	-.0868	.5494	-.4429	-.1237
2	.1186	-.1436	-.3024	-.3345	-.6067	.1767
3	-.0581	.0346	-.0257	.4839	.2347	.1015
4	.0977	.3067	-.1106	-.1805	-.0871	-.5333
5	.3515	.3863	-.2899	-.0562	.2415	.3641
6	.3267	-.2919	-.4452	-.0771	.5172	-.1680

K= 2.82219710

CR

1	.2494	.1326	-.2212	.7125	-.7615	.1100
2	.3558	-.1674	-.2744	-.3823	-.6443	-.1672
3	.4001	-.3530	.1950	.3357	.2970	-.1025
4	.2695	-.0538	.3908	-.2259	-.0390	.5821
5	.3161	.1096	.2939	-.1184	.1780	-.3860
6	.2847	.0118	-.7493	-.1506	.4770	.1512

CI

	1	2	3	4	5	6
1	-.0872	-.3232	-.0048	-.2682	-.1547	.1138
2	.2982	.0763	.1133	.1272	-.1995	-.1316
3	.5027	.3567	.1043	-.2223	.1282	-.1172
4	.2136	-.2489	.0018	.0562	-.0218	.5189
5	.0386	-.6985	-.0306	.0447	.0642	-.3324
6	.0357	-.1653	.1120	.0555	.1567	.1245

K= 3.07921611

CR

	1	2	3	4	5	6
1	.1222	.2255	-.1739	.2899	.1114	.0704
2	.4890	-.3117	-.2901	-.1467	.2219	-.0811
3	.6768	-.2136	.1164	.1251	-.2991	-.0761
4	.3614	.1051	.4165	-.0867	.0075	.3388
5	.2763	.3800	.4049	-.0512	-.0538	-.2158
6	.2471	.1772	-.7282	-.0649	-.1576	.0769

CI

	1	2	3	4	5	6
1	-.0330	.3640	.0066	-.7238	.3533	-.1422
2	.0621	-.0798	.0291	.3583	.6547	.1766
3	.1143	-.4341	.0098	-.3589	-.3138	.1501
4	.0436	.1147	-.0191	.2021	.0284	-.7109
5	-.0032	.5571	-.0251	.1281	-.1642	.4569
6	-.0026	.2562	.0484	.1614	-.4701	-.1650

P0

	1	2	3	4	5	6
1	1.1044	-.0759	.0015	-.0637	.4567	.4711
2	-.0759	.9766	-.0385	.0409	-.8432	.7419
3	.0015	-.0385	.8769	-.0572	-.2041	-.1951
4	-.0637	.0409	-.0572	.9798	.8041	-.3115
5	.4567	-.8432	-.2041	.8041	1.0278	-.0279
6	.4711	.7419	-.1951	-.3115	-.0279	1.0384

ELECTRONIC ENERGY EZERO
-21.43799082

PP

	1	2	3	4	5	6
1	.3112	-.2244	-.1389	-.1477	.0238	-.0001
2	.0126	.1526	-.2640	-.0153	.0126	.0306
3	.4664	-.4768	-.2632	-.3316	-.0069	-.0096
4	.0160	-.0145	-.1867	.1675	.0428	.0131
5	-.0054	-.0418	-.0097	-.0459	-.1916	-.0083
6	-.0345	.0063	-.0417	-.0153	-.0095	-.1765

EPLUS

-.19496426

ELECTRONIC ENERGY

-21.82791935

NUCLEAR REPULSION ENERGY EZERO

4.14307571

NUCLEAR REPULSION ENERGY EPLUS

10.17065262

TOTAL NUCLEAR REPULSION ENERGY

14.31372833

TOTAL ENERGY

-7.51419102

PROCEEDING TO SEGMENT 1 OF CARD NUMBER 1